APPLICATION OF THE GRILLAGE METHODOLOGY TO DETERMINE LOAD DISTRIBUTION FACTORS FOR SPREAD SLAB BEAM BRIDGES

A Thesis

by

JOEL ADAM PETERSEN-GAUTHIER

Submitted to the Office of Graduate Studies of
Texas A&M University
in partial fulfillment of the requirements for the degree of

MASTER OF SCIENCE

Chair of Committee,	Mary Beth Hueste
Co-Chair of Committee,	John Mander
Committee Member,	Mohammed Haque
Head of Department,	Robin Autenrieth

August 2013

Major Subject: Civil Engineering

ABSTRACT

Transverse load distribution behavior amongst bridge girders is influenced by many parameters including girder material properties, spacing, skew, deck design, and stiffening element interactions. In order to simply and conservatively approximate the bridge superstructure load distribution between girders, the American Association of State Highway and Transportation Officials (AASHTO) LRFD Bridge Design Specifications contain load distribution factor (LDF) equations for many common bridge types.

The Texas Department of Transportation (TxDOT) had recently developed a new design for bridge superstructures that utilizes a spread configuration of prestressed concrete slab beams. AASHTO does not contain LDFs for this type of bridge so the load sharing behavior of this superstructure must be investigated further. TxDOT has funded the Texas A&M University Transportation Institute (TTI) to design, model, construct, test, and analyze a full scale spread slab beam bridge. In addition to this testing, an existing slab beam bridge in Denison, Texas will be instrumented and observed for supplementary slab beam behavior data.

To predict bridge behavior, computer models of the Riverside experimental bridge and of the Denison field bridge were developed using both the grillage and finite element methods of analysis. The experimental results from the Riverside and Denison bridges will not be collected by the conclusion of this thesis so a third bridge with existing experimental data, the Drehersville, Pennsylvania bridge, was also modeled for calibration purposes.

The work presented by this thesis focuses on how to accurately model transverse load distribution relationships and LDFs for use in bridge design. The analysis covered is concentrated primarily on the grillage method, with the finite element analysis as part of the larger project scope. From this analysis it was determined that the grillage method was able to accurately model bridge LDFs as compared to FEM modeling and experimental results, for spread slab beam and spread box beam bridges. The critical loading configurations for all bridges placed two trucks side by side and as far to one edge of the bridge as possible. It was also determined that at an ultimate

loading case, the load is distributed much more evenly across the deck than at service loading.

DEDICATION

To my parents, Kris and Stan Petersen-Gauthier.

ACKNOWLEDGEMENTS

The research conducted as part of this thesis would not have been possible without the input of several people. Firstly, I would like to express my gratitude to my advisor, Dr. Mary Beth Hueste. Her preparation, experience, instruction, and guidance have all been crucial to my success at Texas A&M University and to the progress of TxDOT project 0-6722, which I was a part of. I would also like to extend my thanks to Dr. John Mander, who has helped me and this research project immensely with his impressive technical knowledge and practical engineering solutions. Both of these professors, on behalf of the Civil Engineering Department, are also responsible for the generous financial support that allowed me to continue my higher education at Texas A&M.

I would like to thank Dr. Mohammed Haque from the Architecture Department for his support and involvement on my advisory committee. I wish to acknowledge the Texas Department of Transportation (TxDOT) who financed the research presented in this thesis and helped to fund me through the Texas A&M Transportation Institute (TTI). I would also like to acknowledge Texas A&M University and TTI for allowing this project to use the Riverside campus for the construction and testing of our experimental bridge.

I would like to thank Tevfik Terzioglu for his hard work, his continued advice and assistance, and for being a great office-mate and friend. I also wish to thank all of my friends and family for the great support they have shown me over the past two years. My parents and my sister Emma have been extremely helpful during my time in College Station and I cannot thank them enough for the constant love, encouragement, and caring they have given me from afar. Finally, a special thank you to Jenny for her incredible patience, selflessness, and love.

TABLE OF CONTENTS

Page

LIST OF FIGURES

LIST OF TABLES

1. INTRODUCTION

1.1 BACKGROUND

1.1.1 Prestressed Slab Beam Bridges in Texas

Precast, prestressed concrete girders have been used effectively in Texas and other states for over 60 years. The majority of these prestressed concrete bridges are simply supported spans where the deck slab is made composite with pretensioned concrete girders. Currently, the use of precast, prestressed concrete girders provides economical bridges for short to medium spans.

Slab-on-girder bridges with medium spans from 50 to 150 ft are typically constructed by seating the precast prestressed girders on bearing pads on the piers or abutments and then casting a concrete deck on top of the girders. Although different forms of decks have been constructed over the years, nowadays decks are typically 8 in. thick and consist of 4 in. thick stay-in-place precast transversely prestressed concrete panels (PCP) that are placed between girders and a 4 in. thick cast in place (CIP) two-way reinforced concrete topping slab.

For shorter span lengths, up to 50 ft in length, a variety of alternatives exist to the standard I-girder design. The Texas Department of Transportation (TxDOT) often uses prestressed concrete slab beam bridges as a common alternative, as shown in Figure 1.1 and Figure 1.2. While these bridges are used extensively, experience shows they are more expensive than traditional slab-on-I-girder structures on a per square foot basis. To assess this issue TxDOT has shown interest in exploring new and improved types of bridge superstructures that may provide more economical solutions and less complex construction for short-span bridges.

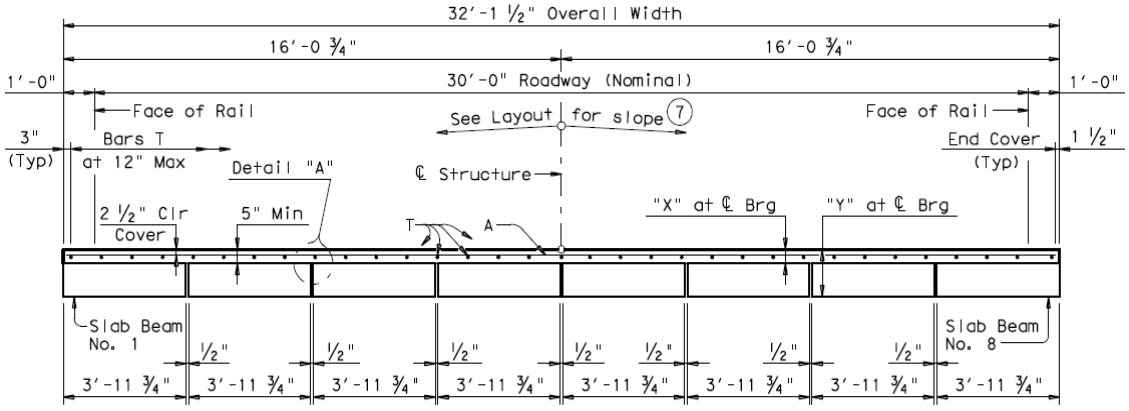

Figure 1.1 Typical TxDOT Prestressed Concrete Slab Beam Bridge Design (TxDOT 2012)

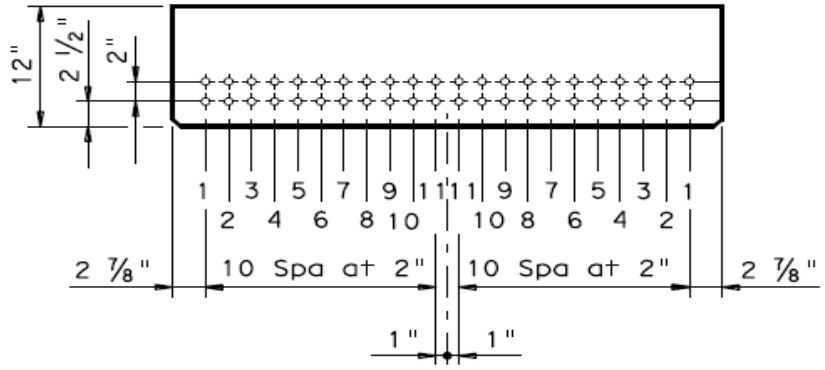

(a) 4SB12 slab beam prestressing locations

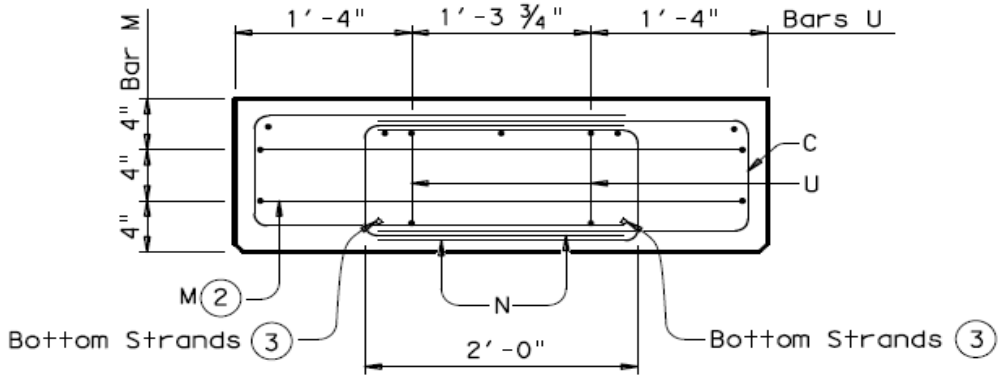

(b) 4SB12 slab beam mild steel reinforcing

Figure 1.2 Typical Details of TxDOT 4SB12 Prestressed Concrete Slab Beams (TxDOT 2012)

One such idea has been developed by TxDOT by modifying the current short-span bridge design that uses the contiguous prestressed concrete slab beams shown in Figure 1.1. The proposed economical solution is to spread out the slab beams and to use a conventional topped panelized deck as shown in Figure 1.3. By spreading out the slab beams in a similar fashion to conventional reinforced concrete slab-on-precast prestressed concrete girders, it is expected that less material is required along with a possible reduction in the overall bridge cost.

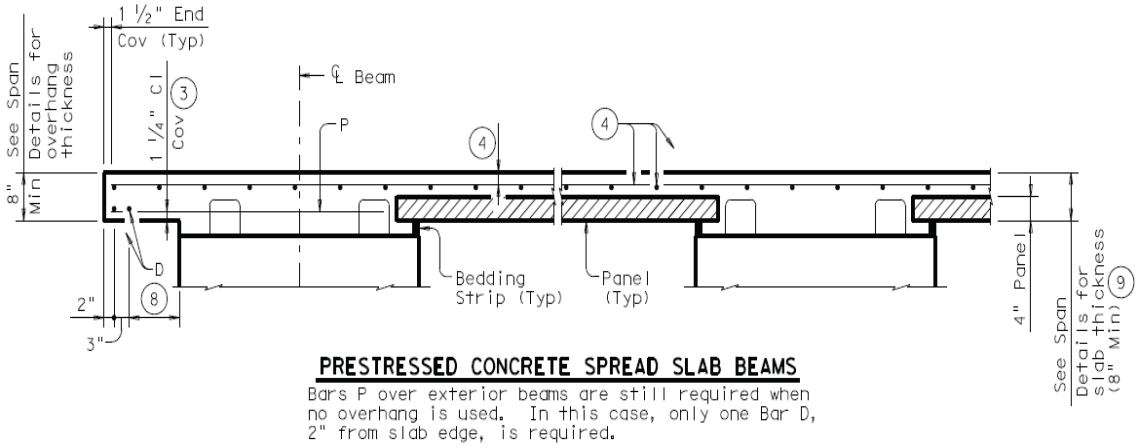

Figure 1.3 Typical Details of TxDOT Prestressed Concrete Spread Slab Beam Bridge Deck with PCPs (TxDOT 2012)

Once the slab beams are spread out across the bridge deck, the moments and shears imposed by eccentrically located truck traffic differ in the individual slab beams across the overall bridge deck cross-section. Appropriate girder distribution factor expressions for this case do not exist and will have to be investigated. While this study will bear in mind the objective of improving the overall economics of the proposed spread-slab beam deck configuration, the principal research focus is directed to recommendations for this bridge type, with a particular emphasis on establishing appropriate live load distribution factors for this class of spread slab beam bridge deck. This thesis focuses on several specific bridge configurations for load distribution investigation, but does not cover all cases of load distribution analysis that will be done for this TxDOT project.

1.1.2 Load Distribution Factors (LDFs)

From the early 1930s to the mid-1990s the simple American Association of State Highway and Transportation Officials (AASHTO) LFD *S/D* equations developed by Newmark (1938) were the primary means to determine the transverse load distribution in bridges in the United States. However, in 1991 the NCHRP 12-26 project (Zokaie et al. 1991) showed that these equations were not accurate for many types of bridges and new, more complex equations were developed to account for additional influential parameters. These formulae were found to predict load distributions for a wide array of bridges much more accurately when compared to values found by experimentation and by computer modeling using grillage or finite element analyses. In 1994 these more advanced equations were then adopted by the AASHTO LRFD Bridge Design Specifications (AASHTO 1994b).

1.1.3 TxDOT Project 0-6722

In order to determine more precisely how the spread beam layout will affect the behavior of prestressed slab beam bridges, and to explore the possible benefits of the spread slab beam bridge configuration, TxDOT has funded Texas A&M University's Civil Engineering Department and the Texas A&M Transportation Institute (TTI) to design, model, construct, test, and analyze a full scale spread slab beam bridge. This bridge will be constructed and tested at Texas A&M University's Riverside campus in Bryan, Texas. In addition to this testing, an existing slab beam bridge in Denison, Texas will be instrumented and observed for supplementary slab beam behavior data.

To make predictions about the bridge behavior, computer models of the Riverside experimental bridge will be developed using both the grillage and finite element methods of analysis. This will be done largely because there has been very little previous research on spread prestressed slab beam bridges and thus there are currently no load distribution factor equations for this type of bridge in the AASHTO LRFD Bridge Design Specifications (AASHTO 2012). Design recommendations and standards

for this bridge type will be developed and bridge behavior for the spread slab beam arrangement will be summarized.

The work presented by this thesis is part of this project, mainly focused on the transverse load distribution relationships of spread slab beam bridges and how to accurately predict load distribution factors. The analysis covered in this thesis focuses primarily on the grillage method, with the finite element analysis (FEA) as part of the larger project scope. It is crucial to assess whether the grillage method is capable of correctly predicting transverse load sharing behavior in spread slab beam bridges.

1.2 OBJECTIVES AND SCOPE

The major objective of the study described in this thesis is to investigate the use of the grillage modeling approach to predict load distribution factors for spread slab beam bridges. This will be accomplished by completing several tasks, including: (1) develop grillage models for the Riverside experimental bridge, the Denison field bridge, and the Drehersville field bridge; (2) calibrate the grillages models using comparisons with finite element models and available experimental data; and (3) analyze the results from the refined Riverside experimental bridge model to predict load distribution relationships, examine spread slab beam load distribution factors, and make final recommendations for the proper use of grillage modeling.

The scope of this thesis covers the history and development of bridge load distribution factors, the use of the grillage methodology to predict these factors for prestressed concrete bridges, and the calibration and selection of grillage modeling assumptions for accurate spread slab beam LDF calculation. It is limited to static wheel loading of the bridge and static point loading of the grillage models. The load sharing between slab beams will be analyzed in depth by the grillage model but other behavior will not be discussed. Development of slab beam load distribution relationships will be done using a combination of grillage and finite element analysis. The current editions of the AASHTO LRFD Bridge Design Specifications (AASHTO 2012) and Standard Specifications for Highway Bridges (AASHTO 2002) will be used in most cases

throughout this project, except when clearly comparing current practices with the older versions and previous formulae.

1.3 METHODOLOGY

The major research objective for this study is to investigate the use of the grillage modeling approach to predict load distribution factors for spread slab beam bridges. The following section outlines the five main tasks that have been identified to meet the research objective.

1.3.1 Task 1: Literature Review and Background Understanding

A comprehensive review of available and relevant literature was conducted to gain background knowledge of the topics involved in this research. The literature covered by this review deals largely with the development and background of the AASHTO LRFD load distribution factors, and the use of the grillage method of bridge analysis to determine load distributions. Other useful sources on the grillage method, its applications and how to use it correctly were also examined. Finally, similar experimental projects to the Riverside experimental bridge testing were studied so preparations for these tests may begin. This aided in deciding which tests needed to be done in order to collect the data that will be the most important to this project, and then how to analyze this data. Other topics that were deemed relevant or significant to certain aspects of the project were also added to this review.

1.3.2 Task 2: Develop Grillage Models

Several computer aided grillage analysis models were created using the structural analysis finite element program SAP2000 (Computers and Structures (2012b)). Models were made for the Riverside experimental bridge, the Denison, Texas bridge, and for the Drehersville, Pennsylvania bridge. Figure 1.4 shows the plan view and transverse section of the Riverside experimental bridge, Figure 1.5 depicts the transverse section and

elevation view of the Drehersville bridge, and Figure 1.6 displays the transverse section and plan view of the Denison bridge.

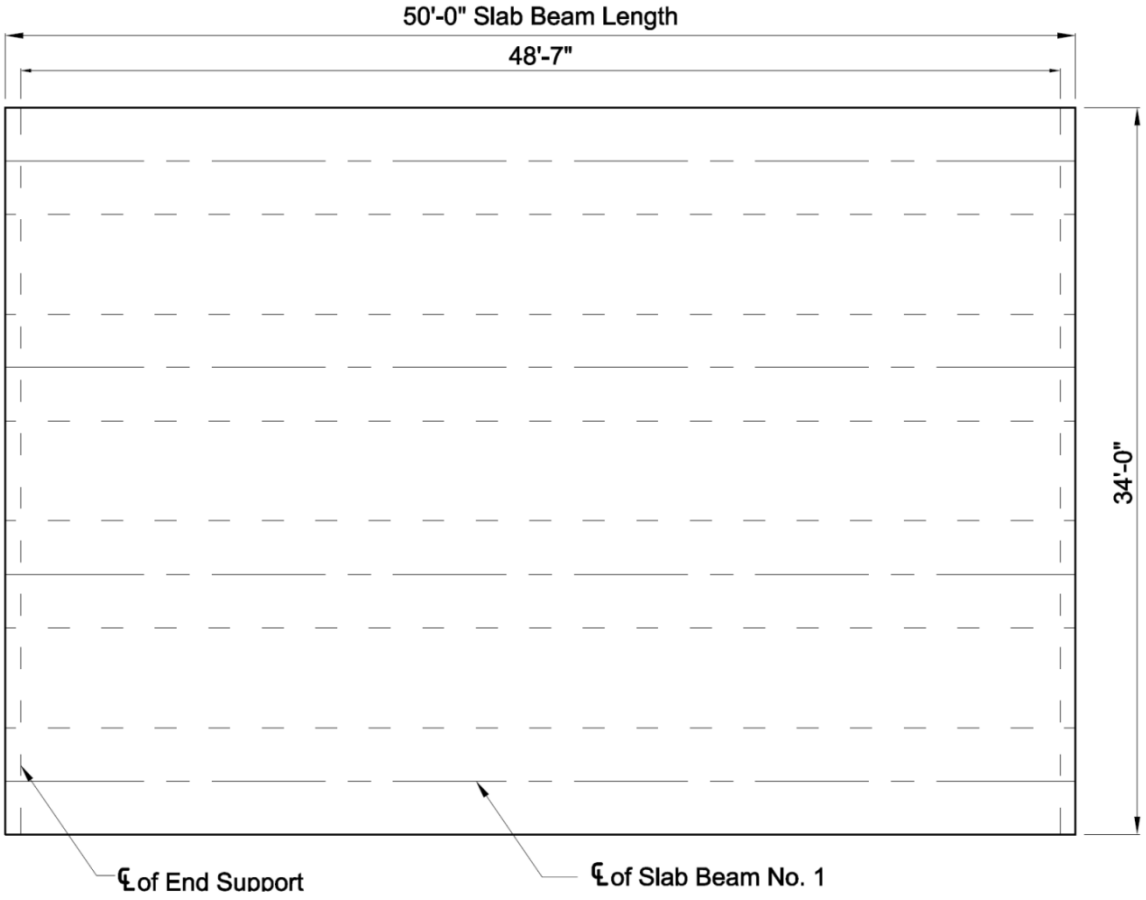

(a) Plan View

(b) Transverse Section

Figure 1.4 Riverside Experimental Bridge (Terzioglu 2012)

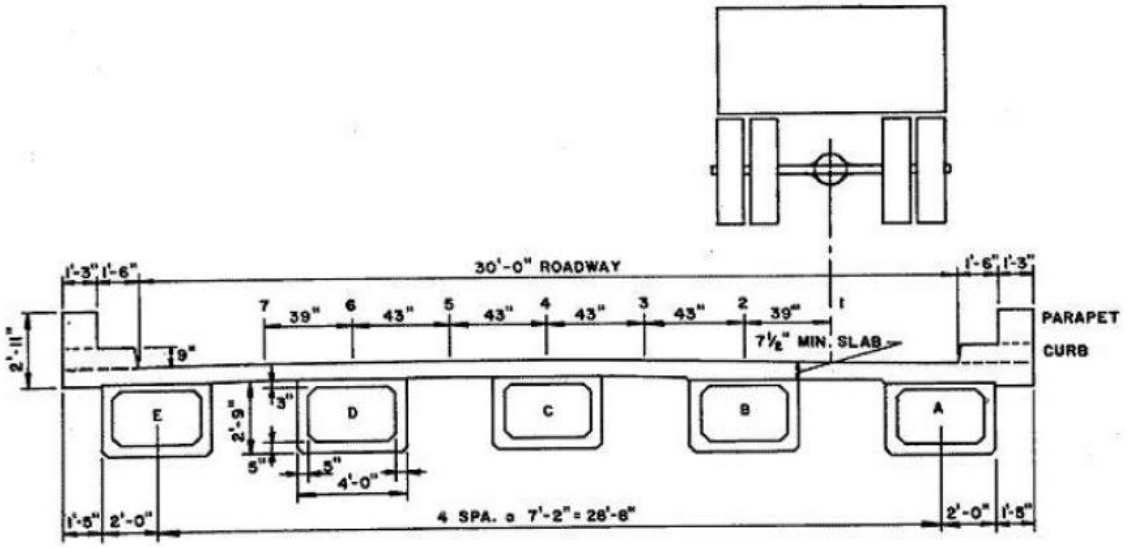

(a) Transverse Section

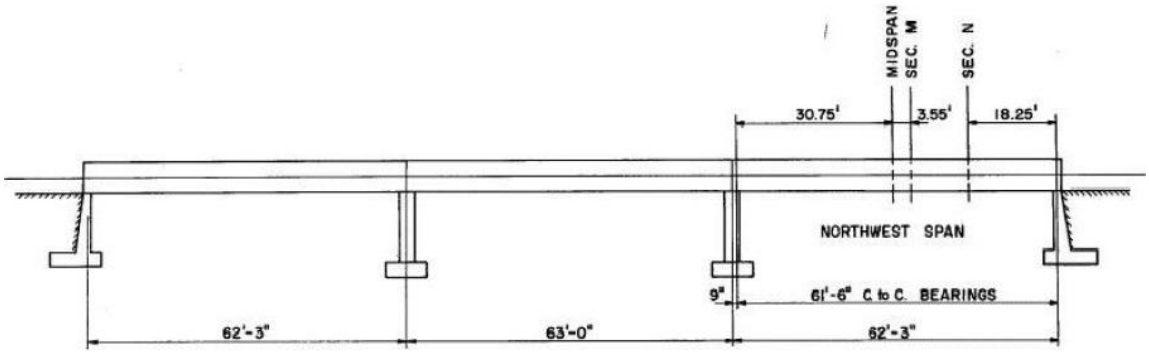

(b) Elevation View

Figure 1.5 Drehersville Bridge (Douglas and Vanhorn 1966)

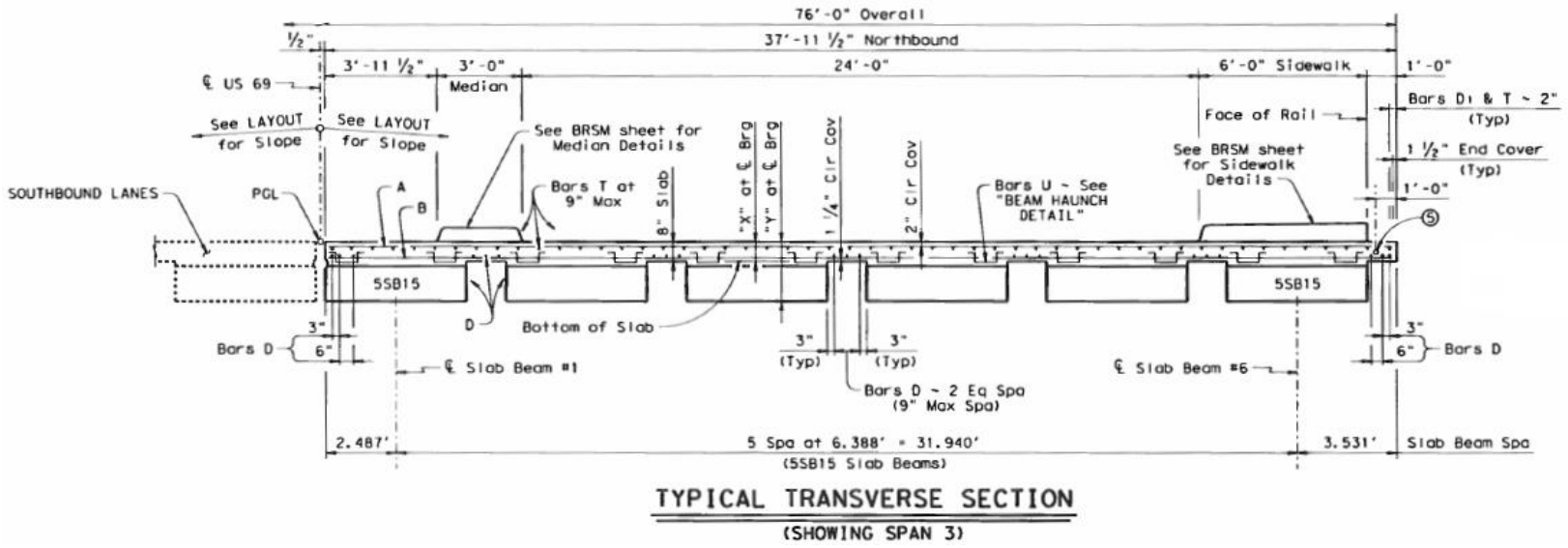

(a) Transverse Section

Figure 1.6 Denison Field Bridge Northbound Lanes (TxDOT 2010)

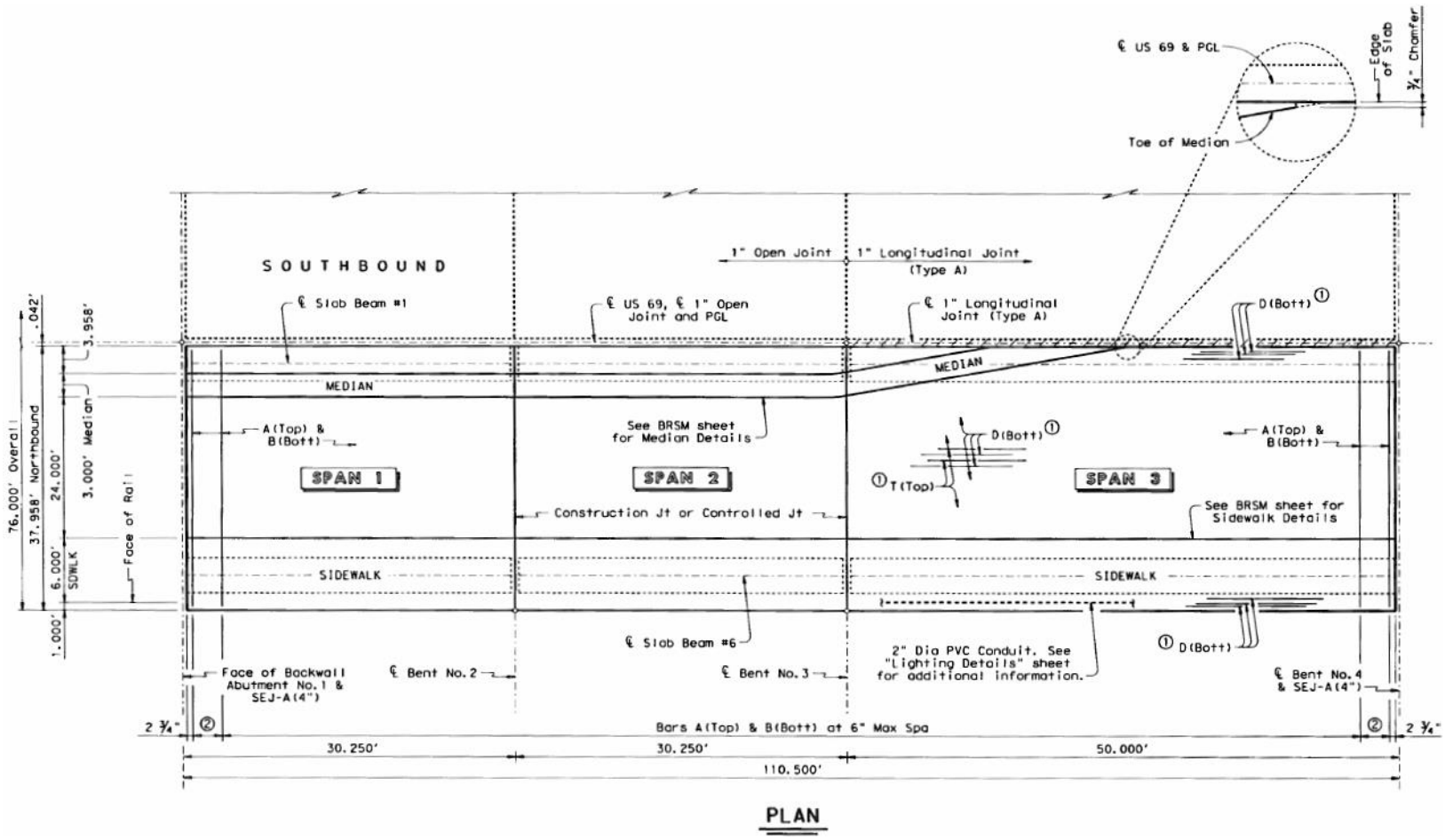

(b) Plan View (Span 3)

Figure 1.6 (cont.)

Several models were developed for the three bridges, each using slightly different modeling parameters to determine the most accurate way to implement the grillage method for load distribution modeling for these types of bridges. The models split the bridge into equivalent beams members, making a grillage, that represent actual sections of the bridge in the same locations. The stiffness parameters of bridge sections, represented by the grillage members, were calculated separately and used to confirm the accuracy of those generated by SAP2000. If these values differed, those calculated according to the appropriate equations for grillage modeling were used by setting property modifiers in SAP2000. For the different loading cases, the resulting moments, shears, and deflections of the longitudinal grillage members, which represent the girders, were used to assess the load sharing among these members and aid in the accurate prediction of the girder load distribution factors.

1.3.3 Task 3: Calibrate Grillage Models

In many cases, the models created in Task 2 captured the bridge behavior relatively accurately, but they were not initially highly accurate in all respects. To improve these models they were calibrated by comparing them to experimental results in the case of the Drehersville bridge, and finite element analysis for the Riverside and Denison slab beam bridges. The grillage models created for the Drehersville bridge were also compared to finite element modeling of this bridge, to ensure that both modeling procedures were similar and to check the calibration of the finite element models. Similarly, the grillage models developed for the Riverside and Denison bridges were compared to the finite element models created for these same bridges so that the grillage models could be adjusted to match the load distributions found from the finite element models as much as practical.

By adjusting the modeling parameters or loading configurations in the grillage models to match the results of more accurate models or experimental data, a common grillage modeling technique to more precisely capture the bridge's load sharing behavior was determined. By comparing the calibration of models for multiple bridges, it was

determined whether similar techniques improved results for different bridges with different parameters. The accuracy of modeling assumptions and how universal these assumptions are was determined for future grillage modeling.

1.3.4 Task 4: Review Load Distribution Relationships for Preliminary LDFs

With final enhanced versions of the grillage models, as well as the data on the relationships between several bridge parameters, the critical load distributions amongst the slab beams were analyzed. From these grillage model load distribution relationships it was possible to investigate the creation of general load distribution factor formulae for spread prestressed slab beam bridges. However, it was shown that at this early stage of spread slab beam bridge research there was still insufficient data to develop load distribution factor equations for this bridge type.

Refined grillage modeling techniques and key assumptions for accurate modeling of spread slab beam bridges and load distribution behavior were recommended after grillage calibration. All changes to the models were described in detail so future grillage modeling may use this procedure or compare with this project. After attaining LDFs from the grillage method, comparisons to the LDFs found from finite element method (FEM) models, and to those given by AASHTO (2012) equations for similar bridge types were made. Modern computation power has made FEA much faster than it was 10 or 15 years ago, but grillage modeling is still considered easier to develop and less computationally expensive. Since the grillage modeling of the bridges in this project proved to be an accurate and expedient alternative to FEA for calculating load distribution factors, this study provided additional guidelines for effectively using this analysis method.

1.3.5 Task 5: Plan the Field Bridge Testing

Based on the preliminary results from the grillage method, the most critical locations for the wheel loads to be placed on the Riverside experimental bridge were determined. This is important for the continuation of the project and will be used in the testing of the experimental bridge. Additional helpful guidelines for the field testing were collected

from similar projects cited in the literature review. The instruments that will be used on the field bridge will have to be placed in the correct positions to capture the maximum moment, shear, and deflection results. These instruments, as well as the cables, and data acquisition units, will also have to be assembled, connected, calibrated, and verified to be working correctly. This advanced preparation will ensure that once the bridge is constructed, testing may follow in an expedient manner.

1.4 ORGANIZATION OF THESIS

This thesis is structured with six major sections. The first section is the background information on the project and introduction to the problem. Section 2 discusses the literature review conducted on the development of load distribution factors and the use of the grillage method of analysis for computer modeling of bridges. The third section describes the development of the Riverside experimental bridge grillage model. In Section 4 calibration of this model as well as the creation and calibration of the Drehersville and Denison field bridges is discussed. The fifth section covers the results of the refined grillage analysis for transverse load distribution factor calculation, comparisons with current AASHTO LRFD load distribution factors, and the effects of overload on LDFs. The sixth and final section presents the project summary, conclusions, and recommendations. Additional information relevant to the thesis is presented in the appendices.

2. LITERATURE REVIEW

2.1 GENERAL

This section covers a wide range of available literature on relevant topics to this research. A review of pertinent information from each source is provided to give a basis as to what has already been accomplished in this field, as well as to provide a helpful knowledge base to build off. The main topics covered by this literature review include the history of the *S/D* live load distribution factors used from the 1930s until 1996 (AASHTO 1996; Newmark 1938); the development, use, and assessment of modern bridge LDFs (AASHTO 1994a; AASHTO 2012); and the use of the grillage method of analysis, which will be used in conjunction with the LDFs to accurately determine and confirm load distribution.

2.2 PRESTRESSED SLAB BEAM BRIDGES

McKee and Turner (1975) conducted a study focused on reducing short-span (up to 50 ft) bridge costs. This project, sponsored by the Louisiana DOT, placed emphasis on superstructure types that can be erected rapidly while progressively using erected portions as a working platform. Solutions used by several other states were reviewed and it was found that popular options included voided slabs, channels, and box sections, generally with positive lateral load transfer mechanisms and either a bituminous or cast-in-place concrete overlay. The research provided designs for box, spread box, and channel sections along with cost estimates. However, McKee and Turner (1975) indicated that the use of new sections did not appear to provide significant savings. It was concluded that substantial progress in both manufacturing and construction procedures, along with increased competition in the industry, were needed to significantly reduce costs.

Panak (1982) also led a project on behalf of TxDOT to investigate the development of economical precast concrete bridges for shorter spans. The study considered five types of precast structural superstructure types including: (1) precast

concrete box beams, (2) prestressed concrete PCI box beams, (3) precast concrete double stem tee beams, (4) precast concrete solid slabs, and (5) precast concrete voided slabs. From a 1981 bid process, Panak (1982) found that a lack of economy was due to the fact that the precast producers were not willing to invest in new forms and associated production hardware that may be used for only one job. Since then however, this issue has been overcome at least for some of the proposed bridge types. Box beams and solid slabs have become common options for TxDOT bridges.

In the last 30 years there has been substantial progress in both the construction and precast manufacturing industry. In addition to the industry making great strides in the past three decades, the design criteria and code requirements have changed quite a bit. Most notably for this project, the load distribution factor equations presented by the AASHTO LRFD Bridge Design Specifications (AASHTO 2012) have been reassessed and reformed greatly during the past 20 years from the AASHTO Standard Specifications for Highway Bridges (AASHTO 1989). Although these new distribution factors have been shown to give more accurate and consistent results, there are still problems with them as they are difficult to use for design and there are no distribution factor equations for several types of bridges including prestressed slab beam bridges. These issues will be investigated thoroughly throughout the project. Due to these changes and the prevalence of slab beam bridges throughout Texas, the proposed project on spread slab beam bridge systems presents a timely opportunity to revisit the task of developing more economical short-span bridge decks.

2.3 LIVE LOAD DISTRIBUTION FACTORS (LDF)

2.3.1 Historical Development of *S/D* LDFs (1938-1996)

Newmark (1938) developed the first empirical load distribution factors. Since that time, Newmark's LDFs were used without any major changes by the American Association of State Highway Officials (AASHO), later to become AASHTO, in all versions of the Bridge Design Specifications until the final edition (AASHTO 1996). These original LDFs, often termed the "*S*-over" equations, used to assess the design moments and

shears applied to individual beams within a bridge deck. The LDFs were found by the calculation of *S/D*, where *S* is the spacing between girders and *D* is a specified value that depends on the type of bridge. For example, a bridge constructed with a concrete deck on spread girders and having two or more lanes of traffic has a *D* value of 5.5. The *D* constant was originally taken as being the distance between wheels of the HS20 design truck, which is 6 ft, but was altered for increased accuracy. Table 2.1 lists the *D* values for several pertinent bridge types, where *S* is in ft (AASHTO 1996).

When load distribution is considered this way it is easy to understand and utilizes the most important parameter, the girder spacing, within a simple formula. Although simple to use, the *S/D* equations ignore the effect of several important parameters such as relative deck stiffness, span length, and skew. Therefore, these equations give accurate results for a few selected bridge geometries, but are considered conservative for long spans, unconservative for short spans, and simply inaccurate for a wide range of bridge geometries and spans. Due to these facts and research on a substantial amount of information for different bridge types, it was decided that revision to the AASHTO Standard Specifications (AASHTO 1989) was needed.

Table 2.1 *S/D* Distribution Factors from AASHTO Standard Specifications for Highway Bridges (US Customary Units) (AASHTO 1996)

Kind of Floor	Bridge Designed for One Traffic Lane	Bridge Designed for Two or more Traffic Lanes
Concrete:		
On steel I-Beam stringers[f] and prestressed concrete girders	S/7.0 If S exceeds 10' use footnote f.	S/5.5 If S exceeds 14' use footnote f.
On concrete T-Beams	S/6.5 If S exceeds 6' use footnote f.	S/6.0 If S exceeds 10' use footnote f.
On timber stringers	S/6.0 If S exceeds 6' use footnote f.	S/5.0 If S exceeds 10' use footnote f.
Concrete box girders[h]	S/8.0 If S exceeds 12' use footnote f.	S/7.0 If S exceeds 16' use footnote f.
On steel box girders	See Article 10.39.2.	
On prestressed concrete spread box Beams	See Article 3.28.	

[f] In this case the load on each stringer shall be the reaction of the wheel loads, assuming the flooring between the stringers to act as a simple beam.

3.28 DISTRIBUTION OF LOADS FOR BENDING MOMENT IN SPREAD BOX GIRDERS*

3.28.1 Interior Beams

The live load bending moment for each interior beam in a spread box beam superstructure shall be determined by applying to the beam the fraction (D.F.) of the wheel load (both front and rear) determined by the following equation:

$$D.F. = \frac{2N_L}{N_B} + k\frac{S}{L} \qquad (3\text{-}33)$$

where,

N_L = number of design traffic lanes (Article 3.6);
N_B = number of beams ($4 \le N_B \le 10$);
S = beam spacing in feet ($6.57 \le S \le 11.00$);
L = span length in feet;
$k = 0.07\,W - N_L\,(0.10N_L - 0.26) - 0.20N_B - 0.12$; (3-34)
W = numeric value of the roadway width between curbs expressed in feet ($32 \le W \le 66$).

3.28.2 Exterior Beams

The live load bending moment in the exterior beams shall be determined by applying to the beams the reaction of the wheel loads obtained by assuming the flooring to act as a simple span (of length S) between beams, but shall not be less than $2N_L/N_B$.

2.3.2 Background and Development of Current AASHTO LDFs (1994-Present)

Zokaie et al. (1991) conducted a study as part of the NCHRP 12-26 project "Distribution of Wheel Loads on Highway Bridges" to assess and fill the need for more accurate and a broader range of LDFs. This study presents updated and more comprehensive formulae for calculating the load distribution. While these equations are also approximate, they give consistently conservative results for the specified range of bridge geometries. All LDF equations were based on finite element analysis and statistical evaluation of typical families of bridge types.

In 1994, more accurate LDF equations based on the work done during NCHRP 12-26 project were introduced as part of the AASHTO Guide Specifications for Distribution of Loads for Highway Bridges (AASHTO 1994a) and the AASHTO LRFD Bridge Design Specifications (AASHTO 1994b). The Guide Specifications formulae are similar to those from the LRFD Specifications, except that they only apply to non-LRFD applications and are to be used only when reverting back to the AASHTO Standard Specifications. Table 2.2 below shows some select bridge types relevant to this project, taken from AASHTO (2012) Table 4.6.2.2.1-1. Table 2.3 and Table 2.4 are similarly select potions of AASHTO (2012) Tables 4.6.2.2.2d-1 and 4.6.2.2.2b-1 that give exterior and interior girder moment LDFs for these bridge types. Table 2.5 and Table 2.6 are excerpts from the AASHTO (2012) exterior and interior girder shear LDF Tables 4.6.2.2.3b-1 and 4.6.2.2.3a-1. All equations are in English units and have not changed since 1994 (AASHTO 2012).

Table 2.2 Common Bridge Deck Superstructures (AASHTO 2012)

SUPPORTING COMPONENTS	TYPE OF DECK	TYPICAL CROSS-SECTION
Steel Beam	Cast-in-place concrete slab, precast concrete slab, steel grid, glued/spiked panels, stressed wood	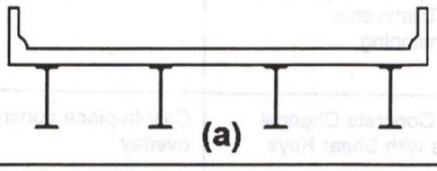 (a)
Closed Steel or Precast Concrete Boxes	Cast-in-place concrete slab	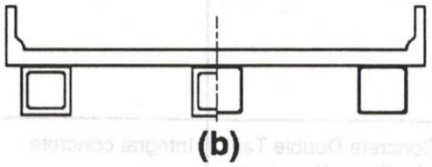 (b)
Precast Concrete I or Bulb-Tee Sections	Cast-in-place concrete, precast concrete	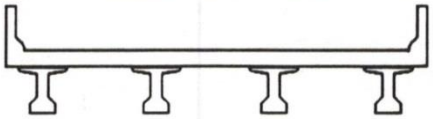 (k)

Table 2.3 Exterior Beam Moment LDFs from AASHTO LRFD Bridge Design Specifications (AASHTO 2012)

Type of Superstructure	Applicable Cross-Section from Table 4.6.2.2.1-1	One Design Lane Loaded	Two or More Design Lanes Loaded	Range of Applicability
Concrete Deck, Filled Grid, or Partially Filled Grid on Steel or Concrete Beams; Concrete T-Beams, T and Double T Sections	a, e, k	Lever Rule	$g = e\,g_{interior}$ $e = 0.77 + \frac{d_e}{9.1}$	$-1.0 \le d_e \le 5.5$
Concrete Deck on Concrete Spread Box Beams	b, c	Lever Rule	$g = e\,g_{interior}$ $e = 0.97 + \frac{d_e}{28.5}$	$0 \le d_e \le 4.5$ $6.0 < S \le 11.5$
			Use Lever Rule	$S > 11.5$
Steel Grid Deck on Steel Beams	a	Lever Rule	Lever Rule	N/A
Concrete Deck on Multiple Steel Box Girders	b, c	As specified in Table b-1		

Table 2.4 Interior Beam Moment LDFs from AASHTO LRFD Bridge Design Specifications (AASHTO 2012)

Type of Beams	Applicable Cross-Section from Table 4.6.2.2.1-1	Distribution Factors	Range of Applicability
Concrete Deck, Filled Grid, or Partially Filled Grid on Steel or Concrete Beams; Concrete T-Beams, T- and Double T-Sections	a, e, k	One Design Lane Loaded: $0.06 + \left(\frac{S}{14}\right)^{0.4}\left(\frac{S}{L}\right)^{0.3}\left(\frac{K_g}{12.0Lt_s^3}\right)^{0.1}$ Two or More Design Lanes Loaded: $0.075 + \left(\frac{S}{9.5}\right)^{0.6}\left(\frac{S}{L}\right)^{0.2}\left(\frac{K_g}{12.0Lt_s^3}\right)^{0.1}$	$3.5 \le S \le 16.0$ $4.5 \le t_s \le 12.0$ $20 \le L \le 240$ $N_b \ge 4$
Concrete Deck on Concrete Spread Box Beams	b, c	One Design Lane Loaded: $\left(\frac{S}{3.0}\right)^{0.35}\left(\frac{Sd}{12.0L^2}\right)^{0.25}$ Two or More Design Lanes Loaded: $\left(\frac{S}{6.3}\right)^{0.6}\left(\frac{Sd}{12.0L^2}\right)^{0.125}$	$6.0 \le S \le 11.5$ $20 \le L \le 140$ $18 \le d \le 65$ $N_b \ge 3$
		Use Lever Rule	**S > 11.5**
Steel Grids on Steel Beams	a	One Design Lane Loaded: S/7.5 If $t_g < 4.0$ IN S/10.0 If $t_g \ge 4.0$ IN Two or More Design Lanes Loaded: S/8.0 If $t_g < 4.0$ IN S/10.0 If $t_g \ge 4.0$ IN	$S \le 6.0$ FT $S \le 10.5$ FT
Concrete deck on Multiple Steel Box Girders	b, c	Regardless of Number of Loaded Lanes: $0.05 + 0.85\frac{N_L}{N_b} + \frac{0.425}{N_L}$	$0.5 \le \frac{N_L}{N_b} \le 1.5$

Table 2.5 Exterior Beam Shear LDFs from AASHTO LRFD Bridge Design Specifications (AASHTO 2012)

Type of Superstructure	Applicable Cross-Section from Table 4.6.2.2.1-1	One Design Lane Loaded	Two or More Design Lanes Loaded	Range of Applicability
Concrete Deck, Filled Grid, or Partially Filled Grid on Steel or Concrete Beams; Concrete T-Beams, T- and Double T-Beams	a, e, k	Lever Rule	$g = e\, g_{interior}$ $e = 0.6 + \frac{d_e}{10}$	$-1.0 \le d_e \le 5.5$
	i, j if sufficiently connected to act as a unit		Lever Rule	$N_b = 3$
Concrete Deck on Concrete Spread Box Beams	b, c	Lever Rule	$g = e\, g_{interior}$ $e = 0.8 + \frac{d_e}{10}$	$0 \le d_e \le 4.5$
			Lever Rule	$S > 11.5$
Steel Grid Deck on Steel Beams	a	Lever Rule	Lever Rule	N/A
Concrete Deck on Multiple Steel Box Beams	b, c	As specified in Table 4.6.2.2.2b-1		

Table 2.6 Interior Beam Shear LDFs from AASHTO LRFD Bridge Design Specifications (AASHTO 2012)

Type of Superstructure	Applicable Cross-Section from Table 4.6.2.2.1-1	One Design Lane Loaded	Two or More Design Lanes Loaded	Range of Applicability
Concrete Deck, Filled Grid, or Partially Filled Grid on Steel or Concrete Beams; Concrete T-Beams, T- and Double T-Sections	a, e, k	$0.36 + \frac{S}{25.0}$	$0.2 + \frac{S}{12} - \left(\frac{S}{35}\right)^{2.0}$	$3.5 \le S \le 16.0$ $20 \le L \le 240$ $4.5 \le t_s \le 12.0$ $10{,}000 \le K_g \le 7{,}000{,}000$ $N_b \ge 4$
	i, j if sufficiently connected to act as a unit	Lever Rule	Lever Rule	$N_b = 3$
Concrete Deck on Concrete Spread Box Beams	b, c	$\left(\frac{S}{10}\right)^{0.8}\left(\frac{d}{12.0L}\right)^{0.1}$	$\left(\frac{S}{7.4}\right)^{0.8}\left(\frac{d}{12.0L}\right)^{0.1}$	$6.0 \le S \le 11.5$ $20 \le L \le 140$ $18 \le d \le 65$ $N_b \ge 3$
		Lever Rule	Lever Rule	$S > 11.5$
Steel Grid Deck on Steel Beams	a	Lever Rule	Lever Rule	N/A
Concrete Deck on Multiple Steel Box Beams	b, c	As specified in Table 4.6.2.2.2b-1		

The NCHRP 12-26 research project focused on the response of bridges to AASHTO HS truck loads (Zokaie et al. 1991). Available methods for wheel load distribution were evaluated for beam and slab, box girder, slab, multi-box beam, and spread box beam bridges. In order to allow more structures to be designed with simplified methods, a complete and consistent set of formulae for LDFs was developed.

In order to cover most of the common bridge types nationwide, a database was compiled of several hundred random bridges from various states. This bridge database was examined to categorize the common values of numerous bridge parameters including beam spacing, slab thickness, overhang, span length, and skew angle, among others. A hypothetical bridge was defined that possessed the average properties and parameters from the database and referred to as the "average bridge." Average bridges for each of the above mentioned bridge types were established. To obtain the effect of

different parameters on wheel load distribution, each parameter was altered while all others were kept constant for the average bridge under consideration. From this technique, wheel load distribution factors for both shear and moment were obtained for each parameter.

The LDF formulae were then established with errors minimized by applying a three-level analysis. Level 1 was defined as the simplified method which uses LDFs for calculating moments and shears. Level 2 included graphical and simplified grillage methods. Level 3 analysis was defined as a detailed finite element analysis.

To derive the simplified formulae, assumptions were made and some parameters were discarded when not particularly relevant. Therefore it was essential to verify the accuracy of these simplified formulae against real bridge behavior to ensure no important bridge characteristics were omitted. The bridge database and average bridges were used for this verification. Five average bridges were evaluated by Level 3 analysis and the LDFs were verified. The distribution factors found from the most accurate method were compared with those found from the simplified method and ratios between the two values were calculated and examined to assess the accuracy of the simplified formulae. The methods or formulae that had smallest standard deviation and an average closest to unity were adopted as the most applicable formulae.

As part of the work to support the development of the LDFs, Nowak (1993) developed new load models for dead, live, and dynamic loads on highway bridges. He built these models based on the available statistical data on dead loads, truck loads and dynamic loads. Considering the lifetime of a bridge as being around 75 years, extreme loads that would have the probability of occurring once in 75 years were determined. During the modeling process LDFs and multiple-presence (more than one truck on the bridge) were considered as important parameters and conditions. Multiple-presence loading was modeled in both one-lane and in side-by-side situations, with different correlations between truck weights. Because live and dynamic loading are random variables in nature, their variations were described by cumulative distribution functions, mean values, bias factors, and correlation coefficients.

The dynamic model in Nowak's project was developed as a function of three main properties: road surface roughness, bridge dynamics (frequency of vibration), and vehicle dynamics (suspension system). Nowak (1993) states that the dynamic deflection was found to be independent of truck weight, thus inferring that with increased truck weight the dynamic load decreases as compared to the live load. From the 75-year live loads, the resultant dynamic load never even reached 15% of the live load for a single truck, and 10% for two trucks side-by-side. The results from this study also indicated that the dynamic load factor (DLF) values were also quite equally based on all three of the main properties listed above. The actual contribution of these parameters will change slightly from bridge to bridge, making this very challenging to predict accurately, so it was recommended that DLF be specified as a percentage of the live load.

The analytical model was also analyzed for the distribution of live load to girders by two-lane loading. The resulting LDFs were then compared with the AASHTO Standard Specifications (AASHTO 1989) values and those recommended by Zokaie et al. (1991). Figure 2.1 shows the calculated and AASHTO moment distribution factors. As can be seen for longer spans and larger girder spacing values, AASHTO (1989) LDFs become overly conservative, often resulting in almost 50% higher factors than the analytical results. The results of the analytical models were also compared with the recommendations of Zokaie et al. (1991) and indicated good agreement with the suggested simplified method, as shown in Figure 2.1.

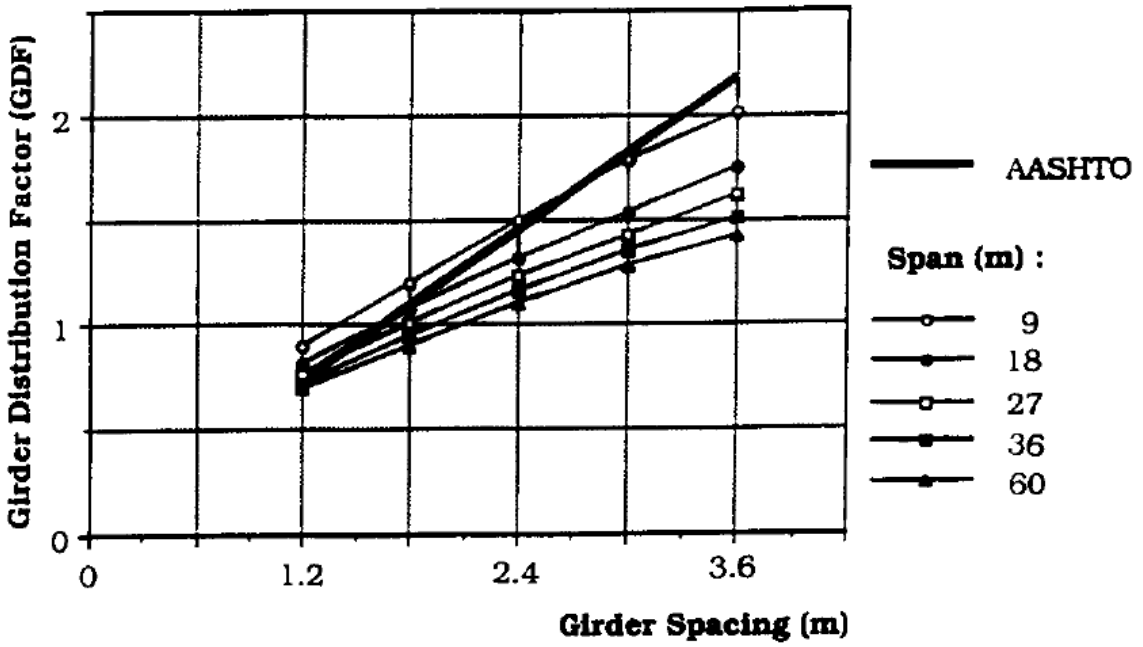

Figure 2.1 Girder Distribution Factors: Calculated and Specified by AASHTO Standard Specifications (Nowak 1993)

Nowak (1993) concluded that for one lane bridges the positive moment from lane live load is governed not by multiple-presence but by a single truck on bridge spans of up to 40 m. Similarly the shear and negative moment are also controlled by a single truck on spans up to 35 m and 15 m respectively. However, two-lane bridge LDFs depend both on span length and on the girder spacing. Nowak stated that this analysis showed that the AASHTO Standard Specifications (AASHTO 1989) equations are too conservative for most cases, especially for larger girder spacings.

2.3.3 Assessment of Current AASHTO LRFD LDFs

Chen and Aswad (1996) studied refined analysis procedures to determine LDFs for simply supported bridges under flexure. AASHTO (1994a) live load distribution factor formulae for flexure were reviewed for prestressed concrete I-girders and spread box beam bridges. The shortcomings of the simplified formulae in the LRFD code were also listed. First, the average bridge span for I-girder bridges was considered to be about 50 ft in the studies of Zokaie et al. (1991). However, this span is rather short when compared

to many modern and future bridge designs. Secondly, the multilane reduction factor was often ignored for bridges with three lanes. This should not be the case because many times when all three lanes are loaded, that situation will be controlling for design and multilane factors will then make a significant contribution in moment and shear reductions. Furthermore the study by Zokaie et al. (1991) conservatively did not take into account the effects of midspan diaphragms.

This study developed refined analysis techniques that allowed the presence of midspan diaphragms and slab orthotropy for beam-slab bridges. Additionally, a parametric study was conducted on a wide array of span-to-depth ratios for spread box and I-girder bridges. This revealed that for reasonably large span to depth ratios, the refined methods of analysis (FEA or grillage analysis) gave midspan moments that were about 20% smaller than those returned by the simplified formulae in the AASHTO LRFD Bridge Design Specifications (AASHTO 1994b). Similarly in spread box beams the FEA showed results that were about 10% lower than the equations. The most severe case of this FEA reduced results occurred in the exterior girders when midspan diaphragms were used; the refined analysis indicated 30% smaller load distribution values than the LRFD formulae. Therefore the author recommended that finite element analysis or grillage analysis be used for longer span bridges as this permits a significant reduction in the release strength or alternatively for lengthening the span capability.

Zokaie (2000) discussed further details of the new simplified LDFs developed during NCHRP 12-26, and presented the background on the development of the formulae, comparing their accuracy with the previous *S/D* method. Although the NCHRP 12-26 project considers five different types of bridges, Zokaie only concentrated on slab-on-girder bridges in his study, so as to further detail the methods used to develop the LDF formulae. The computer program GENDEK5A (Powell and Buckle 1970) was used for modeling these slab-on-girder type bridges. The average slab-and-beam bridge was then modeled using this chosen computer program. To identify which parameters have considerable influence on the load distribution, a sensitivity study was performed.

HS20 truck loads were used to load the FE model of the bridge deck to determine the live load distribution factors for shears and moments. This analysis was then repeated many times, each time for a different parameter in question, keeping all other parameters as their mean values while changing the one being investigated from its minimum to maximum value. Parameters investigated included girder area, girder eccentricity, girder moment of inertia, girder spacing, span length, and slab thickness. To assess how important each parameter was to the overall load distribution, the results for each parameter were plotted together on the same graph for visual inspection. From this examination, Zokaie decided that the girder spacing, span length, and girder and slab stiffness were the most significant parameters related to load distribution (Zokaie 2000).

Results obtained from Zokaie's proposed formulae were compared with a more accurate FEA results. The so called *g*-ratio was calculated by taking the ratio of distribution factor obtained from the formula to the one obtained from FEA. These ratios were used for fine tuning of the simplified formulae. The intention of this was to obtain a standard deviation less than the earlier *S/D* AASHTO (1996) formulas. Also the average value of the *g*-ratios must be larger than unity in order to create some conservatism, but not overly conservative. By visually inspecting the plots and examining the trends, the formulae were given their final form. However, many of the final equations presented by Zokaie were modified with slightly different or more conservative coefficients when they were implemented in AASHTO (1994b).

Figure 2.2 shows the histogram of the *g*-ratios for the historic *S/D* equations and the proposed approach. It can be seen that the standard deviation and accuracy of the proposed approach is significantly improved as compared to the historic *S/D* equations.

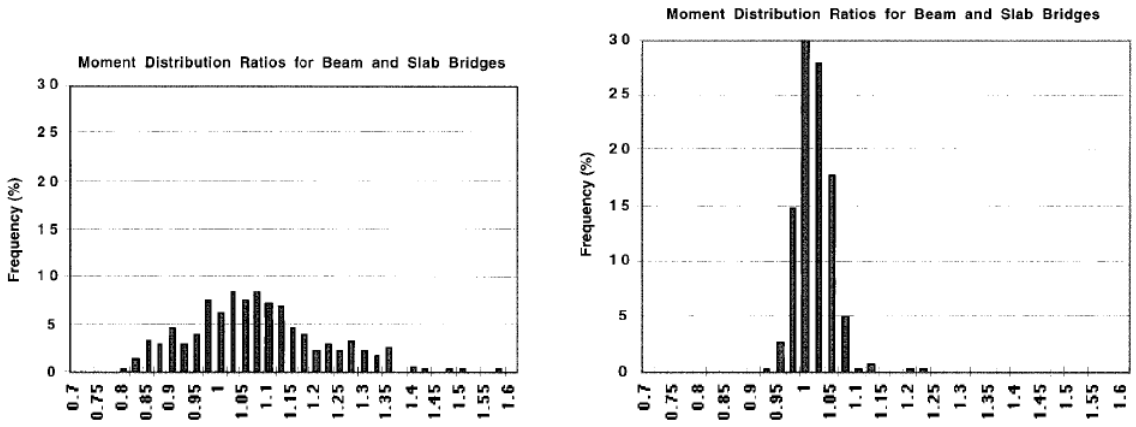

(a) AASHTO *S/D* (b) Proposed Formulas

Figure 2.2 Comparison of G-Ratios for Simple Formulae with G-Ratios for More Accurate Analysis (Zokaie 2000)

2.3.4 Research Studies Evaluating AASHTO LRFD Load Distribution Factors

2.3.4.1 Goodrich and Puckett (2000)

Goodrich and Puckett (2000) explored the effects of nonstandard axles gauges on the wheel live load distribution. They also developed a simplified method for calculating the LDFs caused by trucks with axle gauge widths differing from the specified 6 ft in the AASHTO LRFD Bridge Design Specifications (AASHTO 1994b). This simplified method was based on a rigorous finite strip method analysis and was compared with the results from the program BRASS-Dist (WYDOT 1996) for several combinations of axle configurations and bridge geometries. The simplified method presented by Goodrich and Puckett (2000) generally gives conservative results that show a strong relation to the results found from the rigorous analysis.

2.3.4.2 Tabsh and Tabatabai (2001)

Tabsh and Tabatabai (2001) studied the effects of oversized trucks on the live load distribution in bridges. The load distribution factors in the AASHTO LRFD Bridge Design Specifications (AASHTO 1994b) are based on specific truck geometries and loads. There are however some cases where trucks with larger gauge widths, axle spacing, or loads are used. In these cases engineering analysis is needed before a permit may be acquired. To make this process easier Tabsh and Tabatabai (2001) proposed

modification factors for the specification based LDFs to account for these overload situations and thus make it possible to design for these events. Through a parametric study involving FEA the authors found that the LDFs for oversized loads were less than those found using the expressions in the AASHTO LRFD Bridge Design Specifications (AASHTO 1994b). The main overload parameter investigated (a larger truck gauge width) was also shown to have a greater influence on the shear distribution than the flexural distribution between girders.

2.3.4.3 Barr et al. (2001)

Barr et al. (2001) conducted a study to further verify the LDFs by experimentation. The project was based on the experimental results of a continuous high-performance prestressed concrete I-girder bridge designed by the Washington State Department of Transportation (WSDOT). The measured response of this bridge during static live load testing was used to confirm the analytical FE model created. Then twenty-four variations of this model were studied in order to evaluate flexural live load distribution factors. These finite element models were also analyzed to evaluate the effects of lifts, intermediate diaphragms, continuity, skew angle, end diaphragm, and load type on the LDFs. The finite element models returned LDFs for bridges with fairly standard geometries within 6% of the code equation values. However, the bridge in question for this study had a more irregular geometry and therefore the code values were conservative by 28%. Barr found that lifts, skew angle, end diaphragms, and load type significantly reduced the LDF while continuity and intermediate diaphragms had little effect on the load distribution.

2.3.4.4 Eom and Nowak (2001)

Eom and Nowak (2001) conducted a study to evaluate the LDFs of truck loads on girder bridges. Previous studies showed that the LDFs specified in the earlier AASHTO Standard Specifications (AASHTO 1996) were not accurate for longer span bridges and for large girder spacings. Therefore, this research was intended to validate LDFs for steel girder bridges with spans of 10 – 45 m. An experimental field test on 17 steel girder

bridges was conducted by the Michigan DOT to help understand their load distributions. The bridges were instrumented by strain gages and loaded with heavy trucks (up to 761 kN or 171 kips). Trucks were placed on the bridges and from the recorded strains LDFs were calculated for one lane and two lane loaded cases. An analytical study was also conducted using FEA with three different boundary conditions (simple supports, hinged supports, and partially fixed supports). The final LDFs obtained through experimental tests and analytical models were then compared with AASHTO Standard Specifications (AASHTO 1996) and AASHTO LRFD Specifications (AASHTO 1998).

For all of the bridges that were tested, the experimentally obtained LDFs from the field tests were less than the code formulae values. The ratios of these two different LDF values were then compiled for all bridges analyzed and their patterns were studied. The results indicate that for short span bridges, AASHTO Standard Specifications (AASHTO 1996) and AASHTO LRFD Specifications (AASHTO 1998) specify LDFs that are overly conservative. This difference between the code LDFs and those found from FEA may mean that the real bridge conditions were different than what was assumed in the AASHTO specifications. Eom and Nowak (2001) also state that the results of the study showed that particularly for larger span bridges AASHTO LRFD Specifications (AASHTO 1998) provide more consistent LDFs than the AASHTO Standard Specifications (AASHTO 1996).

Different boundary conditions were used in the FEA to determine which ones returned the most accurate results. Eom and Nowak (2001) claim that the LDFs were found to be more uniform for ideally simply supported bridges. The strain values for simply supported cases as compared to ones with some fixity were shown to be much higher, which made the measured strain in the tests lower than predicted by the simply supported analysis. In essence the field testing led to the belief that there was some support fixity but the FEA conflicted with this and showed the most accurate results for simply supported. The authors then states that for bridges with ideal simple supports, the more realistic LDFs for one lane loaded come from the AASHTO LRFD Specifications

(AASHTO 1998). However, for the use of these code formulae it is important to consider some partial fixity of the supports to avoid overly conservative results.

2.3.4.5 Eamon and Nowak (2002)

Eamon and Nowak (2002) investigated how edge stiffening secondary elements effect the load distribution in bridges. The specific secondary elements that were investigated by this study included barriers, sidewalks, and diaphragms. Only two-lane highway bridges with composite steel and prestressed concrete girders were considered and FEA was used to develop the models of these bridges. During the elastic range of deformations, these types of edge stiffening secondary elements were shown to reduce the girder distribution factors by 10 to 40%, while for the inelastic range the reductions tended to be one-half as large being only 5 to 20%. Barriers and sidewalks carried some of the load that would have been otherwise distributed to interior girders, while it was observed that diaphragms have the effect of lowering the differences between girder deflections across a bridge deck. This resulted in more even load distributions by essentially pulling down the exterior girders and raising interior girders.

2.3.4.6 Sotelino et al. (2004)

Sotelino et al. (2004) conducted a study to develop a simplified equation based on the AASHTO LRFD Bridge Design Specifications (AASHTO 1998) load distribution formula that can be used easily in design and does not require an iterative procedure. Although the equations presented by Zokaie et al. (1991) are more accurate and consistently conservative than the previous *S/D* equations, they still have their limitations and drawbacks. Due to the fact that Zokaie's equations include a longitudinal stiffness parameter, these LDF formulae are much more difficult to use during design than analysis due to the fact that the stiffness parameters may not yet be known. In addition to this main goal, the project also focused on other potential flaws in Zokaie's equations. These additional objectives included investigating the effects of several bridge features that were not included in the AASHTO (1998) LDF equations, such as cross bracing diaphragms, parapets, and deck cracking.

The project successfully developed a new simplified load distribution equation for design. After analyzing 43 steel girder bridges and 17 prestressed concrete girder bridges with a finite element model and with the AASHTO (1998) LDF equations and the new simplified equation, the results were compared. It was determined by Sotelino et al. (2004) that the proposed equations always returned more conservative values than the FEA and was also typically more conservative than the AASHTO equations, thus giving an appropriate simplified design equation for LDFs. The study also found that the use of secondary elements such as cross bracing diaphragms and parapets could reduce the LDF found by the AASHTO (1998) equations by up to 40%. However, longitudinal cracking was shown to increase the AASHTO (1998) LDFs by up to 17%, while transverse cracks did not seem to affect the load distribution. The range of application for Sotelino's simplified formula is shown in Table 2.7. In addition to the range of application of these parameters, it was shown that the simplified formula works best if the longitudinal stiffness parameter, K_g, is less than $189940e^{\left(\frac{L}{59}\right)}$ in^4. The actual proposed wheel load distribution equation for concrete slab on steel girder bridges is shown in Table 2.8 and is compared to the current AASHTO LRFD LDFs as well as the previous *S/D* method.

Table 2.7 Range of Application for Simplified LDF Formula for Concrete Slab on Steel Girder Bridges (Sotelino et al. 2004)

Parameters	Girder Spacing: S, ft (mm)	Span Length: L, ft (mm)	Slab Thickness: t_s, in (mm)	Skew Angle (θ, degree)
Applicable Range	4 - 10 (1220 - 3050)	44 – 122 (13400 – 37200)	8 (200)	0 - 45

Table 2.8 Simplified LDF Equations for Concrete Slab on Steel Girder Bridges (Sotelino et al. 2004)

Specification	Basic LDF Formula	Skew correction factor
AASHTO Standard	$\frac{S}{5.5}$	N/A
AASHTO LRFD	$0.15+\left(\frac{S}{3}\right)^{0.6}\left(\frac{S}{L}\right)^{0.2}\left(\frac{K_g}{12Lt_s^3}\right)^{0.1}$	for $\theta \geq 30°$ $1-0.25\left(\frac{K_g}{12Lt_s^3}\right)^{0.25}\left(\frac{S}{L}\right)^{0.5}(\tan\theta)^{1.5}$
Simplified	$0.15+0.73\cdot\frac{S^{0.8}}{L^{0.3}}\cdot e^{\left(\frac{L}{590}\right)}$	for $\theta \geq 30°$ $1-0.59\cdot\frac{S^{0.5}}{L^{0.75}}\cdot(\tan\theta)^{1.5}\cdot e^{\left(\frac{L}{236}\right)}$

* Units of S, L, K_g, and t_s are ft, ft, in^4, and in, respectively.

2.3.4.7 Kocsis (2004)

Kocsis (2004) evaluated the AASHTO Guide Specifications (AASHTO 1994a) and AASHTO Standard Specifications (AASHTO 1996) in terms of line load and live load distribution factor requirements for I-girders. He also introduced a user-friendly software program, SECAN that more accurately predicts live load distribution factors and line load distributions. Previous studies have shown that the AASHTO (1996) line load distribution (line load distributed equally among all girders) was not accurate. Kocsis concluded that for line load distributions more accurate results could be obtained by using the SECAN software.

The analysis program SECAN was developed by comparing the results of established analytical methods and field experimental testing. The author also states that the live load distribution factors for AASHTO trucks, from the Guide Specifications for Distribution of Loads for Highway Bridges (AASHTO 1994a), provide more accurate results than those given by AASHTO Standard Specifications (AASHTO 1996). These

LDFs from the AASHTO Guide Specifications (AASHTO 1994a) are shown to be similar in accuracy to those found from SECAN, and considerably easier to use.

2.3.4.8 Puckett et al. (2005)

Puckett et al. (2005) conducted a broad study to develop new formulae for calculating LDFs. This project, similar to that of Zokaie et al. (1991), focused on a wide array of bridge types as well as several different analysis methods. The goal of project was to improve upon the current NCHRP 12-26 based equations in the AASHTO LRFD Bridge Design Specifications (AASHTO 2004). An automated process that compared the live load distribution factors from several simplified analysis methods to those calculated by a grillage analysis was used to determine which analysis methods should be considered for the project. The lever rule was investigated further as a good and simple load distribution analysis tool and was converted into equation form. This lever rule equation was then calibrated and combined with an adjusted uniform distribution method to give the final load distribution method. According to Puckett et al. (2005), this new method provides more accurate load distribution factors than those within AASHTO (2004) and without many of the restricted ranges of application.

2.3.4.9 Harris et al. (2010)

Harris et al. (2010) studied a new type of steel bridge termed the sandwich plate system (SPS), focusing on the load distribution, and evaluated how well the AASHTO LRFD Bridge Design Specification (AASHTO 2007) LDF equations worked for this new bridge system. Sandwich plate system bridges use a thin deck made from two steel face plates and a polyurethane core. This system will have a different deck stiffness as compared to typical reinforced concrete decks, which will in turn affect the results from the AASHTO (2007) LDF equations developed by Zokaie during the NCHRP 12-26 project (Zokaie et al. 1991) due to the deck stiffness parameter in these equations. After investigating this difference and its effects, Harris found that the deck stiffness differences may cause a 20% difference in the LDFs but that the AASHTO LRFD (AASHTO 2007) equations for concrete decks may be used to estimate the load

distribution factors for SPS bridges. The lever rule was also shown to be conservative for these types of bridges but was not quite as accurate as the AASHTO (2007) equations.

2.3.4.10 Harris (2010)

Harris (2010) also conducted a study assessing flexural load distribution methodologies used for analysis of stringer bridges. Potential discrepancies within several methods of load distribution factor analysis for slab-girder bridges that are investigated include relationships of member load effects, impact of boundary conditions, and effects of secondary members. The project's objective was to define what methods are most appropriate and when it is best to use them. Harris (2010) concluded that most current methodologies have similar trends as long as the internal member load effects and boundary conditions are modeled correctly and considered properly.

2.4 GRILLAGE METHOD OF ANALYSIS

2.4.1 Overview

Bridge live load distribution factors can be assessed using simple grillage or finite element models (Hueste et al. 2006b). Guidelines for developing grillage models for bridge decks are available in several journal articles (Hambly 1975; Zokaie et al. 1991) as well as multiple books and manuals (Barker and Puckett 2007; Hambly 1976; Ryall et al. 2000; Surana and Agrawal 1998). Instructions and recommendations for properly developing finite element models can also be found in a multitude of scholarly articles and books (Barker and Puckett 2007; Puckett et al. 2005; Ryall et al. 2000; Zokaie et al. 1991). A three-dimensional finite element analysis is a more computationally intensive approach that can also be calibrated with comparisons to actual measured bridge response data, but for load distribution factor calculation grillage analysis is a much simpler method that can still give reasonable results.

2.4.2 Principals of the Grillage Method

2.4.2.1 Lightfoot and Sawko (1959)

The grillage method was developed in the early days of matrix structural analysis by Lightfoot and Sawko (1959). Since that time the grillage method has become increasingly accurate and easy to use with the advancement of computational capability. The strategy behind the method is to simply divide a bridge deck into several equivalent longitudinal and transverse beams resembling a grillage. Figure 2.3 gives examples of grillage idealizations for bridge decks.

2.4.2.2 Hambly (1975)

Hambly (1975) outlines the use of the grillage method for cellular bridge decks and gives guidelines for accurately modeling many types of forces and reactions within the bridge deck. Development of the grillage mesh, as well as longitudinal bending, transverse bending, distortion, torsion, shear lag, skew, and load application are all covered by this paper.

2.4.2.3 Hambly (1976)

Hambly (1976) discusses several different types of structural bridge decks, their components and the analysis types that can be used to better understand them. Details of the grillage method of analysis are also explained. Hambly states that grillage analysis was one of the more popular computer-aided analysis methods for bridge decks at the time he wrote his book because of how accurately it can predict the bridge behavior while still being relatively easy to understand and easy to use.

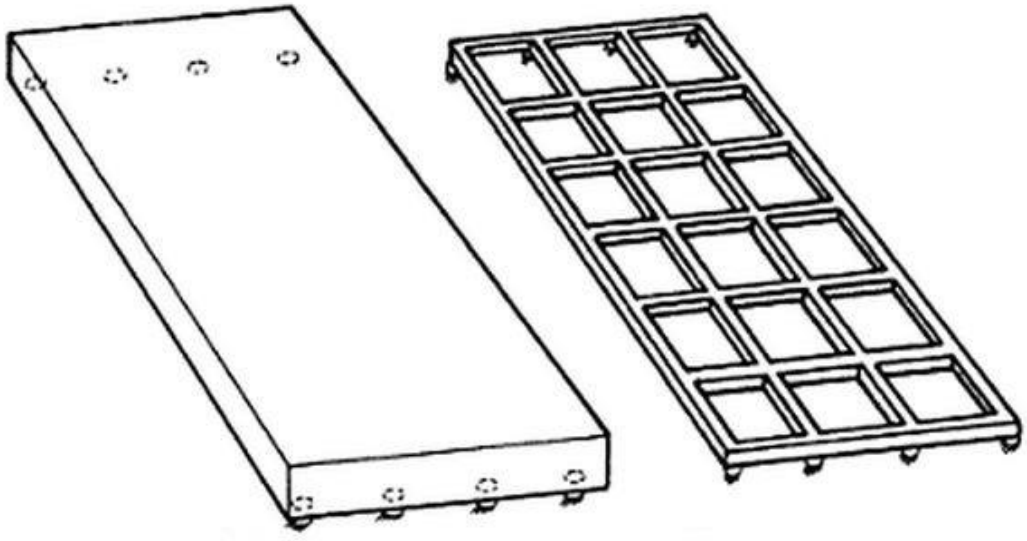

(a) Slab Bridge Deck (Hambly 1991)

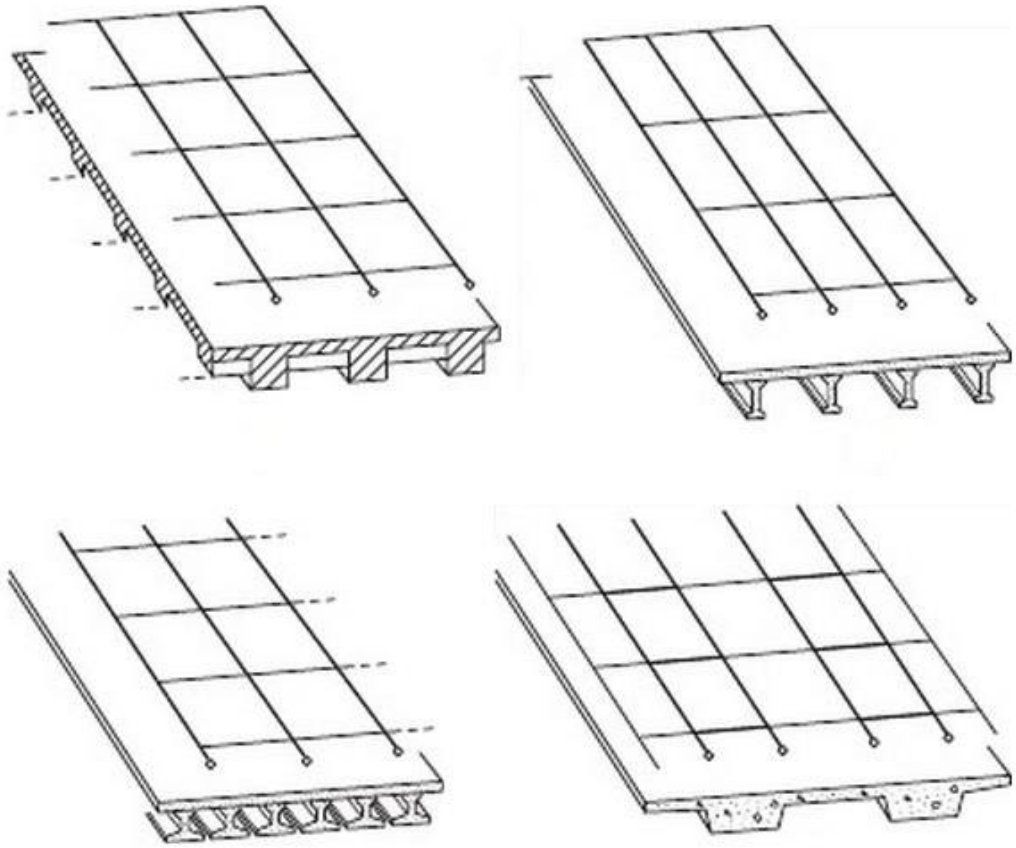

(b) Waffle, Spaced I-Girder, Adjacent I-Girder, and Solid Box Beam Bridge Decks (Parke and Hewson 2008)

Figure 2.3 Examples of Grillage Idealizations of Bridge Decks

Hambly (1976) and Barker and Puckett (2007) state that for analysis purposes, the grillage members are assigned the same bending and torsional stiffness parameters as the section of the bridge that they represent. Generally for slab-on-girder bridges, in the longitudinal direction, the grillage members coincide with the centerlines of the girders, thereby keeping those stiffness elements concentrated where they have the largest influence in the physical bridge system. Cross-beams are used at appropriate spaces to represent the deck slab. Placing grillage members at locations known to have high force and stress magnitudes, such as supports and prestressing strands, is also good practice. If the analysis is set up appropriately, the grillage model should deflect in the same fashion as the bridge deck; the portion of moments, shears, and torsions in the grillage elements should be similar to those in the section of the bridge they represent.

The grillage spacing in both directions should be similar so as to accurately model load distribution in between members. Once an appropriate grillage mesh is developed and set up with the correct parameters in a computer program, the grillage model may be loaded. Point loads and line loads are used in grillage analysis and may be placed anywhere on the grillage. Any type of static load may be applied to the bridge with equivalent point and line loads. Dynamic loading is typically dealt with as a percentage increase of the static loading so these loads may be similarly modeled by the grillage method. If the intended location of a load lies in the gap between grillage beams the load may be split to the two nearest transverse beams by use of the lever rule, so that the resultant force of the two new forces is at the same location and of the same magnitude as the originally intended load.

2.4.2.4 Surana and Agrawal (1998)

Surana and Agrawal (1998) discuss a wide array of aspects involved in the grillage method of analysis, and the bridge types it can be used with. Comparisons with several other analysis techniques including the finite element method are also explored. The grillage method and the finite element method can both be used accurately for numerous types of bridges; the finite element method can be somewhat more complex, thus more time consuming and costly to implement and run. However, despite the grillage method

being less complex, it can still be applied to complicated bridge designs, such as those that incorporate edge stiffening beams, large skew angles, and unusual support conditions.

Due to the high deck stiffness in the horizontal plane, translation displacements in the longitudinal and transverse directions will be very small and can be ignored during the grillage method of analysis. For the same reason, the horizontal rotation of the deck will also be negligible. This leaves one translation, and two rotation degrees of freedom left to be calculated by the grillage analysis. These three degrees of freedom are the vertical displacement and the rotation about the longitudinal and transverse directions. These degrees of freedom are calculated at every node of the grillage model. Nodes are automatically created at the intersection of grillage members but for increased accuracy it is recommended that additional nodes be set at closer intervals between intersections. The computer program being used to run the analysis will solve a set of simultaneous equations obtained by the loading, stiffness, and geometry properties of the bridge, to determine the displacements for the three degrees of freedom at every node. These displacements may then be used along with the grillage parameters to calculate the forces and moments in each member.

2.4.2.5 Barker and Puckett (2007)

Barker and Puckett (2007) list numerous useful equations for checking grillage section properties to ensure the grillage model is setup correctly. The torsional stiffness coefficient, *J,* is one of the most important properties for load distribution determination. This is because the twisting resistance that the members have directly effects how the beams will distribute eccentric loads throughout the bridge. Barker and Puckett (2007) state that for grillage modeling the *J* torsional constant can be calculated by summing the constants from all rectangular sub sections of the cross-sections. Two approximations for *J* of rectangular sections are also given:

$$J = \sum k_1 b h^3 \tag{2.1}$$

where:

b = Length of long side, in.

h = Length of short side, in.

k_1 = Shape factor = $\frac{1}{3}$ for thin rectangles $(b/h \to \infty)$

$$J = \frac{A^4}{40 I_p} = \frac{3b^3 h^3}{10(b^2 + h^2)} \tag{2.2}$$

where:

A = Cross-sectional area, in.^{2}

I_p = Polar moment of inertia, in.^{4} = $\frac{bh}{12}(b^2 + h^2)$

The first equation is also found in Ugural and Fenster (2011) for sections consisting of rectangular shapes. Boresi and Schmidt (2003) list this equation with a full k_1 equation:

$$k_1 = \frac{1}{3}\left[1 - \frac{192}{\pi^5}\left(\frac{h}{b}\right)\sum_{n=1,3,5,\ldots}^{\infty}\frac{1}{n^5}\tanh\left(\frac{n\pi b}{2h}\right)\right] \tag{2.3}$$

Young et al. (2012) also gives this first equation with a simplified k_1 equation that gives results with errors less than 4%:

$$k_1 = \frac{1}{3} - 0.21\frac{h}{b}\left(1 - \frac{h^4}{12b^4}\right) \tag{2.4}$$

Equation (2.2) can also be found in AASHTO (2012) as an approximation for stocky open sections such as prestressed I-beams, T-beams, and solid sections. These equations will be very important for checking the torsional constant *J* that is calculated by the computer program being used for the grillage model. The sources above state that these rectangular torsional constant equations are derived from St. Venant torsion theory. SAP2000 also calculates the torsional constant for bridge deck sections through finite-element analysis using St. Venant torsion equations (Computers and Structures 2012a). However, since SAP2000 does not have a rectangular T-section template another template will have to be altered. This could cause errors in the calculation of this

constant because other templates might utilize different torsion equations derived for that particular shape. Modifiers may be applied to the automatically calculated values given in SAP2000 to give the hand calculated values from the equations listed above and thus ensure accurate torsional stiffness.

2.4.2.6 Parke and Hewson (2008)

Parke and Hewson (2008) have written a comprehensive source of bridge engineering information covering everything from ancient bridge development to loading, analysis, dynamics, substructure systems, design, construction, monitoring, and repair of various types of modern bridges. The grillage method of analysis is covered in length with many helpful examples for developing a grillage model with a structural engineering software package. A few concerns that can arise in the grillage idealization of the slab structure are stated to ensure they are accounted for properly.

Despite the fact that the grillage method attempts to take the real bridge's properties and shape into account, it is simplifying the bridge and some aspects of the physical bridge are lost in the model. Equilibrium of all elements in the slab states that torques and twists at any location must be equal in both the longitudinal and transverse directions. The grillage model does not contain any principle to meet this criterion for locations other than grillage intersections. However, it can be shown that if the grillage mesh is fine, meaning that if the grillage members are spaced more closely, this orthogonal twisting behavior is modeled approximately as it actually is. By making the grillage mesh more fine the distance between grillage beam member intersections is reduced and therefore twisting behavior is modeled accurately in more locations. This will then ensure that the bridge will deflect in a smooth shape, rather than a wavy shape found in coarse grillage meshes. Another concern with the grillage method is that the moment in a grillage beam is proportional only to the curvature in that grillage, while in the real bridge the curvature in both directions affects the moment. Fortunately, this difference has again been shown to be negligible for a fine mesh for similar reasons.

2.4.3 Application and Verification of Grillage Method for LDF Confirmation

2.4.3.1 Zokaie et al. (1991)

Zokaie et al. (1991) recommended more complex load distribution factor equations than the early "*S*-over" equations, based on grillage and FE analysis for a wide array of bridges. The AASHTO (1994a) LRFD code then adopted these formulae to better calculate the load distribution in bridges.

Zokaie (2000) reviewed his work from the 1991 NCHRP project 12-26 to further ensure that these formulae accurately calculate the load distribution factors. To do this it was necessary to compare their output with proven methods, such as grillage analysis and FEA. In order to prove the accuracy of the FEA and grillage analysis, these methods were used to determine and compare the load distribution factors for several field bridges. These bridges were instrumented and experimentally loaded with trucks at different locations across the bridge width to determine their load distributions. Once the finite element and grillage models were calibrated based on these results and confirmed to be working correctly within their computer programs, similar grillage and finite element models were made for several "average bridges" as defined in Section 2.3.2.

The load distribution factors found for these bridges from the grillage and finite element methods were then compared to the distribution factors given by the new AASHTO LRFD (AASHTO 1998) equations. In addition to this comparison, the parameters that were found to have the most impact on the load distribution were investigated to ensure they were accounted for in the equations. It was concluded that the formulae were generally quite accurate, often giving load distributions within 5% of FEM results. The grillage analysis results were also often close to those found from the FEM analysis. For cases when the formulae could not be applied it was recommended that a finite element or grillage model be made to determine the load distribution factors.

2.4.3.2 Schwarz and Laman (2001)

Schwarz and Laman (2001) used the grillage method to model three test bridges and predict the live load distribution factors in each. These values were then compared to

experimental data from each bridge under static and dynamic truck loading, as well as the calculated load distribution and dynamic impact from AASHTO Standard Specifications (AASHTO 1996) and AASHTO LRFD Specifications (AASHTO 1998) equations. The grillage models tested a few different grillage characteristics to see what aspects were most effective in attaining the true nature of a bridge. For instance, their Bridges 2 and 3 were each modeled with and without a midspan diaphragm (which was present in both test bridges). Meanwhile, the small skew of Bridge 2 resulted in the diaphragm being set perpendicular to the longitudinal direction, while the large skew in Bridge 3 caused the diaphragm to be modeled perpendicular to the girders (skewed from the longitudinal direction).

It was found that the AASHTO LRFD Specifications (AASHTO 1998) and the AASHTO Standard Specifications (AASHTO 1996) equations for girder distribution factors gave higher values than the distribution factors measured from the experiment. However, the grillage model closely predicted the transverse load distribution observed by the experimental loading of the bridges. It was also shown that for shorter spans, ignoring the diaphragms in the grillage modeling provided more accurate results.

2.4.3.3 Hueste et al. (2006)

Hueste et al. (2006) investigated the TxDOT bridge design changes that would occur by switching from the AASHTO Standard Specifications for Highway Bridges (AASHTO 1996) to the AASHTO LRFD Bridge Design Specifications (AASHTO 2004). During a parametric study, the grillage analysis technique was used to assess the accuracy of the live load distribution factors found by the AASHTO LRFD (AASHTO 2004) equations. The bridges analyzed for this project had maximum spans over the 140 ft limit for the load distribution factor equations. These equations were still used despite exceeding this formula limit, but to determine if the equations were still accurately predicting the load distribution, grillage models were developed and calibrated for each of these bridges. Detailed development and calibration information about each model, completed using the program SAP2000, is included in the report.

From the equations and the grillage analysis, the critical locations for placing the HL-93 design truck were found. Load distribution results for one and two or more lanes loaded were also taken into consideration by both the grillage method and the AASHTO LRFD Specifications (AASHTO 2004). It was concluded that the LRFD distribution factor formulas were conservative, in some cases very conservative; however it was recommended that grillage results be confirmed by an even higher method of analysis such as FEA.

2.4.4 Use of Grillage Method for Other Verification Purposes

Srinivas and Ramanjaneyulu (2007) utilized the grillage method of analysis to accurately determine the structural response and deflections of a test bridge, in order to train an artificial neural network to be able to predict this data on its own. Details about the grillage methodology and how the analysis was performed for this research are provided. The grillage model was calibrated to give very accurate results. The model was loaded many times while the artificial neural network took note of the model's reactions so that after learning its behavior the neural network would eventually be able to predict the reactions from the loading on its own.

Kaveh and Talatahari (2010) attempted to use a computer algorithm to optimize the inputs and the use of the grillage method of analysis for bridge decks. Both steel and concrete girders were investigated and their behavior under loads influenced the degrees of freedom used at the joints and the way the bridge was split into grillages. A large focus of the project was to ensure accurate calculation of cross-sectional properties of both the longitudinal and transverse grillages, as these values have a strong influence on the end result. Examples of using the optimized grillage method to analyze two bridges and then compare the results to previous solutions of other advanced heuristic methods were shown in the paper. It is concluded by the authors that warping is a very important effect to take into account in grillage models and that the charged system search developed in this project performs very well for most cases.

3. GRILLAGE DEVELOPMENT

3.1 INTRODUCITON

The load distribution factor equations given by the LRFD Specifications (AASHTO 2012) pertain only to certain types of bridges and under certain parametric constraints. This method is also known to be a conservative approximation of the load distribution among girders rather than a rigorous computation of the actual values. Since there is currently no load distribution factor formulae for slab bream bridges, equations for similar bridge types may be used as a very general approximation or else the bridges must be modeled by a computer program. Modeling of these bridges will take much more time than using other equations but if the modeling is done correctly it will produce far more accurate and defendable load distributions than assuming the bridge acts similarly to another bridge type.

Several degrees of modeling for the Riverside experimental bridge were explored and compared to one another and to the results given by LDF equations intended for other bridge types. The most basic type of modeling was the grillage method of analysis. As stated in Section 2.3.4, grillage analysis is a method used for bridge superstructures that assumes the deck and girders to be made up of a mesh of beam elements, dramatically reducing the number of degrees of freedom within the bridge system and simplifying the bridge mechanics. These simplifications also decrease the time required to model a bridge and if done correctly may still return reasonable and conservative results at a fraction of the effort involved in finite element modeling.

The level of accuracy given by the grillage method will be determined by its comparison to finite element models using frame, shell, and solid elements, as well as experimental results. Grillage models may be easily calibrated to these more precise methods by changing beam element parameters or support conditions, or loading arrangement. Once calibrated for one bridge, the same parameter assumptions and modeling techniques should be able to be used to create a model of another bridge of a similar geometry while maintaining the calibrated accuracy.

This section discusses the development of an equivalent grillage model of the Riverside experimental bridge. A similar technique was used on the Drehersville, Pennsylvania bridge and the Denison, Texas bridge. The steps used to calibrate and verify the load distribution accuracy of these models will be discussed in Section 4. Final grillage assumptions and techniques will be stated in the following sections and recommendations will be made for correctly constructing grillage models for load distribution calculation for similar bridge types.

3.2 PROBLEM STATEMENT

The transverse load distribution amongst girders is a very important aspect of bridge behavior for both design and analysis. This complex relationship has been studied rigorously for many bridge types. But for those that are not as commonly used, specifically spread slab beam bridges, can a simplified analysis method such as the grillage analogy be used effectively to determine load distribution factors?

3.3 GRILLAGE MODEL DEVELOPMENT

3.3.1 General

This section discusses the procedure for creating a computerized equivalent grillage model of the physical Riverside experimental bridge. Calculations of the grid member properties will be presented. The grillage modeling techniques used are based on guidelines found in literature and described in Section 2.3.4. SAP2000 Version 15 (Computers and Structures (2012b)) was used to build and analyze this model.

3.3.2 Grillage Model Geometry

The Riverside experimental bridge is 34 ft wide and 50 ft long. However, the center-to-center longitudinal distance between the supports is 48’-7”. This is the length that will be used for modeling purposes. There are four 5SB15 prestressed concrete slab beam girders equally spaced at 9’-8” center-to-center, with the external girders located at the very edges of the bridge. The 5SB15 slab beams are 5 ft wide and 15 in. deep, with two

rows of prestressing strands near the bottom of the beam. Resting on the girders and spanning the spaces in between the girders are 5 ft wide, 4 in. thick transversely prestressed concrete panels (PCPs). The girders have a specified 28 day strength of 8.5 ksi, while the PCPs are specified as 5 ksi. The deck is made up of 4 ksi cast-in-place (CIP) reinforced concrete and is 10 in. thick over the girders and 6 in. thick over the PCPs. The bridge plan view and transverse section are shown in Figure 1.4.

The location of the four longitudinal grillage members was taken to be the centerline of the four slab beam girders. This is the typical strategy for grillage modeling and it is especially helpful to use this longitudinal grillage member arrangement for load distribution calculation. This is because each longitudinal grillage member will represent one girder and therefore the moments and shears in these members may be taken directly for load distribution calculations. The spacing of these longitudinal beams is the center-to-center spacing between girders, 9'-8". As a rule of thumb the spacing in both directions should be somewhat similar. The reasons for this involve load application and distribution, and to keep roughly the same mesh fineness, and therefore precision, in both directions. A transverse grillage spacing of 6'-0.875" was chosen because the longitudinal spacing was fairly high and this would split the model into nine equally spaced transverse grillage members. Figure 3.1 shows the grillage beam elements spaced as stated above.

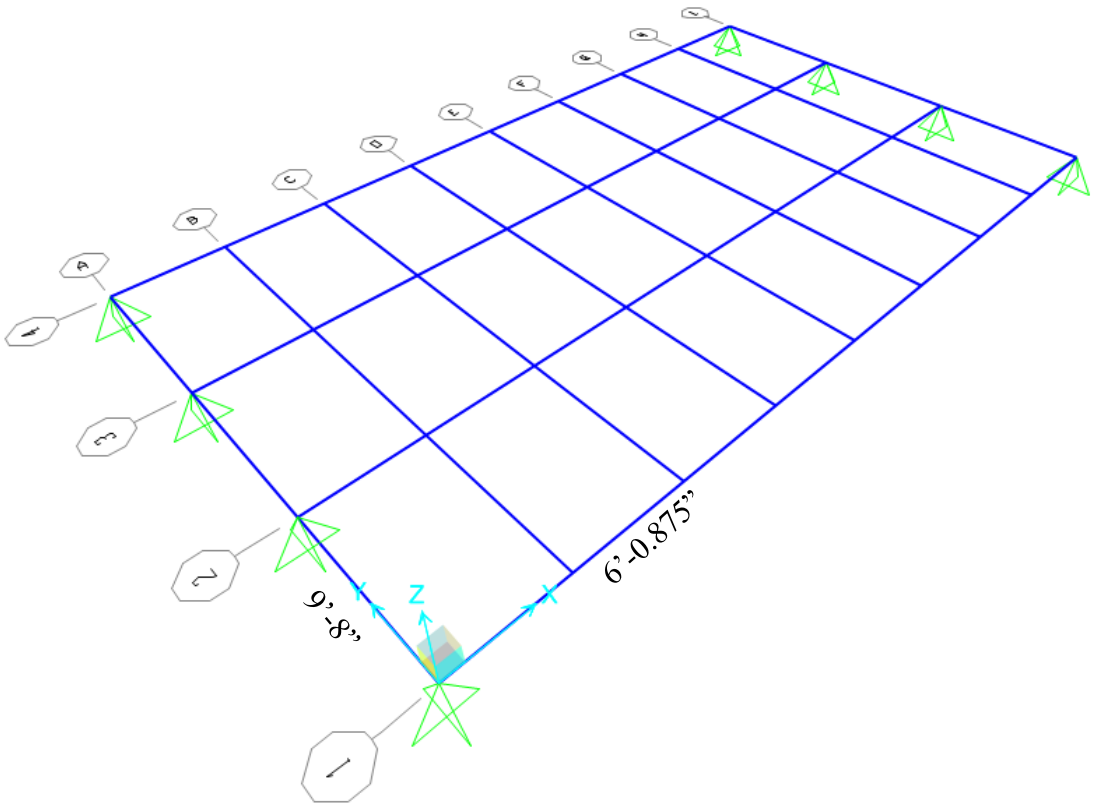

Figure 3.1 Evenly Spaced Riverside Experimental Bridge Grillage Model

3.3.3 Grillage Member Properties and Support Restraints

The two most important member properties for grillage modeling are the torsional stiffness and the bending stiffness. These properties will greatly affect the load sharing for each member and will therefore also greatly affect the load distribution factors given by the model. Torsional stiffness depends on the parameters of member length, *L*, shear modulus of elasticity, *G*, and torsional moment of inertial (or torsional constant), *J*. Bending stiffness relies on member length, *L*, bending modulus of elasticity, *E*, and bending moment of inertia, *I*. SAP2000 automatically determines the member length from the model's nodal coordinates and the modulus of elasticity value is found based on the specified concrete material properties. A default Poison's ratio of 0.2 was used for all concrete in the model, and this is used to compute the shear modulus from the bending modulus.

The torsional and bending moments of inertia are automatically calculated by SAP2000 based on the member's cross-sectional dimensions. All members used in all grillage models made were composed of a rectangular cross-sections or a combination of rectangular shapes so the calculation of a member's bending moment of inertia is very basic and was verified to be correctly calculated by SAP2000. The torsional moment of inertia is a complex parameter that has different equations for different types of cross-sections. SAP2000 uses equations derived from St. Venant torsion equations that are specific to a member type's cross-section (Computers and Structures 2012a). However, SAP2000 does not have a template for a concrete T-shape (the longitudinal members are T's because of the wider deck on top of the beams) so an I-beam shape had to be modified to create the correct cross-section. Due to this template modification SAP2000 was shown to be incorrectly computing the torsional moment of inertia, *J*, for the longitudinal members.

Section 2.4.2 discusses in detail the equations that should be used for the correct calculation of the parameter *J*. Equations (2.1) and (2.2) give almost identical answers, but for bridge parameter calculation AASHTO (2012) should be referenced. The AASHTO LRFD Specifications commentary C.4.6.2.2.1 states that the St. Venant torsional inertia, *J*, may be determined as:

- For thin walled open beams:

$$J = \frac{1}{3}\sum bt^3 \tag{3.1}$$

- For stocky open sections, e.g., prestressed I-beams, T-beams, etc., and solid sections:

$$J = \frac{A^4}{40I_p} \tag{3.2}$$

- For closed thin-walled shapes:

$$J = \frac{A_o^2}{\sum \frac{s}{t}} \tag{3.3}$$

where:

b = Width of beam element, in.

t = Thickness of beam element, in.

A = Area of cross-section, in.^{2}

I_p = Polar moment of inertia, in.^{4}

A_o = Area enclosed by centerlines of elements, in.^{2}

s = Length of a side element, in.

Because the deck portion of the superstructure is present in both the transverse and longitudinal directions it is important to not overcompensate for the torsional stiffness and count it fully in both portions. The deck's torsional constant is therefore cut in half (Parke and Hewson 2008). To do this, Equation (3.1) must be used because this equation calculates the torsional constants from each rectangular section and then sums them. The bending moment of inertia does not need to be similarly cut in half as this parameter only affects one primary direction. To adjust the SAP2000 values to the desired hand calculated values, property modifiers that are multiplied by the SAP2000 values were applied to the members for the properties being altered.

3.3.3.1 Longitudinal Members

The four longitudinal grillage members are modeled as concrete T-beams composed of the bridge deck and slab beam girders. Due to the placement of the outside edges of the to coincide with the edge of the bridge, the tributary deck width associated with these girders is less than that associated with the interior girders. This arrangement makes these composite exterior members slightly less stiff than the interior members.

SAP2000 only allows the use of one material per member and it does not allow two members to be placed on top of one another. This is an issue for bridge superstructures like the Riverside experimental bridge because it utilizes three different strength concretes. To account for the correct strength and cross-section in the model, the PCPs were conservatively assumed to be the same material as the reinforced CIP deck. This entire 10 in. thick deck was then transformed to the strength of the precast

slab beams by factoring the effective flange width by the modular ratio, which is the ratio of the modulus of elasticity of the precast beam to that of the CIP deck. This allows for the entire cross-section to be specified in the model as one material. The transformation was shown to not have a significant effect on the torsional and bending stiffness, as shown below.

Table 3.1 gives the different torsional inertia and shear modulus values for different subsections of an interior longitudinal grillage member. The J_{kl} and J_{AASHTO} values come from Equations (2.1) and (2.2) respectively. Table 3.2 compares the untransformed and transformed *JG* values for each *J* equation. The percent difference between transformed and untransformed sections averages to be 0.5% for the two different equations. The difference between the two *J* equations is about 1%. The torsional stiffness is defined as a constant times *JG/L*. The length parameter, *L*, has been left of out of the calculations below for simplicity and because it is constant throughout the transformations.

$$\eta = \frac{E_d}{E_b} \tag{3.4}$$

$$b_{dt} = b_d \eta \rightarrow J_{dt} \approx J_d \eta \tag{3.5}$$

$$E = 2G(1+\nu) \therefore E_{dt} = \frac{E_d}{\eta} \rightarrow G_{dt} = \frac{G_d}{\eta} \tag{3.6}$$

$$J_{dt} G_{dt} \approx J_d \eta \frac{G_d}{\eta} = J_d G_d \tag{3.7}$$

Where:

η = Transformation constant

E_d = Deck modulus of elasticity, ksi

E_b = Beam modulus of elasticity, ksi

b_{dt} = Transformed deck width, in.

b_d = Tributary deck width, in.

J_{dt} = Transformed deck torsional moment of inertia (beam moment of inertia), in.^{4}

J_d = Deck torsional moment of inertia, in.^{4}

ν = Poison's ratio

E_{dt} = Transformed deck modulus of elasticity (beam modulus of elasticity), ksi

G_{dt} = Transformed deck shear modulus of elasticity (beam shear modulus of elasticity), ksi

G_d = Deck shear modulus of elasticity, ksi

Table 3.1 Torsional Inertia, *J*, and Shear Modulus, *G*, of Riverside Bridge Sections

Sub-Section	J_{kI} [in.^{4}]	J_{AASHTO} [in.^{4}]	G [ksi]
Untransformed Deck	36,567	34,543	1502
Beam	56,872	57,176	2190
Transformed Deck	24,433	23,509	2190

Table 3.2 Comparison of Untransformed and Transformed Member Torsional Stiffnesses

Section	$J_{kI}G$ [k-in.^{2}]	$J_{AASHTO}G$ [k-in.^{2}]	Difference [%]
Untransformed	179,454,222	177,079,610	1.3%
Transformed	178,025,428	176,667,876	0.8%
Difference [%]	0.8%	0.2%	-

Physical bridges like the Riverside experimental bridge may contain curbs, sidewalks, and parapets along the edges of the bridge. Depending on how these edge structures are constructed they could induce additional edge stiffening or loading. These elements could have an effect on the load distributions and exterior girder behavior and should be accounted for in modeling. However, the Riverside experimental bridge will not contain these elements as it will be in a controlled testing environment. Therefore, the models of this bridge will not contain any of these edge stiffening or loading

elements. Section 4.4 includes a discussion of edge stiffening elements for the Drehersville, Pennsylvania bridge.

The final calculated dimensions and parameters for the two exterior and two interior 5SB15 slab beams and tributary deck sections used in the model are listed in Table 3.3. All longitudinal members were meshed at every 1 ft and at every intersection with a transverse member. This allows for higher accuracy in the model and more points where all forces are calculated, rather than just the intersection points.

Table 3.3 Riverside Bridge Grillage Longitudinal Member Parameters

Parameters	**Exterior**	**Interior**
Deck Width, b_d [in.]	60.34	79.6
Deck Depth, d_d [in.]	10	10
Beam Width, b_b [in.]	60	60
Beam Depth, d_b [in.]	15	15
Concrete Strength, f'_c [ksi]	8.5	8.5
Modulus of Elasticity, E [ksi]	5255	5255
Shear Modulus, G [ksi]	3190	3190
Moment of Inertia, I [in.^{4}]	78,340	89,509
Torsional Constant, J [in.^{4}]	65,879	69,089

3.3.3.2 Transverse Members

The nine transverse grillage members are modeled simply as rectangular sections representing the 10 in. thick deck. The tributary width of each of the interior transverse members is the center-to-center spacing of the transverse grillage members, 6’-0.875”, while the end members is half that. Since there is only one material (PCPs are assumed to be the same as the deck) present in the transverse members no transformation is needed. Also because SAP2000 has a rectangular concrete section template the torsional moment of inertia, along with all other automatically calculated values, were shown to

be correct for these simple cross-sections. The torsional constant is again multiplied by 0.5 as the deck section is also present in the longitudinal members.

Although the transverse grillages in this model were fairly basic, for some bridges and certain loading cases the transverse grillage members will become very important and will need modeling adjustments. For instance when diaphragms are present in a bridge, the transverse grillage members model these elements. Section 4.4 covers the grillage modeling of diaphragms in the Drehersville, Pennsylvania bridge. As discussed further in Section 3.4, the axle loads applied to grillage models will be placed directly on the transverse members, which must correctly distribute these loads to the girders. Also, the maximum shear loading case for LDF calculation may require loads to be placed at the end transverse grillages, which have complicated response behavior due to the end supports along these members. The stiffness properties or load placement at the end transverse members may need to be adjusted to correctly model this end support and load distribution behavior.

The final calculated dimensions and parameters for the two exterior and seven interior transverse deck sections entered into the model are listed in Table 3.4. All transverse members were meshed at 1 ft and at every intersection with a longitudinal member. This was done to keep the same level of accuracy in the transverse direction as in the longitudinal direction, and to give a higher resolution for monitoring changes in the internal moments, shears, and deflections along the member lengths.

Table 3.4 Riverside Bridge Grillage Transverse Member Parameters

Parameters	Exterior	Interior
Deck Width, b_d [in.]	36.4375	72.875
Deck Depth, d_d [in.]	10	10
Strength, *f'c* [ksi]	4	4
Modulus of Elasticity, *E* [ksi]	3605	3605
Shear Modulus, *G* [ksi]	1502	1502
Moment of Inertia, *I* [in.^{4}]	3036	6073
Torsional Constant, *J* [in.^{4}]	5023	11,096

3.3.3.3 Support Restraints

There are no end diaphragms or other end stiffening elements in the Riverside experimental bridge. Supports are placed at both ends of all longitudinal members. All supports were modeled simply as pinned connections as this was determined to be the most similar condition to the actual bridge. Pinned connections fix the translation in all three directions but leave all rotations free. The actual bridge will be resting on an unusual support system that includes a set of steel bearing plates and bearing pads and a small pancake load cell in between. This is so that the end reactions may be measured during all tests, allowing for an accurate calculation of applied load and for load distribution confirmation.

3.4 APPLICATION OF LOADS

3.4.1 Overview

AASHTO LRFD Bridge Design Specifications (AASHTO 2012) Art. 3.6.1.2 states that "vehicular live loading on the roadways of bridges or incidental structures, designated as HL-93, shall consist of a combination of the design truck or design tandem, and design lane load." The tandem load is a two axle loading, spaced 4 ft apart and having point loads of 25 k at each axle. The design truck is shown in Figure 3.2 below, taken from

Figure 3.6.1.2.2-1 in AASHTO (2012), and consists of 3 axles. The first axle has a load of 8 k, while the middle and back axles are each 32 k. The spacing from the first axle to the middle is set as 14 ft and the back axle spacing can vary from 14 ft to 30 ft depending on which configuration causes the highest moments or shears in the bridge superstructure.

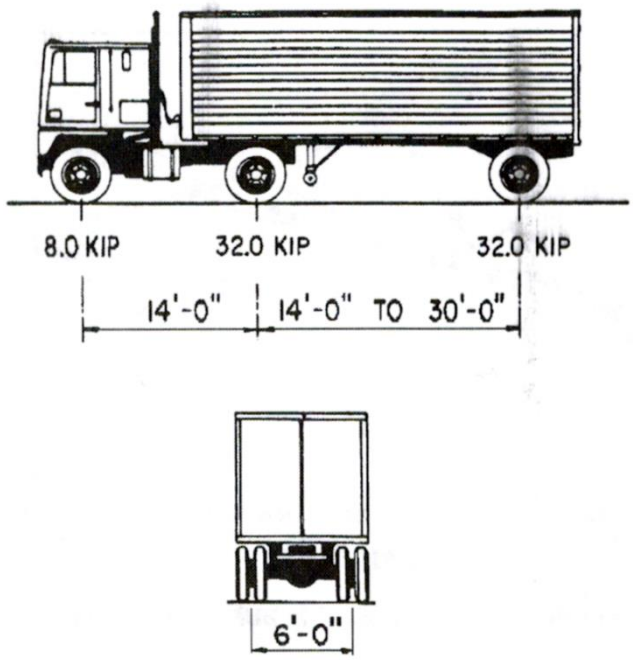

Figure 3.2 Design Truck Load Configuration (AASHTO 2012)

The loading configuration that gives the highest moments and the highest shears is used and then combined with a 0.64 k/ft uniform live load over the lane area for bridge design calculations. The maximum moments and shears acting on the Riverside experimental bridge were induced by the 3 axle design truck load when the back axle spacing was set to 14 ft. This is also the service load that will be used for modeling and experimentally testing the Riverside experimental bridge. The uniform lane live load is a part of the design criteria for this bridge but is not included in the models for LDF calculation. This is a common procedure for bridge LDF modeling and testing (Adnan 2005; Eom and Nowak 2001; Tabsh and Tabatabai 2001; Trimble et al. 2003).

3.4.2 Longitudinal Positioning

For the maximum bending moment case the resultant of the three axles is longitudinally located equidistant and opposite from the center of the bridge as the second axle. The maximum shear case was found by placing the rear 32 k axle over the support location at one end of the bridge. Both of these locations also provided the respective maximum moment and shear in the single simply supported beam that was used to determine the LDFs, which was to be expected because the loads needed to be applied in the same locations for a correct comparison.

St. Venant's shear principle states that the actual maximum shear in a bridge will be the member depth away from the end (Ugural and Fenster 2011) and that this is where the load should be placed. This is due to the way shear force acts within the cross-section and the 45 degree shear plane associated with this force. However, for load distribution factor modeling and calculation the standard procedure is to simply load the very end of the bridge so that the single beam modeling shear is greatest. This end loading also happens to be the location of the maximum shear in the FE comparison models as well. The longitudinal distance of the three truck axles for both trucks for moment and shear loading is shown by Table 3.5. Figure 3.3 depicts the maximum shear and moment loading cases.

Table 3.5 Truck Loading Longitudinal Distance from Riverside Bridge End

Loading Type	8k Axle [ft]	32k Axle [ft]	32k Axle [ft]
Moment	8.15	22.15	36.15
Shear	28	14	0

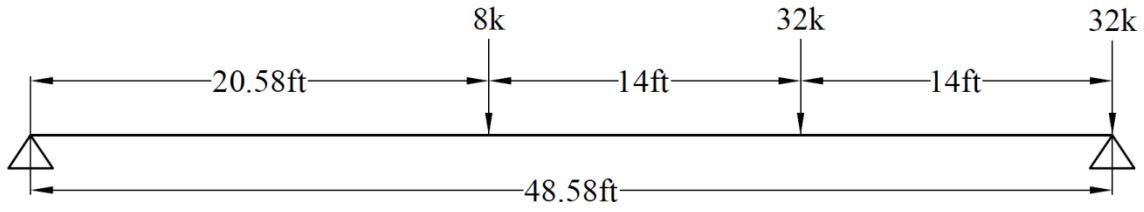

(a) Maximum Shear

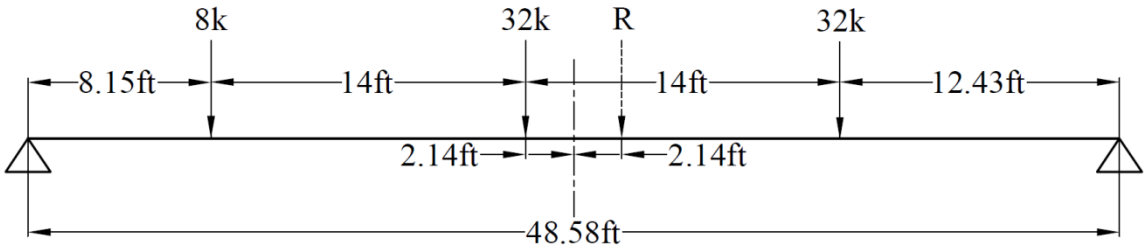

(b) Maximum Moment

Figure 3.3 Maximum Shear and Moment Longitudinal Truck Loading

3.4.3 Transverse Positioning

The critical case for bridge moments and shears is when there are two trucks both at the same longitudinal location on the bridge. In the transverse direction, loading lanes are made for the two side by side trucks, starting with the outside axle load of the outside truck being located at 3 ft away from the edge of the bridge. This distance from the edge of the bridge is specified by AASHTO (2012) Art. 3.6.1.3.1 which states that the design load shall be placed 2 ft away from the outside rail, which is assumed to be 1 ft wide and at the edge of the bridge.

The trucks axles are spaced 6 ft apart, meaning that the other half of the axle load is placed 6 ft inwards from the edge load. The specified transverse spacing between the closest axle loads of the two trucks is 4 ft. Both trucks are then moved 1 ft at a time towards the center of the bridge, until the trucks are centered on the bridge. Each 1 ft transverse movement creates another load case. For this bridge there are seven loading cases for both shear and moment, with the first one having the closest axle loading to the edge being 3 ft, and the last one being 10 ft away from the edge which transversely centers the two trucks on the bridge. The term loading case is also used interchangeably

with loading lane in this thesis as each loading case represents a different modeling lane. Table 3.6 describes the transverse truck wheel loading locations for all loading cases.

Table 3.6 Truck Loading Transverse Distance from Riverside Bridge Edge

Loading Case	Truck 1 Wheels [ft]		Truck 2 Wheels [ft]	
	Outside	Inside	Outside	Inside
1	3	9	13	19
2	4	10	14	20
3	5	11	15	21
4	6	12	16	22
5	7	13	17	23
6	8	14	18	24
7	9	15	19	25

3.4.4 Lever Rule Loading

The loading locations and magnitudes listed above describe how the experimental loading will be set up on the physical bridge, but the grillage model can only be loaded along beam member centerlines. To accomplish the same loading in the grillage model as on the physical bridge the loads that do not fall on grillage members must be distributed to the two nearest transverse grillages by use of the lever rule. When done correctly the two new loads will add up to the same magnitude as the original load and the resultant will be located at the original intended position of the load. This should simulate a very similar load situation to the physical loading, especially if the grillage mesh is sufficiently fine.

Once all loads were split up to the nearest transverse grillages there were 24 total point loads for the two trucks in the maximum moment configuration for every load case. The maximum shear configuration placed the rear axle directly on the end transverse grillage, therefore making it unnecessary to split this load to other grillage

members. This configuration resulted in a total of 20 point loads for every lane load case. Figure 3.4 shows these loading configurations for moment and shear Load Case 1 with the rear 32 k axle being on the transverse grillage A (close) side.

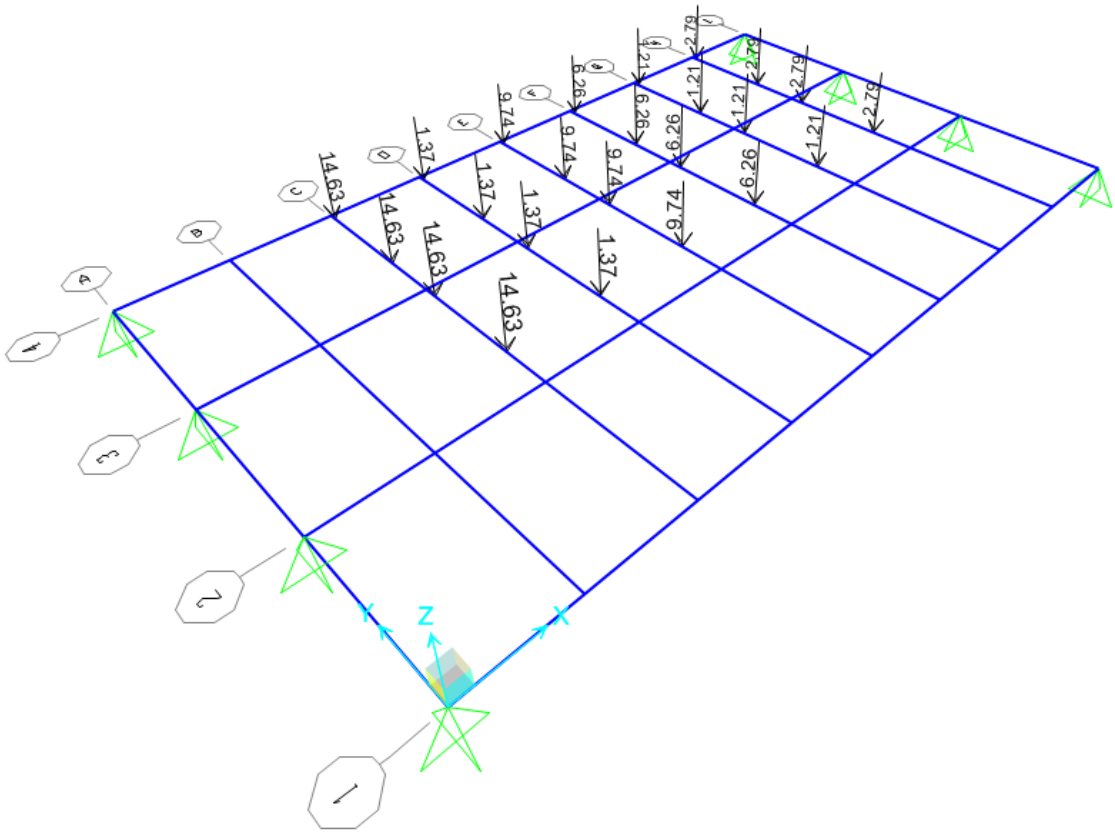

(a) Maximum Moment

Figure 3.4 Loading Case 1 Distributed Axle Loads

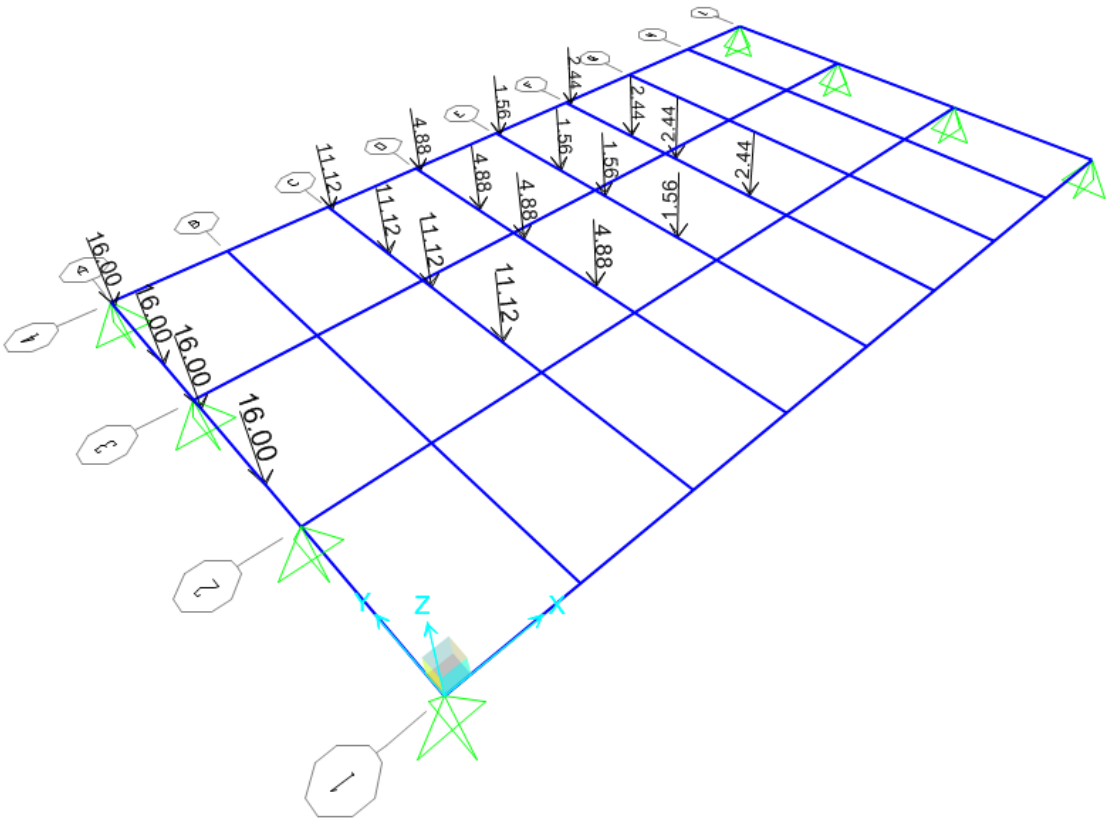

(b) Maximum Shear

Figure 3.4 (cont.)

4. GRILLAGE CALIBRATION

4.1 GENERAL

This section covers the adjustments made to the original Riverside grillage model described in Section 3 with the goal of getting better correlation of the load distributions as compared to those found by FE analysis. Seven different Riverside grillage models were developed to address errors found in the shear values and four more models were created to explore the effects of transverse grillage spacing and loading arrangement. In addition to improving the Riverside experimental bridge's grillage model, additional models were made for the Drehersville bridge, using the same assumptions and procedure as stated in Section 3 for the Riverside experimental bridge. This model was created to compare the grillage methodology with experimental testing results, to serve as a second case for finite element model (FE) comparisons and to confirm the modeling approach used for the Riverside bridge models. Finally, a second slab beam bridge, the Denison field bridge, was modeled using the grillage methodology developed above and was again compared to FE results for a third calibration case.

4.2 RIVERSIDE EXPERIMENTAL BRIDGE FINITE ELEMENT MODELS

4.2.1 Finite Element Comparisons

TxDOT Project 0-6722 includes additional research efforts beyond the scope of this thesis to develop two finite element models of the Riverside experimental bridge. These models were created in the bridge analysis program CSiBridge Version 15 (Computers and Structures (2012c)), from the developers of SAP2000. Both models were made with similar assumptions to the grillage model, such as support conditions, material strengths, section sizes and parameters, loading positions, etc. A frame and a shell element model were created to compare the differences between the two types of FE models available in CSiBridge. Shell elements are generally regarded to be the more accurate of the two. There will be no experimental data for the Riverside bridge until after the construction

and testing is completed so these FE models were used as more refined models for girder load distribution comparisons. The frame and shell element models are shown in Figure 4.1 and Figure 4.2, respectively.

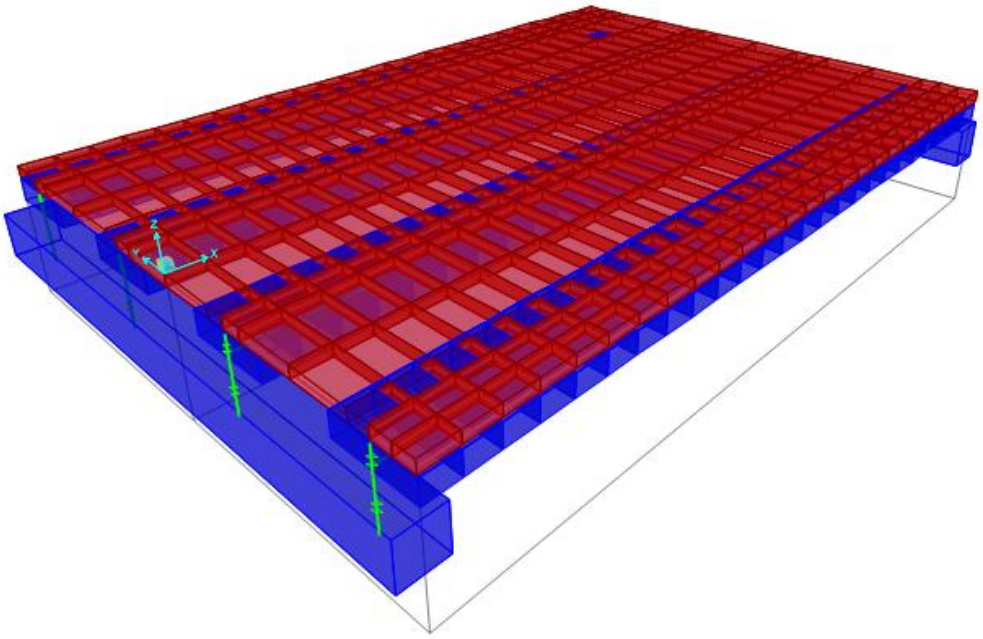

Figure 4.1 Riverside Bridge Frame Element Model (Hueste et al. 2014)

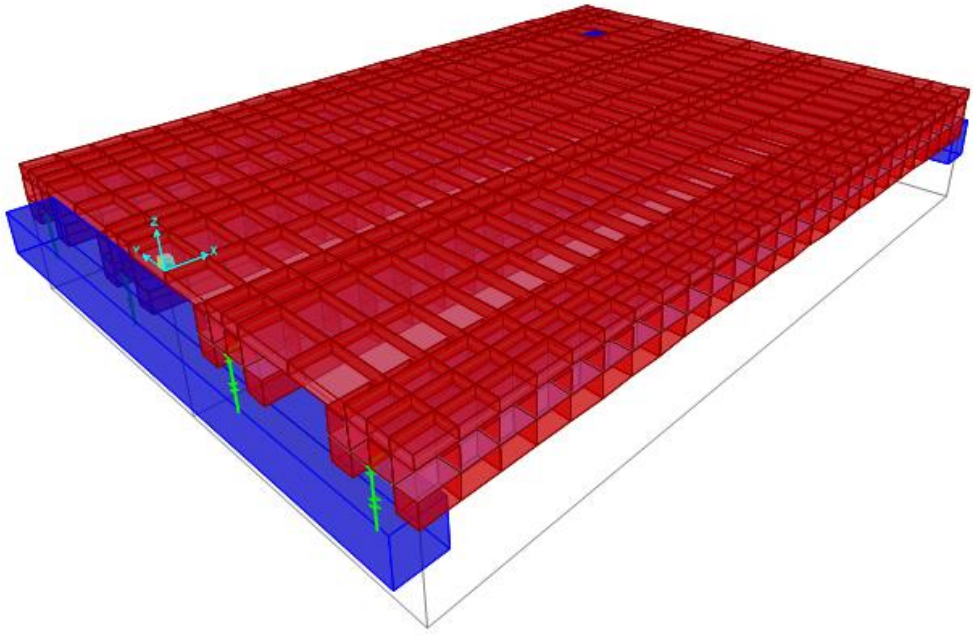

Figure 4.2 Riverside Bridge Shell Element Model (Hueste et al. 2014)

CSiBridge allows the use of a moving truck load that runs a truck over the bridge down a specified lane, statically analyzing the loading at points along the bridge span. From this analysis the shear and moment results at every finite element mesh intersection can be examined to determine the maximum shear and moment values and longitudinal loading locations. Similarly to the grillage models, a mesh spacing of 1 ft was used in both directions. For all seven transverse loading lane cases described in Table 3.6 the maximum shear occurred when the rear 32 k axle was placed directly over the bridge supports, and the maximum moment occurred when this axle was placed at 12 ft 5 in. from the support. These are the same longitudinal locations that produce the maximum shear and moment in the grillage models and in the single beam element used for LDF calculation. Verification of this observation can be found in Table 3.5.

The maximum girder moment and shear values found in each transverse lane loading case from the FE models and from the grillage model were compared to determine whether adjustment to the grillage model was necessary. Girder deflections were also investigated for additional bridge model behavior comparisons but these results were not viewed as necessary for adjusting the grillage model because there are no LDFs for deflections and additional deflection calibration may not be favorable for the shear and moment results. There are two interior and two exterior girders in the Riverside experimental bridge, but values were only recorded for the critical exterior and the interior girders nearest to the loading side. This is because these are the girders with the highest shears and moments and thus the appropriate ones to use for LDF and design calculations. Tables 4.1 through 4.6 show the initial FE comparisons.

Table 4.1 Exterior Girder Grillage vs. FE Moment Comparison

Loading Case	Exterior Girder - Moment				
	Grillage M_{max} [k-ft]	FE Frame M_{max} [k-ft]	FE Shell M_{max} [k-ft]	G/FE Ratio	
				Frame	Shell
1	387.0	372.4	397.2	1.039	0.974
2	355.3	344.4	364.2	1.032	0.976
3	324.6	315.6	329.7	1.029	0.985
4	295.5	288.9	298.0	1.023	0.992
5	267.8	262.9	265.2	1.019	1.010
6	241.1	238.5	234.7	1.011	1.027
7	215.7	214.9	205.0	1.004	1.052

Table 4.2 Interior Girder Grillage vs. FE Moment Comparison

Loading Case	Interior Girder - Moment				
	Grillage M_{max} [k-ft]	FE Frame M_{max} [k-ft]	FE Shell M_{max} [k-ft]	G/FE Ratio	
				Frame	Shell
1	413.6	401.6	429.7	1.030	0.963
2	410.7	396.8	426.2	1.035	0.964
3	406.3	392.4	423.5	1.035	0.959
4	400.3	385.3	416.0	1.039	0.962
5	392.2	377.1	408.8	1.040	0.959
6	382.0	365.9	397.0	1.044	0.962
7	369.8	353.8	383.7	1.045	0.964

Table 4.3 Exterior Girder Grillage vs. FE Shear Comparison

Loading Case	Exterior Girder - Shear				
	Grillage V_{max} [k]	FE Frame V_{max} [k]	FE Shell V_{max} [k]	G/FE Ratio	
				Frame	Shell
1	35.9	36.2	35.8	0.991	1.002
2	29.8	32	31.5	0.930	0.945
3	24.1	27.6	27.0	0.875	0.894
4	19.1	23.5	22.9	0.811	0.833
5	14.6	19.2	18.2	0.762	0.804
6	10.8	15.5	14.1	0.694	0.762
7	7.4	11.8	10.2	0.630	0.728

Table 4.4 Interior Girder Grillage vs. FE Shear Comparison

Loading Case	Interior Girder - Shear				
	Grillage V_{max} [k]	FE Frame V_{max} [k]	FE Shell V_{max} [k]	G/FE Ratio	
				Frame	Shell
1	56.6	47.8	49.1	1.185	1.154
2	57.5	47.7	49.1	1.206	1.172
3	57.7	47.9	49.4	1.204	1.167
4	57.2	47.3	48.5	1.208	1.178
5	55.8	46.6	48.0	1.197	1.163
6	53.6	45	46.6	1.191	1.150
7	50.7	43.3	44.9	1.172	1.130

Table 4.5 Exterior Girder Grillage vs. FE Deflection Comparison

Loading Case	Exterior Girder - Deflection				
	Grillage δ_{max} [in]	FE Frame δ_{max} [in]	FE Shell δ_{max} [in]	G/FE Ratio	
				Frame	Shell
1	0.382	0.400	0.330	0.956	1.158
2	0.350	0.369	0.306	0.948	1.143
3	0.319	0.337	0.283	0.946	1.126
4	0.289	0.308	0.262	0.940	1.104
5	0.261	0.280	0.241	0.933	1.084
6	0.235	0.252	0.220	0.931	1.066
7	0.209	0.225	0.200	0.929	1.046

Table 4.6 Interior Girder Grillage vs. FE Deflection Comparison

Loading Case	Interior Girder - Deflection				
	Grillage δ_{max} [in]	FE Frame δ_{max} [in]	FE Shell δ_{max} [in]	G/FE Ratio	
				Frame	Shell
1	0.358	0.365	0.290	0.981	1.235
2	0.356	0.360	0.287	0.990	1.242
3	0.353	0.356	0.283	0.992	1.247
4	0.348	0.350	0.278	0.994	1.252
5	0.341	0.340	0.273	1.003	1.249
6	0.332	0.332	0.260	1.000	1.278
7	0.322	0.322	0.257	1.001	1.253

The grillage moment distribution between girders was shown to be very similar to that of the FE models (see Tables 4.1 and 4.2). Due to the close correlation of the results (within five percent), and the fact that two different models will never give exactly the same results, it is presumed that the grillage modeling techniques and

assumptions used in the moment modeling are appropriate. The accuracy of the moment results is more easily compared in a graphical format as shown by Figure 4.3. It is interesting to note that the grillage moments tend to fall between those for the two FE models.

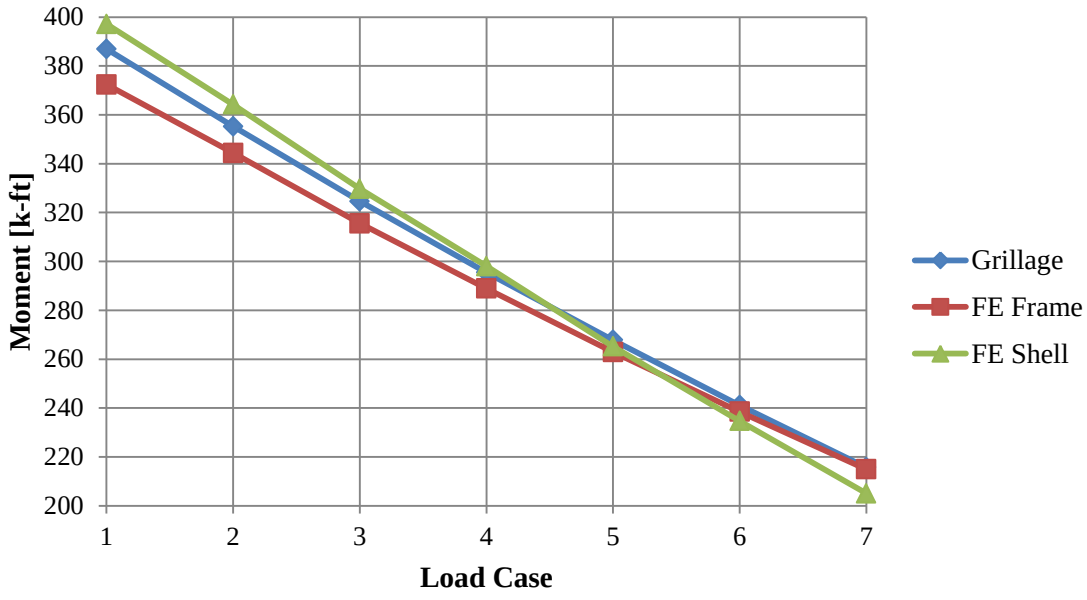

(a) Exterior Girder

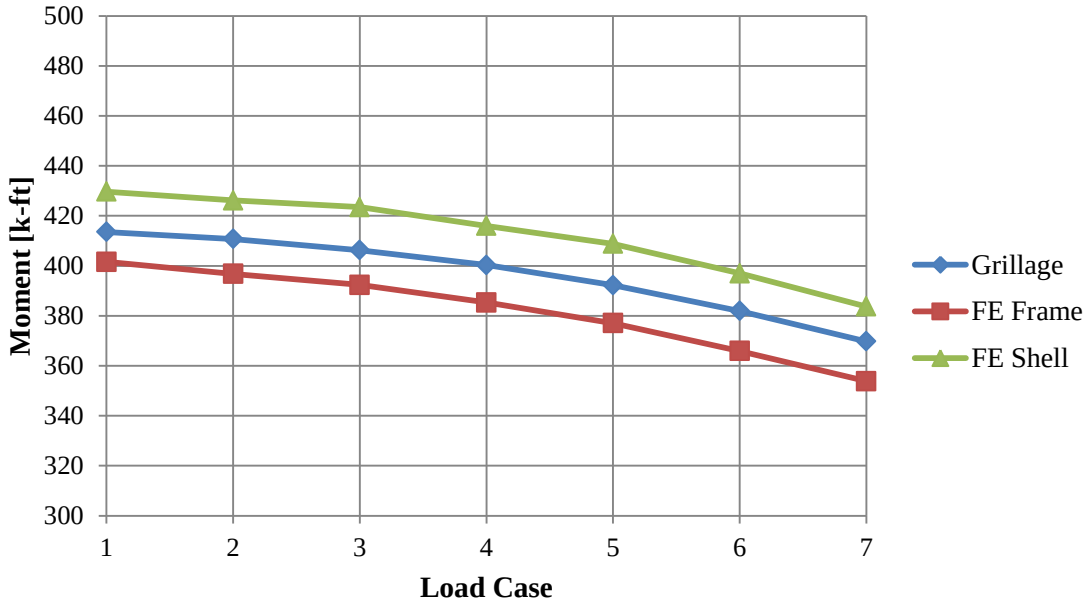

(b) Interior Girder

Figure 4.3 Riverside Experimental Bridge Moment Comparison

The moment results match relatively well. However, the shear comparisons (see Tables 4.3 and 4.4) show that the grillage model gives very high shears in the interior girder (up to 21 percent higher) and very low shears in the exterior girder (up to 37 percent lower) when compared to the FE models. Additional adjustment to the model seems necessary to improve these initial girder shear distributions.

The deflection results were investigated for supplemental model comparison and to ensure that the variability in their results as compared to the FE models is not excessive. It was found that the deflection results from the grillage model are within 10% of the frame FE model and within 30% of the shear FE model. No further adjustment is deemed necessary with respect to deflections since the distribution factors are for used on beam moments and shears.

4.2.2 Grillage Spacing Altered for Loading

The grillage model described above contained equally spaced transverse grillage members, as recommended by relevant literature. However, this caused axle point loads to be manually distributed to the two nearest transverse grillages if they did not fall directly on a grillage member centerline in the model. The effect of this manual load distribution to grillage members should be minimal, but to test how much it was impacting the results and to see if it was responsible for the shear errors, two more grillage models were created.

The two new models were made identically to the original model but had altered transverse grillage spacing from the evenly spaced version. One model spaced the transverse members so that the maximum moment loading case point loads would directly align with the members. The other was spaced for the shear loading. Both of the new loading spaced models contained eight transverse members, as compared to the nine members in the evenly spaced model, so the spacing was still very similar.

The inconvenience with this way of modeling maximum shear and moment values is that two separate models are required, making the creation of the models more time intensive. However, because these models are spaced for the specific loading cases, fewer point loads are required and the axle loads do not need to be manually distributed

to the nearest grillages, making the application of loads to these models less time intensive. Figure 4.4 shows the lane 1 loading case of the moment spaced grillage model while Figure 4.5 displays the lane 1 loading of the shear spaced model. These figures can be compared with Figure 3.4 for the evenly spaced grillage model.

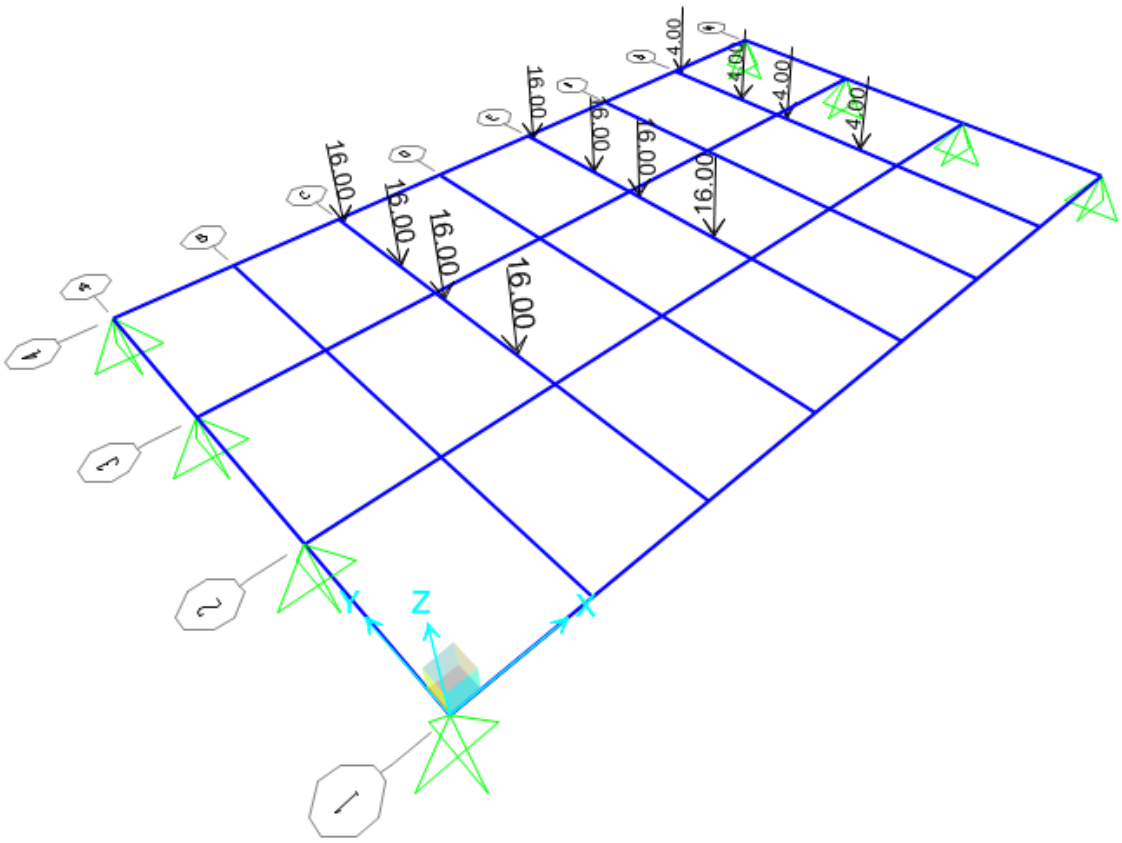

Figure 4.4 Moment Spaced Grillage Model Loading Case 1

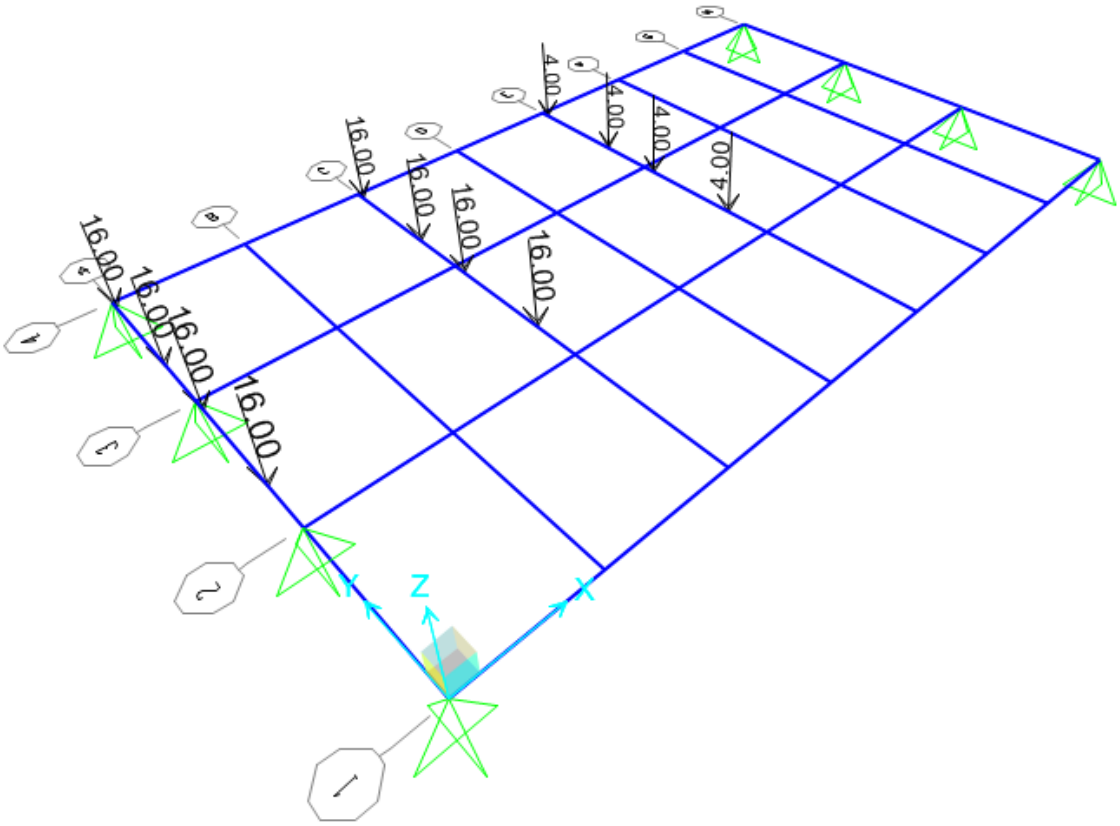

Figure 4.5 Shear Spaced Grillage Model Loading Case 1

The moment and shear results from these loading spaced models are shown in Table 4.7 through Table 4.10 and compared to the FE values. It can be seen that these results are very similar to the evenly spaced grillage results presented in Table 4.1 through Table 4.4 with the moment values being slightly farther away from the FE models and the shear results still having a great deal of error. This indicates that the transverse grillage member spacing is not the cause of the shear errors and that manually distributing the axle loads that do not fall on a grillage centerline does not decrease accuracy. Deflection results also show a very high correlation between the two grillage models and have again been helpful for comparison but have been neglected for calibration. Additional steps to improve shear results are discussed in the following section.

Table 4.7 Exterior Girder Loading Spaced Grillage vs. FE Moment

Loading Case	Exterior Girder - Moment				
	Grillage M_{max} [k-ft]	FE Frame M_{max} [k-ft]	FE Shell M_{max} [k-ft]	G/FE Ratio	
				Frame	Shell
1	397.2	372.4	397.2	1.066	1.000
2	364.0	344.4	364.2	1.057	0.999
3	331.9	315.6	329.7	1.052	1.007
4	301.5	288.9	298.0	1.043	1.012
5	272.7	262.9	265.2	1.037	1.028
6	244.8	238.5	234.7	1.027	1.043
7	218.4	214.9	205.0	1.016	1.065

Table 4.8 Interior Girder Loading Spaced Grillage vs. FE Moment

Loading Case	Interior Girder - Moment				
	Grillage M_{max} [k-ft]	FE Frame M_{max} [k-ft]	FE Shell M_{max} [k-ft]	G/FE Ratio	
				Frame	Shell
1	431.4	401.6	429.7	1.074	1.004
2	428.7	396.8	426.2	1.080	1.006
3	424.3	392.4	423.5	1.081	1.002
4	418.5	385.3	416.0	1.086	1.006
5	410.2	377.1	408.8	1.088	1.003
6	399.2	365.9	397.0	1.091	1.006
7	386.0	353.8	383.7	1.091	1.006

Table 4.9 Exterior Girder Loading Spaced Grillage vs. FE Shear

Loading Case	Exterior Girder - Shear				
	Grillage V_{max} [k]	FE Frame V_{max} [k]	FE Shell V_{max} [k]	G/FE Ratio	
				Frame	Shell
1	35.9	36.2	35.8	0.990	1.001
2	29.7	32	31.5	0.929	0.944
3	24.1	27.6	27.0	0.874	0.893
4	19.1	23.5	22.9	0.811	0.832
5	14.6	19.2	18.2	0.761	0.803
6	10.7	15.5	14.1	0.693	0.762
7	7.4	11.8	10.2	0.629	0.727

Table 4.10 Interior Girder Loading Spaced Grillage vs. FE Shear

Loading Case	Interior Girder - Shear				
	Grillage V_{max} [k]	FE Frame V_{max} [k]	FE Shell V_{max} [k]	G/FE Ratio	
				Frame	Shell
1	56.6	47.8	49.1	1.185	1.153
2	57.5	47.7	49.1	1.206	1.172
3	57.7	47.9	49.4	1.204	1.168
4	57.2	47.3	48.5	1.208	1.179
5	55.8	46.6	48.0	1.198	1.163
6	53.6	45	46.6	1.192	1.151
7	50.8	43.3	44.9	1.172	1.130

Table 4.11 Exterior Girder Loading Spaced Grillage vs. FE Deflection

Loading Case	Exterior Girder - Deflection				
	Grillage δ_{max} [in.]	FE Frame δ_{max} [in.]	FE Shell δ_{max} [in.]	G/FE Ratio	
				Frame	Shell
1	0.387	0.400	0.330	0.968	1.173
2	0.355	0.369	0.306	0.961	1.158
3	0.323	0.337	0.283	0.959	1.142
4	0.293	0.308	0.262	0.954	1.120
5	0.265	0.280	0.241	0.948	1.101
6	0.238	0.252	0.220	0.946	1.083
7	0.213	0.225	0.200	0.945	1.063

Table 4.12 Interior Girder Loading Spaced Grillage vs. FE Deflection

Loading Case	Interior Girder - Deflection				
	Grillage δ_{max} [in.]	FE Frame δ_{max} [in.]	FE Shell δ_{max} [in.]	G/FE Ratio	
				Frame	Shell
1	0.363	0.365	0.290	0.994	1.251
2	0.361	0.360	0.287	1.002	1.257
3	0.357	0.356	0.283	1.004	1.263
4	0.352	0.350	0.278	1.007	1.268
5	0.345	0.340	0.273	1.016	1.265
6	0.337	0.332	0.260	1.013	1.295
7	0.326	0.322	0.257	1.014	1.268

4.2.3 Modifications to Model for Shear Distribution

There are several possible reasons that the shear distribution is not modeled accurately by the grillage analysis. Due to the nature of the maximum shear loading case, the entire rear 32 k axle of each truck is placed on the very end transverse grillage member.

Because this loading in the model takes place a longitudinal distance of 0 ft, or directly over the support, the loading is being transferred to the supports under the girder ends rather than to the girders. This caused the internal shear in the girders as calculated by SAP2000 to be much lower than the actual maximum values, so to find the actual maximum end shears the end reactions were used. This led to some inaccuracies with the shear distribution between girders.

The rear axle loading for the maximum shear case is meant to be applied only at a distance of 0 ft from the bridge end, but because the end transverse member is 3 ft 0.4375 in. wide it may be too flexurally or torsionally stiff. This could cause the end member to distribute the loads differently compared to a real bridge. To correct the end transverse stiffness and allow the model to distribute the loads simply to the closest girders by relative distance several model changes were tested on the shear loading spaced grillage model. Table 4.13 lists the grillage alterations attempted and the average improvement of their results over the seven shear loading cases as compared to the original shear results listed in Tables 4.3 and 4.4. The detailed results of all modifications made can be found in Appendix A. The two modifications that were the most successful in correcting the shear modeling of the grillage models are described in additional detail below.

Table 4.13 Grillage Shear Modifications and Improvements

Mod. No.	Modification	Improvement
1	*I* of both end transverse members was set to 0	~5%
2	*I* of loaded end transverse member was set to 0	~6%
3	*I* and *J* of loaded end transverse member were set to 0	~6%
4	End axle loading was manually distributed to locations of two nearest girders but still placed on transverse member	~8%
5	Same as (4) but placed on longitudinal member	~8%
6	(3) and (4) combined	~11%
7	Same as (5) but placed 0.0001 in. into bridge instead of at 0 in.	~12%

Modifications (6) and (7) from Table 4.13 both brought the shear load distribution difference between the grillage model and the FE models down to about 5%. These modifications both distributed the shear end axle loading away from the end transverse grillage member, placing it directly on the two nearest longitudinal members. This reduced the effect of the end transverse grillage and the error that resulted from this interaction. However, when this load was distributed to the very ends of the longitudinal members, at 0 in. from the bridge end, the end transverse member was still causing incorrect load distributions. To deal with this, modification (6) also set the bending and torsional stiffnesses of the end transverse member to 0. These shear results were still found by checking the reactions at the end of every beam rather than investigating the internal beam shear of the longitudinal members.

When the end shear loads were distributed to the longitudinal members and placed 0.0001 in. into the beam, the load was found to be properly transferring into the bridge system. This loading configuration in modification (7) gave the same end reactions as modification (6) but produced correct internal shears within the beam members, giving the closest shear results to the FE models of any modification attempted. This method of shear loading was also found to be better than the sixth modification because it did not change any of the bridge properties, only the application of loads, and therefore it maintained the moment accuracy found initially, while separately improving the shear results.

Model modification (6) and (7) were also made to the evenly spaced grillage model to determine if it would improve the shear distributions in that model too. The results were nearly identical to those found from the shear loading spaced grillage model, an improvement of about 10% to 12%. Modification (7) improved grillage shear accuracy when compared to both FE models but brought the distributions even closer to the shell model than the frame model, which is reassuring as the shell element model was considered to be more accurate.

Further improvement to bring shear results below 5% difference between models was shown to be very difficult and unnecessary as all the results discussed above are the

averages over all seven loading cases for interior and exterior girders, and for the modification (7) the new results gave values ranging from slightly above to slightly below those found from the FE models, averaging within 2% of the average FE shear values for all loading cases. Figure 4.6 shows the lane 1 loading case for shear after load configuration modification (7), with all end loads placed at girder ends.

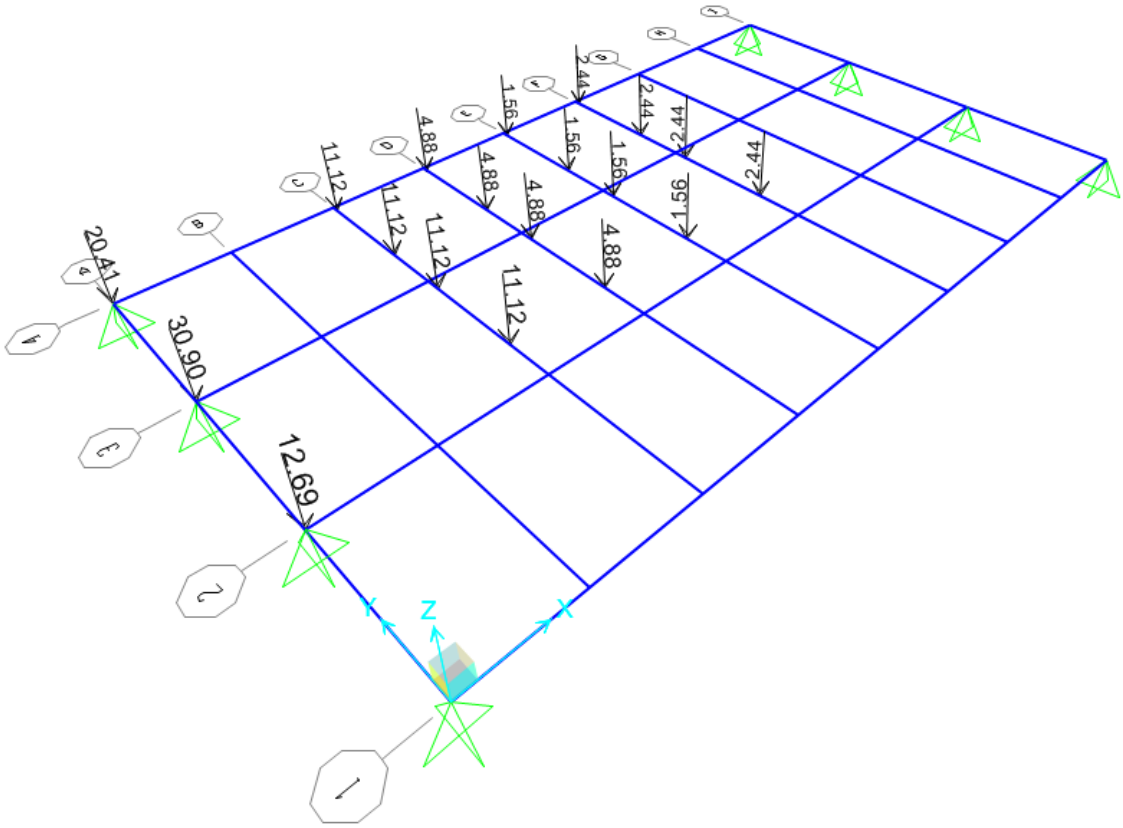

Figure 4.6 Shear Load Case 1 Using End Load Distribution to Girders

Table 4.14 and Table 4.15 below show the shear results for evenly spaced grillage model after modification (7) was applied. Additional tables of results for the modified models are shown in Appendix A.

Table 4.14 Exterior Girder Grillage vs. FE Shear after Modification (7)

Loading Case	Exterior Girder - Shear				
	Grillage V_{max} [k]	FE Frame V_{max} [k]	FE Shell V_{max} [k]	G/FE Ratio	
				Frame	Shell
1	37.8	36.2	35.8	1.044	1.056
2	32.4	32	31.5	1.013	1.029
3	27.2	27.6	27.0	0.984	1.006
4	22.1	23.5	22.9	0.939	0.963
5	18.5	19.2	18.2	0.963	1.015
6	15.3	15.5	14.1	0.988	1.086
7	12.3	11.8	10.2	1.038	1.201

Table 4.15 Interior Girder Grillage vs. FE Shear after Modification (7)

Loading Case	Interior Girder - Shear				
	Grillage V_{max} [k]	FE Frame V_{max} [k]	FE Shell V_{max} [k]	G/FE Ratio	
				Frame	Shell
1	51.8	47.8	49.1	1.083	1.054
2	51.9	47.7	49.1	1.089	1.058
3	51.9	47.9	49.4	1.084	1.051
4	52.0	47.3	48.5	1.100	1.073
5	50.5	46.6	48.0	1.085	1.053
6	48.3	45	46.6	1.073	1.036
7	45.9	43.3	44.9	1.061	1.023

Not only are the modified grillage models much more accurate as compared to the FE models for all loading lane cases, but in almost all cases they are also slightly conservative. This is ideal for the grillage method to give conservative values when used for LDF prediction for design. To display this trend of the grillage model being accurate

and yet conservatively covering most FE results the values from Tables 4.14 and 4.15 are plotted in Figure 4.7. This figure displays the improved shear predictions from the model with grillage modification (7) in a graphical comparison.

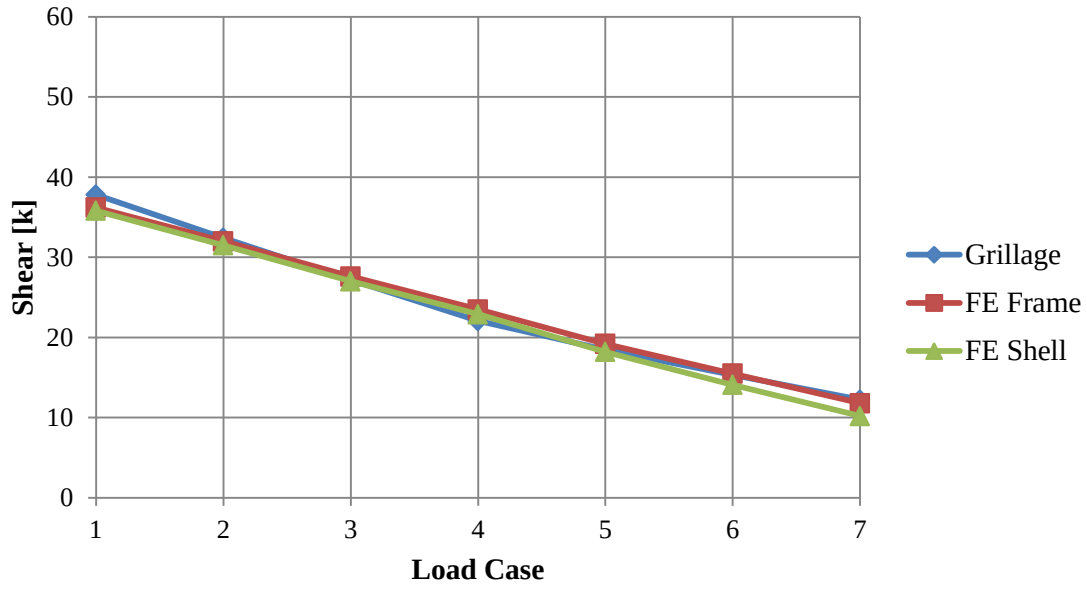

(a) Exterior Girder

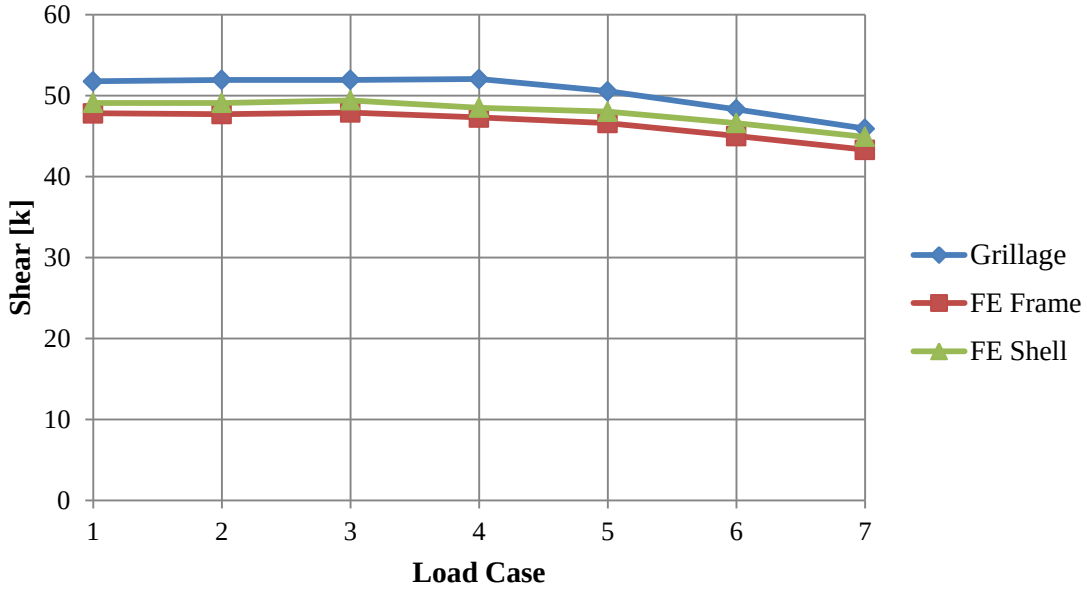

(b) Interior Girder

Figure 4.7 Riverside Bridge Shear Comparison after Modification 7 to Grillage Model

4.3 MESH SENSITIVITY STUDY

A grillage mesh fineness sensitivity study was conducted on the final evenly spaced Riverside bridge grillage model. The goal of this study was to determine if the transverse grillage spacing used for the Riverside bridge models was sufficiently fine to correctly model load distributions and bridge behavior. Two models were created with the same procedure as defined in Section 3 and with the shear loading modification that places the end loads on the girders as described in Section 4.2.3. These models however had transverse grillage spacings of half and twice that in the previous evenly spaced model. No additional longitudinal grillage members were added or subtracted from the models as it is best to keep longitudinal members only at girder locations for LDF calculations. The two mesh sensitivity models are shown below in Figure 4.8 and Figure 4.9.

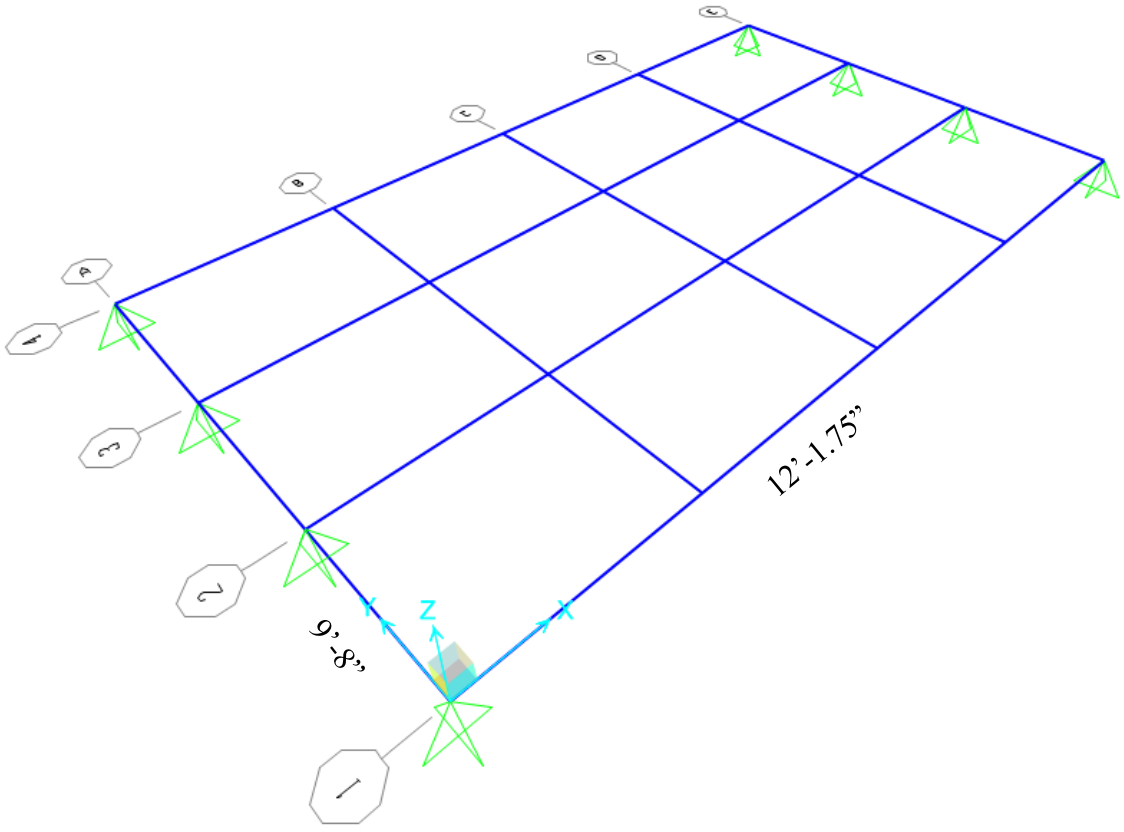

Figure 4.8 Double Spacing Grillage Model

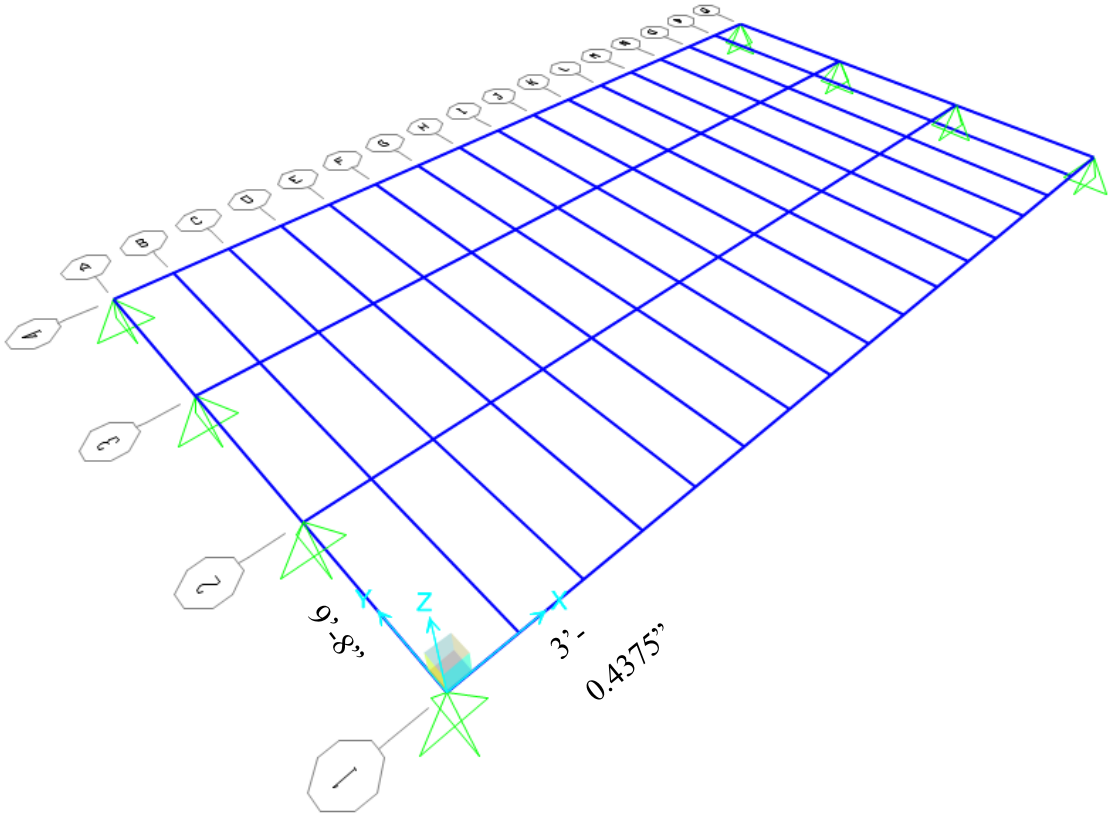

Figure 4.9 Half Spacing Grillage Model

The shear and moment results from these two mesh sensitivity models varied only slightly from the original evenly spaced model. In general the finer mesh produced results that were about 1% closer to the shell FE model, while the model with half as many members gave results that were about 1% farther away. The averages of these models when compared to the shell FE model are shown in Table 4.16. The red fill signifies that the values for all seven loading cases were unconservative for the grillage model, the yellow means that some loading cases were conservative and some were unconservative, and the green indicates that all loading cases gave conservative results in the grillage model. Additional mesh sensitivity results may be found in Appendix A.

Table 4.16 Mesh Sensitivity Results

Average Difference |1-(G/FE Shell)|				
Spacing	**Moment**		**Shear**	
	Exterior	**Interior**	**Exterior**	**Interior**
Original	0.023	0.038	0.062	0.050
Double	0.029	0.045	0.074	0.041
Half	0.021	0.020	0.047	0.064

The first three columns all show the finer grillage mesh giving reduced differences as compared to the shell element model and the more coarse mesh resulting in higher error. However, the interior shear in the fine mesh model becomes even more conservative than the original model, resulting in a larger difference from the FE model, while the double spaced model becomes a little more accurate. Overall this is a slight difference and not that important as further investigation of both mesh sensitivity models clearly show the half spacing model to be more accurate. One instance of this is that the largest difference between the double spacing grillage model and the FE shell model is over 25% at the exterior girder for shear loading case 7. The largest difference between the half spacing grillage model and the FE shell model is less than 16% at the exterior girder for shear loading case 4.

Overall the averages of all loading cases might still be close for both sensitivity models, but their standard deviations shown a much higher discrepancy when compared to the FE models on a single load case basis. The mesh sensitivity study concluded that the original transverse spacing of 6’-0.875” was sufficiently fine to accurately model the load distribution and bridge behavior. The 12’-1.75” spacing was too large and created high errors, while the 3’-0.4375” spacing was unnecessarily small and did not significantly improve the results from the original model. It is recommended that a transverse grillage spacing between 0.5 and 1 times the longitudinal member spacing be used for grillage modeling.

4.4 DREHERSVILLE EXPERIMENTAL RESULTS

4.4.1 Background

To supplement the finite element calibration of the Riverside experimental bridge grillage model and to further verify the methods in Section 3, a grillage model was made for the Little Schuylkill River bridge near Drehersville, Pennsylvania. This model was made similarly to the evenly spaced model including the more accurate shear loading modeling approach described above, with a few additional features to deal with different bridge attributes. The bridge crosses the Little Schuylkill River but for simplicity will be called the Drehersville bridge in this thesis.

The Drehersville bridge was instrumented and experimentally tested in 1966 as part of a Lehigh University research project to study the lateral distribution of static loads (Douglas and Vanhorn 1966). The bridge consists of three simply supported spans with no skew angle. The northwest span was instrumented and tested. This span has a length of 61.5 ft and a roadway width of 30 ft. The three-span bridge elevation view is shown in Figure 1.5 along with the two test loading locations of the central truck axle that were used.

The structural components included five prestressed concrete box-beam girders in a spread configuration, a reinforced concrete deck, sidewalks and parapets on both sides, and end and midspan diaphragms. The box girders have an overall depth of 2 ft 9 in. and an overall width of 4 ft, with web thicknesses of 5 in., a top flange thickness of 3 in., and a bottom flange thickness of 5 in. The bridge deck is specified as 7.5 in. thick and the diaphragms are 10 in. thick and as deep as the beams. Figure 4.10 below is the SAP2000 image of the cross-section of the midspan transverse grillage member with the diaphragm. The deck in this grillage section is 6 ft 1.8 in. wide.

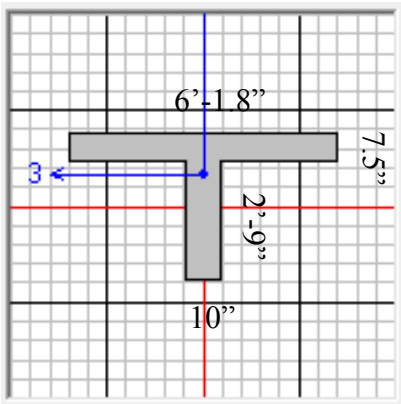

Figure 4.10 Midspan Diaphragm Member of Drehersville Grillage Model

The beam modulus was experimentally obtained and shown to be 6806 ksi, while the concrete compressive strength at the time of testing was calculated to be 7.022 ksi (Douglas and Vanhorn 1966). The deck strength was assumed to be 5 ksi and the beam strength was set as 7 ksi. These were the strengths used in the three FE models and the grillage models for this bridge, but the actual deck strength at the time of testing is unknown. The bridge cross-section including test lane loading is shown in Figure 1.5. Figure 4.11 shows the two test truck loadings used.

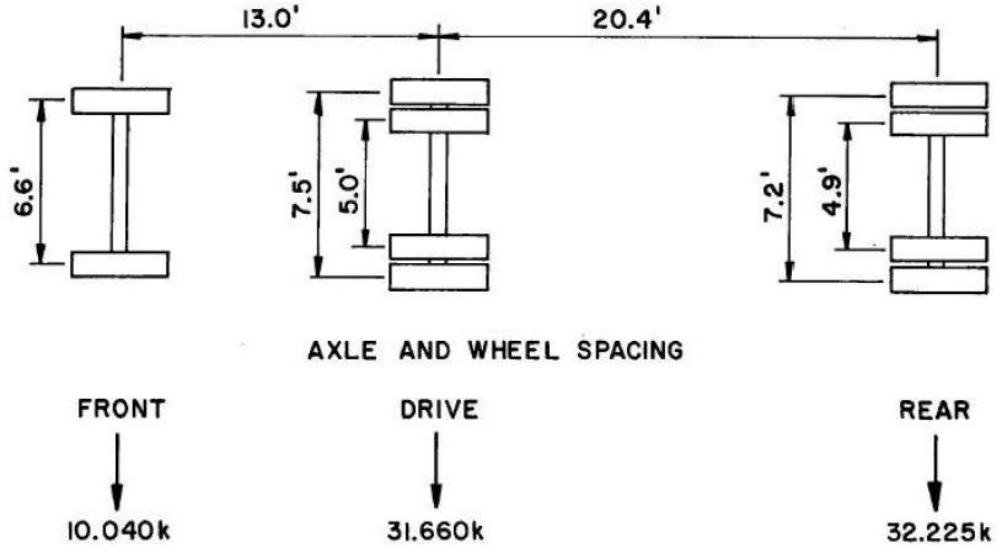

(a) Test Vehicle T1

Figure 4.11 Axle Loads of Drehersville Bridge Test Trucks (Douglas and Vanhorn 1966)

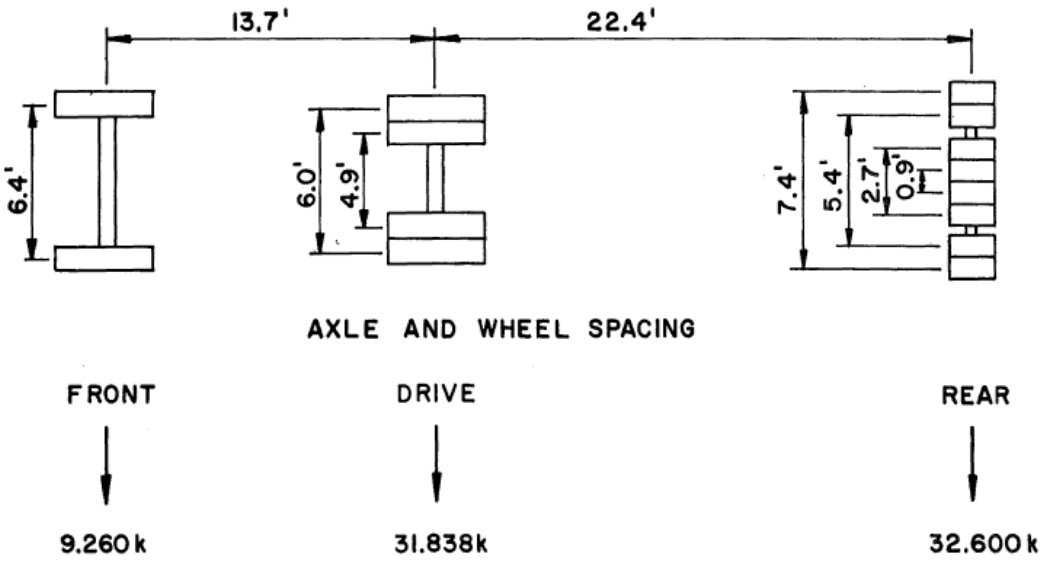

(b) Test Vehicle T2

Figure 4.11 (cont.)

The Drehersville bridge was not only investigated by Douglas and Vanhorn (1966), but was also modeled by Adnan (2005) as part of a study that involved calibration of FE and grillage models for precast, pretensioned concrete bridges (Hueste et al. 2006a). The finite element model results from this study will also be used for comparisons to this grillage model, as well as those found by three new Drehersville FE models created by other researchers as part of TxDOT project 0-6722 (Hueste et al. 2014). Between these four FE models and the experimental results from the Drehersville bridge experimental testing, the grillage model techniques and calibration processes will be well tested.

The FE model created by Adnan (2005) was developed using SAP2000 and was built with frame finite elements. Similarly to the Riverside experimental bridge, two new FE models utilizing frame and shell elements were made with CSiBridge for the Drehersville bridge. The most comprehensive and technically accurate model was built in the finite element program Abaqus Version 6 (Dassault Systemes (2013)) and used only solid or continuous elements. The new frame and shell element models were again made with similar assumptions to the grillage model for the Drehersville bridge, but the

old frame model and the new solid model were both made with the curb and parapet edge stiffening elements as well. The solid element model is shown in Figure 4.12.

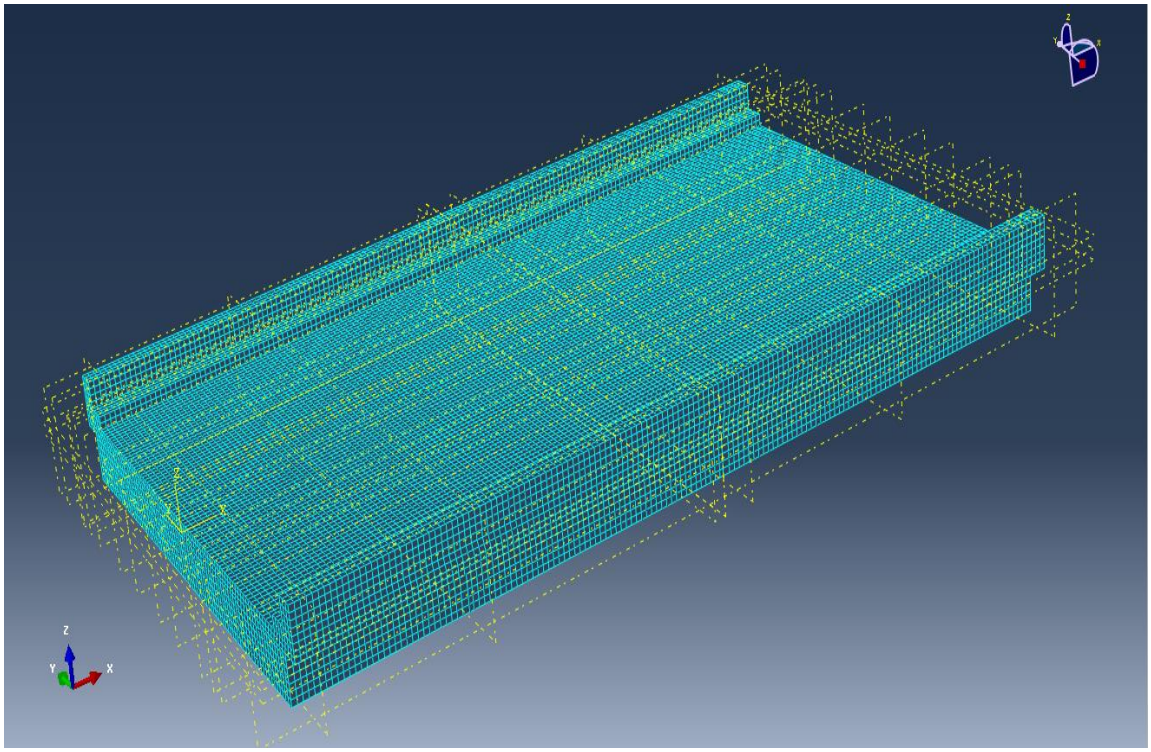

Figure 4.12 Drehersville Bridge Finite Solid Element Model (Hueste et al. 2014)

Figure 4.13 shows the lane 4 moment loading of the Drehersville grillage model. All loading cases tested were for done by placing the test truck(s) facing west with their central axles at the location of Section M in Figure 1.5 to create the maximum moment and to replicate the loading during testing. The transverse location of the axle loadings was determined again in a testing lane format as shown in Figure 1.5, where there were 7 possible testing lanes.

All moment values were also recorded at the longitudinal location of section M, where the bridge was instrumented. The reported experimental values correspond to this location. The analysis of the single beam LDF reference model did show that the maximum moment occurred at section M when the axle loads were placed as stated above. However, due to the presence of the midspan diaphragm in the full structure the

maximum moments in the models were in slightly different positions in each girder. These maximum moment values were not used for calibration but show a higher correlation to the experimental values while being slightly conservative. These values are provided in Appendix B. No side stiffening members were included in the grillage model as it is unclear if these members were composite with the bridge, but all three diaphragms were modeled in the two end and the middle transverse grillages.

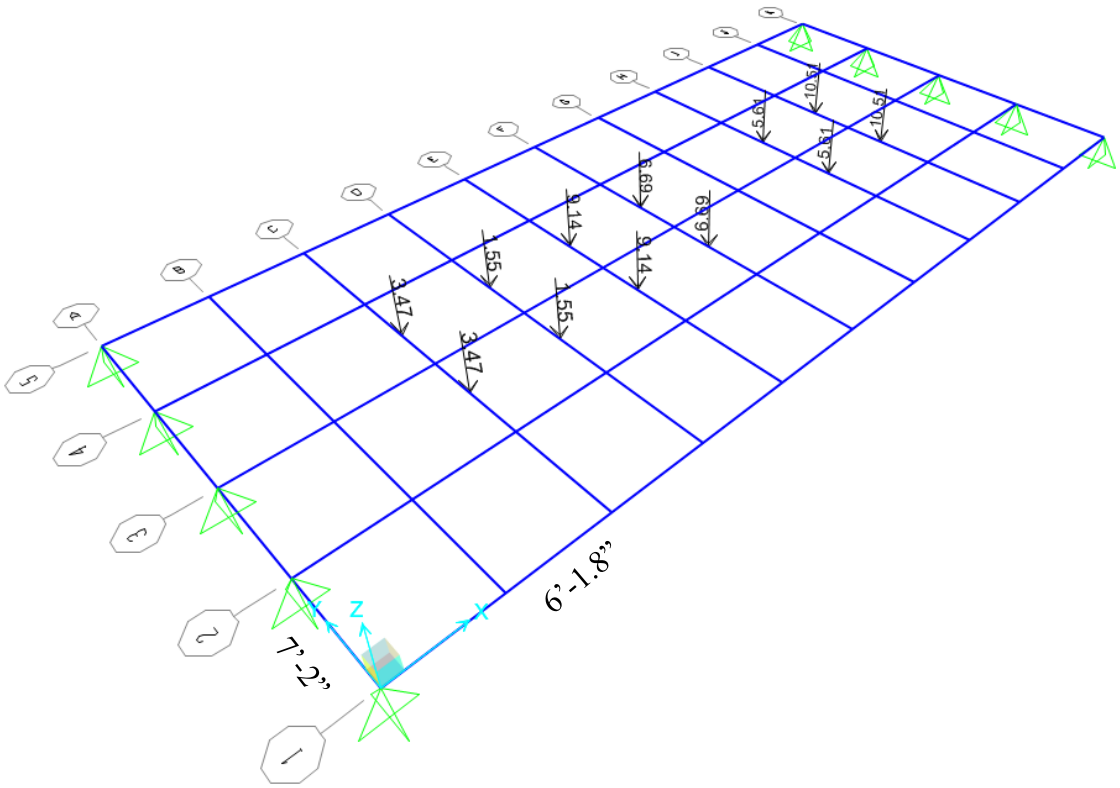

Figure 4.13 Drehersville Bridge Grillage Model Lane 4 Moment Loading

4.4.2 Results and Calibration

The experimental (Douglas and Vanhorn 1966), grillage, and FE (Adnan 2005; Hueste et al. 2014) results from this bridge are compared in Tables 4.17 through 4.20. Only two loading cases are investigated for simplicity and because these two also have FE model results from Adnan (2005). The lane 4 loading case is a centered load so

moment results should be symmetric about the longitudinal centerline of the bridge. Lanes 1 and 4 loaded gives the maximum external girder moment, and only the results from the two girders on that side and the center girder are recorded by Adnan (2005).

Table 4.17 Drehersville Bridge Lane 4 Moment Distribution Comparisons

Girder Location	Moment [k-ft]					
	Experiment	2005 FEA	FE Frame	FE Shell	FE Solid	Grillage
A	144.0	108.5	136.5	137.6	139.6	123.1
B	158.5	162.7	152.4	151.5	150.8	156.2
C	178.3	210.9	161.3	160.8	172.8	159.4
D	135.5	162.7	152.4	151.5	150.8	156.2
E	132.0	108.5	136.5	137.6	139.5	123.1

Table 4.18 Drehersville Bridge Lanes 1 & 4 Moment Distribution Comparisons

Girder Location	Moment [k-ft]					
	Experiment	2005 FEA	FE Frame	FE Shell	FE Solid	Grillage
A	477.1	280.0	381.3	364.8	358.4	470.5
B	373.0	339.6	350.7	342.1	343.1	391.0
C	273.8	295.6	304.5	303.3	314.6	301.6
D	203.2	-	248.9	256.7	261.0	199.6
E	190.9	-	192.5	211	234.0	73.6

Table 4.19 Drehersville Bridge Lane 4 Moment Distribution Ratios

Girder Location	Moment Ratio to Experimental				
	FEA/Exp	Frame/Exp	Shell/Exp	Solid/Exp	G/Exp
A	0.753	0.948	0.955	0.969	0.855
B	1.027	0.962	0.956	0.951	0.986
C	1.183	0.904	0.902	0.969	0.894
D	1.201	1.125	1.118	1.113	1.153
E	0.822	1.034	1.043	1.057	0.933

Table 4.20 Drehersville Bridge Lanes 1 & 4 Moment Distribution Ratios

Girder Location	Moment Ratio to Experimental				
	FEA/Exp	Frame/Exp	Shell/Exp	Solid/Exp	G/Exp
A	0.587	0.799	0.765	0.751	0.986
B	0.910	0.940	0.917	0.920	1.048
C	1.080	1.112	1.108	1.149	1.102
D	-	1.225	1.263	1.285	0.982
E	-	1.008	1.105	1.226	0.385

These tables again show the grillage method gives fairly accurate moment results. The grillage model closely predicted the highest four girder experimentally recorded moments for the two lane loaded case and was generally conservative, but returned results that were mostly unconservative for the single lane loading. Additionally, the single lane case for the lane 1 loading showed much different results than the recorded behavior. The model showed girder E rising and containing a negative moment for this case where the loading was nearest to girder A. However, the experimental results for the lane 1 loading showed negative deflections and positive moments of similar magnitude but opposite sign to those found from the model.

The experimental results of girder D and girder A in the lane 4 loading case show particularly high error when compared to all models. This girder error may actually have

more to do with the experimental testing than the model because it should have been symmetrically loaded and girder D would be expected to be similar to the moment found in girder B, and similarly A and E moments should also be the same. All models give a much higher moment value for girder D than was actually recorded in the experiment and a lower moment in girder A. This trend for the central loading case hints at a possibility of the truck actually being placed slightly to the girder A side of the centerline, which would cause the recorded moment in D to be lower than it should have, and the opposite for girder A. Another possible reason for this error could be material flaws or strength differences between girders.

Differences between the FEA done by Adnan (2005) and the models done for this project could be due to the edge stiffening elements in the Adnan's FE model, which included elements that were not present in any of the new models except the solid element Abaqus model. The edge stiffening elements in this older model were created to account for the curb and parapet along each side of the bridge. The new models were initially created without these pieces to examine the behavior without these elements. If these elements were continuous and tied into the deck with rebar then they would be considered structural elements and would bring additional stiffness to the edges. However, it is unknown if these elements were in fact continuous and connected to the deck.

From the initial grillage analysis without these edge stiffnening elements, the results are reasonable in most cases, and comparable to the FE analysis. However, the unexpected load sharing behavior for lane 1 loading and the lower grillage model exterior girder moments require additional investigation. The midspan transverse diaphragm is most likely responsible for the rising and negative moment found in girder E during lane 1 loading. This diaphragm is contributing too strongly in the model and may have cracked during or before experimentation, which would greatly reduce its torsional and bending stiffnesses. An additional model with reduced midspan diaphragm stiffnesses was created to explore this behavior. The lower exterior girder moments found from the modeling could be due to the curb, sidewalk, and parapet not being

included in the model. Another model that included these edge stiffening elements was also created.

To model cracking in the midspan diaphragm, the web of the midspan transverse grillage member was modified. The stiffnesses of the deck section were left as their previous values. The web (diaphragm) torsional and bending moments of inertia were reduced to 5% of their original value by adjusting the SAP2000 property modifiers. This change effectively reduced the overall bending stiffness of this transverse member by 25% and the torsional stiffness by 40%. The results from the cracked diaphragm modeling are shown in Appendix B.

The curb, sidewalk, and parapet were modeled as structural components by modifying the torsional and bending moments of inertia of the exterior longitudinal grillage members to include the effects of these edge stiffening elements. These additions increased the edge members' bending stiffness by 20% and the torsional stiffness by 250%. The results from this case may be found in Appendix B.

Upon review of both of these model changes, neither seemed to improve the agreement between models. The results indicate that they have opposite effects on the interior vs. exterior moment changes. One more model was created using both the cracked diaphragm and edge stiffening elements to investigate how these modifications would work together. The results showed much improved values over either one of the single change and generally improved the grillage results from the original Drehersville bridge model when compared to the experimental values. These results are listed below in Tables 4.21Table 4.21 through 4.24.

Table 4.21 Edge Stiffening and Cracked Diaphragm Lane 4 Grillage Moment Comparisons

Girder Location	Moment [k-ft]					
	Experiment	2005 FEA	FE Frame	FE Shell	FE Solid	Grillage
A	144.0	108.5	136.5	137.6	139.6	128.8
B	158.5	162.7	152.4	151.5	150.8	150.9
C	178.3	210.9	161.3	160.8	172.8	158.7
D	135.5	162.7	152.4	151.5	150.8	150.9
E	132.0	108.5	136.5	137.6	139.5	128.8

Table 4.22 Edge Stiffening and Cracked Diaphragm Lanes 1 and 4 Grillage Moment Comparisons

Girder Location	Moment [k-ft]					
	Experiment	2005 FEA	FE Frame	FE Shell	FE Solid	Grillage
A	477.1	280.0	381.3	364.8	358.4	495.4
B	373.0	339.6	350.7	342.1	343.1	360.6
C	273.8	295.6	304.5	303.3	314.6	289.7
D	203.2	-	248.9	256.7	261.0	197.7
E	190.9	-	192.5	211	234.0	92.9

Table 4.23 Edge Stiffening and Cracked Diaphragm Lane 4 Moment Ratios

Girder Location	Moment Ratio to Experimental				
	FEA/Exp	Frame/Exp	Shell/Exp	Solid/Exp	G/Exp
A	0.753	0.948	0.955	0.969	0.894
B	1.027	0.962	0.956	0.951	0.952
C	1.183	0.904	0.902	0.969	0.890
D	1.201	1.125	1.118	1.113	1.114
E	0.822	1.034	1.043	1.057	0.976

Table 4.24 Edge Stiffening and Cracked Diaphragm Lanes 1 and 4 Moment Ratios

Girder Location	Moment Ratio to Experimental				
	FEA/Exp	Frame/Exp	Shell/Exp	Solid/Exp	G/Exp
A	0.587	0.799	0.765	0.751	1.038
B	0.910	0.940	0.917	0.920	0.967
C	1.080	1.112	1.108	1.149	1.058
D	-	1.225	1.263	1.285	0.973
E	-	1.008	1.105	1.226	0.487

It is clear that edge stiffening elements and diaphragm members are very important for load distributions. A stronger diaphragm will increase interaction and load sharing amongst girders, while edge stiffening members will draw higher moments into the edge members. When test data is available it is recommended that bridge models be made without these elements initially and if further calibration in necessary, add these structural elements to the model to see if their presence improves the results. Figure 4.14 depicts the final comparison between different modeling moment results and the experimental results in a graphical representation.

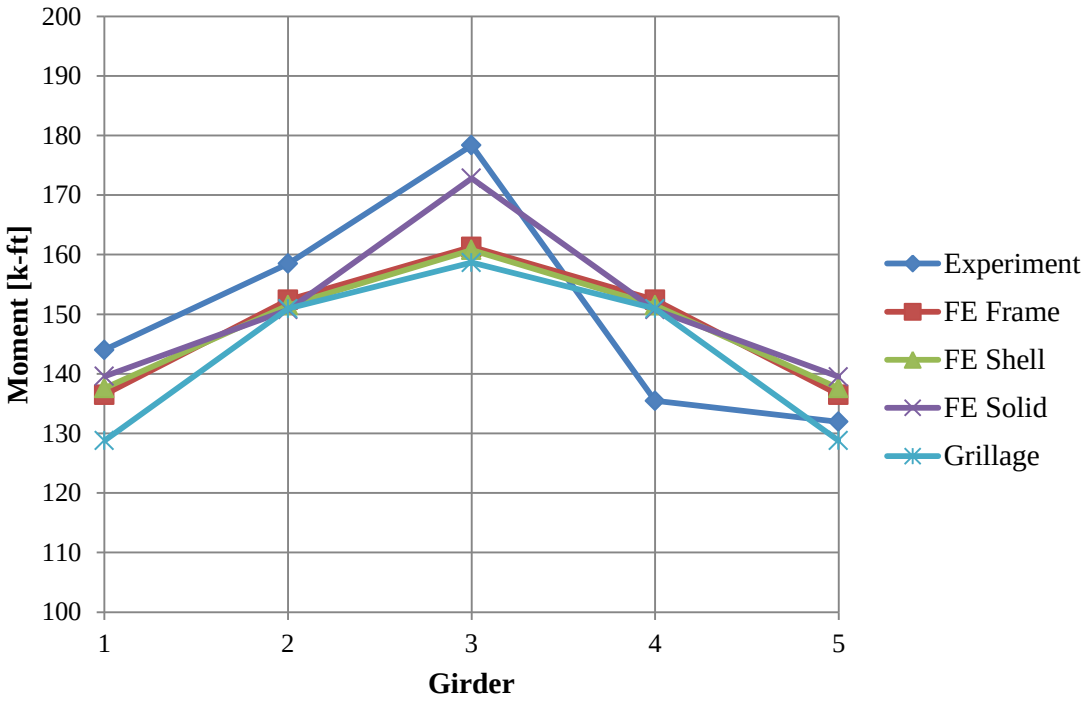

Lane 4 Loaded

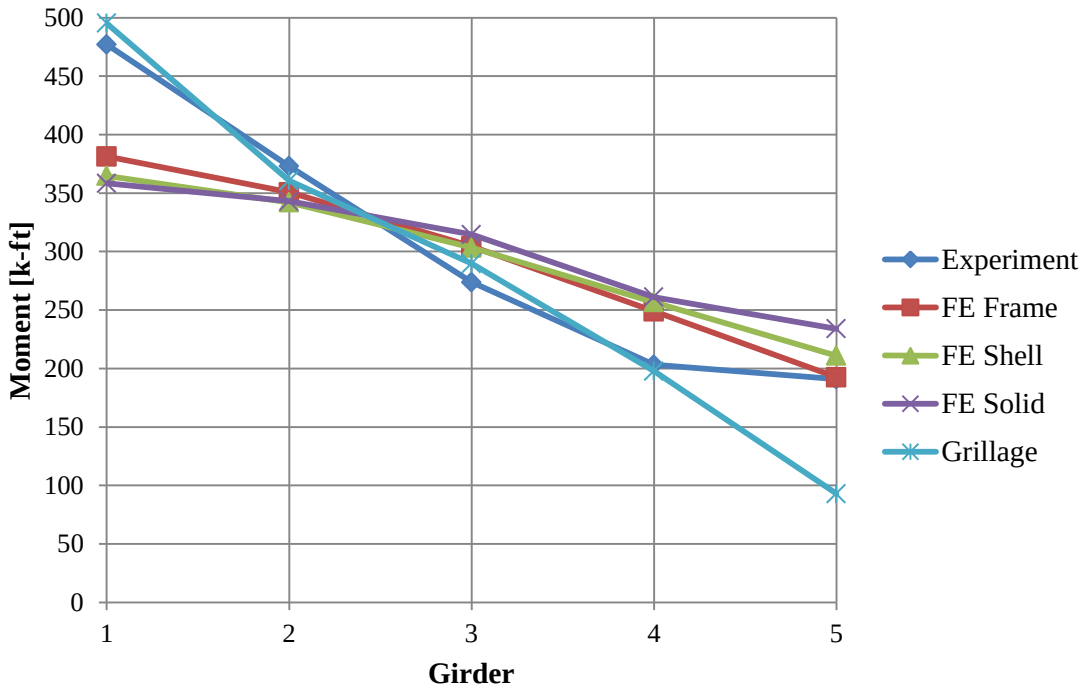

(a) Lanes 1 and 4 Loaded

Figure 4.14 Drehersville Bridge Moment Comparisons

The refined grillage model utilizing a cracked midspan diaphragm and edge stiffening elements clearly models the moment in each of the first four girders most accurately for the critical case of lanes 1 and 4 loaded. The fifth and lowest moment girder is not modeled well by the grillage model in this case. However, this is not as critical because for LDF calculation it is more important to accurately and conservatively model the critical girders with the highest moment.

While the main goals of the LDF modeling are to give accurate moment and shear distributions, the Drehersville bridge also has experimental deflection data that can be compared with model deflections for additional bridge behavior verification. The maximum deflections found from the models were generally moderately accurate but not highly accurate in all cases when compared with the deflections found from experimentation. The models tend to give conservative deflections as compared with the experimental findings, which is acceptable for design. The deflection comparisons from the original Drehersville grillage model are shown in Tables 4.25 through 4.28.

Table 4.25 Drehersville Bridge Lane 4 Deflection Comparisons

Girder Location	Deflection [in.]				
	Experiment	**FE Frame**	**FE Shell**	**FE Solid**	**Grillage**
A	0.0398	0.0600	0.0600	0.060	0.0510
B	0.0574	0.0680	0.0650	0.066	0.0701
C	0.0700	0.0740	0.0690	0.070	0.0797
D	0.0552	0.0680	0.0650	0.066	0.0701
E	0.0404	0.0600	0.0580	0.060	0.0510

Table 4.26 Drehersville Bridge Lane 4 Deflection Ratios

Girder Location	Deflection Ratio to Experimental			
	Frame/Exp	Shell/Exp	Solid/Exp	G/Exp
A	1.509	1.509	1.509	1.282
B	1.185	1.133	1.151	1.222
C	1.057	0.985	1.000	1.138
D	1.233	1.178	1.196	1.270
E	1.484	1.434	1.484	1.260

Table 4.27 Drehersville Bridge Lanes 1 and 4 Deflection Comparisons

Girder Location	Deflection [in.]				
	Experiment	FE Frame	FE Shell	FE Solid	Grillage
A	0.115	0.170	0.156	0.154	0.207
B	0.127	0.157	0.146	0.146	0.179
C	0.120	0.137	0.130	0.133	0.139
D	0.086	0.110	0.110	0.115	0.088
E	0.061	0.085	0.090	0.099	0.031

Table 4.28 Drehersville Bridge Lanes 1 and 4 Deflection Ratios

Girder Location	Deflection Ratio to Experimental			
	Frame/Exp	Shell/Exp	Solid/Exp	G/Exp
A	1.477	1.355	1.338	1.797
B	1.234	1.147	1.147	1.406
C	1.141	1.083	1.108	1.162
D	1.283	1.283	1.341	1.021
E	1.398	1.481	1.629	0.513

The deflection results show larger differences between the model and experimental values as compared to the moment results. However, the important point for the load distribution modeling is that the grillage model is conservative for all beams except the very lowest one in the Lanes 1 and 4 loading case. Also, the grillage modeling results follow the experimental deflection profile across the bridge width when viewed graphically. All other models also give conservative results but do not have a similar shape to experimental results. This can be seen in Figure 4.15.

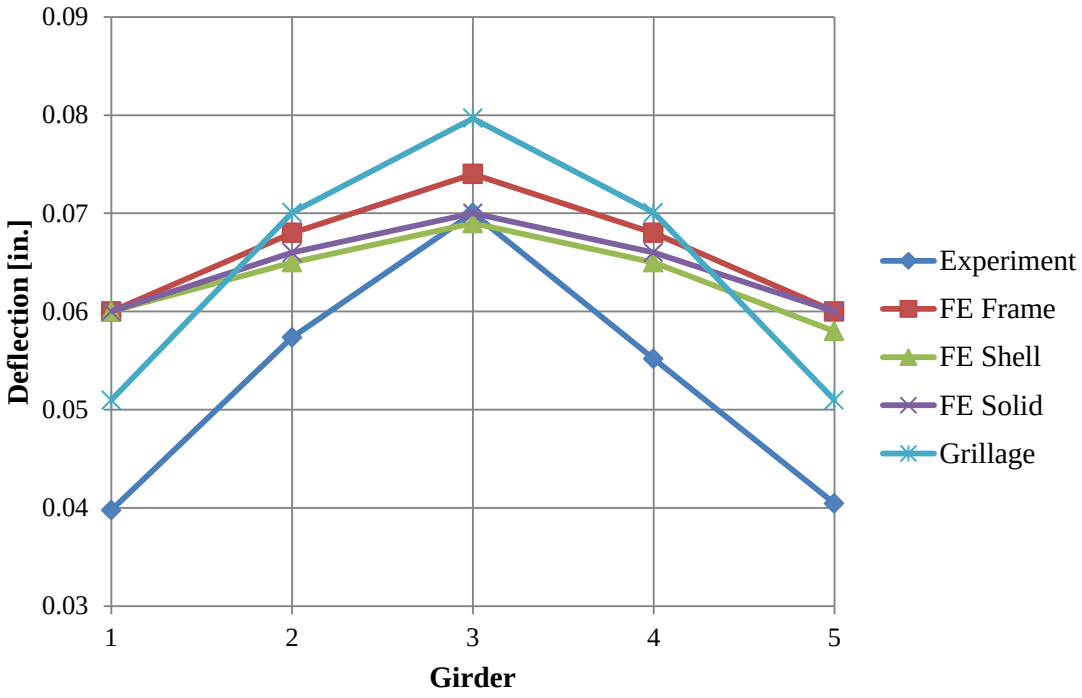

Figure 4.15 Drehersville Bridge Lane 4 Loading Deflection

No further adjustments were deemed necessary for the grillage model. The deflections found by the refined grillage analysis that incorporated a cracked midspan diaphragm and edge stiffening elements were less accurate than those shown above from the original model and are listed in Appendix B.

4.5 DENISON FIELD BRIDGE FINITE ELEMENT MODELS

4.5.1 Background

In order to examine how the spacing between slab beams affect load distribution behavior, and to further verify the grillage assumptions and modeling changes used above, a grillage model was created for the US Highway 69 slab beam bridge in Denison, Texas. This bridge was designed by TxDOT in 2010 (TxDOT 2010) and incorporates two independent bridges in a side-by-side layout, with one bridge servicing the northbound lanes and the other the southbound. The northbound bridge is currently completed, while the southbound bridge is under construction. Both bridges contain 18 spans, with the first three spans on the South end of both bridges utilizing slab beams as the structural girders. Span 3 is the longest of the three slab beam spans and is the span that will be modeled. This span will also be instrumented as part of TxDOT project 0-6722 so that the bridge's behavior under service loading may be observed and analyzed. The results from the modeling will later be compared to this instrumentation data when the testing is complete.

As shown by the drawings in Figure 1.6, span 3 of the Denison bridge has a center-to-center of supports length of 50 ft. The bridge width is 37.958 ft, with a 1 ft rail and 6 ft sidewalk on one edge, and a median along the other edge. However, the distance from the central edge to the median changes along span 3, as shown in Figure 1.6. For modeling purposes, the median location at the far south end, where it is fully in on the northbound bridge, will be used for the entire length of span 3, and no trucks will be allowed closer to the edge than 1 ft away from this median. The median, the sidewalk, and the rail were not considered structural elements and therefore were not modeled.

There are six evenly spaced 5SB15 slab beams in span 3 with gaps between the slab beams of 1.388 ft. The reinforced concrete deck above these gaps is supported by a non-structural corrugated metal sheet, while the rest of the deck is placed directly on top of the slab beams. The thickness of the deck above the beams is 1 ft, but the plans list the thickness between beams as 8 in. because the concrete within the corrugated sheet is not counted. For modeling simplicity the slab will be considered to be 1 ft thick across the

entire bridge and no corrugated metal will be modeled. The slab beams have a specified minimum 28 day strength of 5.4 ksi, while the deck has a required strength of 4 ksi. Figure 4.16 below shows images of the slab beams in span 3 from underneath the bridge.

(a) South Side Bent of Span 3, Showing Slab Beam Bearing and Close Spacing

(b) Underside of Span 3, Showing Centered Bearing Pads, Corrugated Metal Sheet, and Narrow Slab Beam Spacing

Figure 4.16 Photos Showing Span 3 from Underside

All modeling assumptions made for the Denison grillage and FE model are similar to those described above for the Riverside experimental bridge and for the Drehersville bridge. The grillage model was made using six longitudinal members spaced at 6.388 ft so that they are centered along the six slab beams centerlines. These longitudinal members include a transformed deck section that factors the deck torsion constant by one half. There are nine transverse grillage members, spaced at 6.25 ft and again factor the torsion constant by one half. Similarly to the Drehersville bridge modeling, a full solid element model was also created for the Denison bridge in Abaqus as part of this project for grillage calibration and comparison (Hueste et al. 2014).

Due to the wide sidewalk and the initial wide location of the median, the roadway surface on the Denison bridge is only 24 ft wide at the beginning of span 3, and it will be taken to be this width over the entire length for loading purposes. The outside axle load of the first truck for the first load case is placed 1 ft away from the curb of the sidewalk. The same axle and truck spacing, and 1 ft load case movements used for the Riverside experimental bridge (detailed in Section 3.4.3) are also used for the Denison bridge. This setup results in four different transverse locations of the two truck loading before the trucks reach the midspan of the bridge. This means that there are four moment and four shear load cases.

The back axle spacing of the three axle design truck load was investigated for the Denison bridge and a spacing of 14 ft was again determined to give the highest moments and shears. The longitudinal moment configuration again placed the resultant force of the three axles equidistant and opposite of the bridge centerline as the middle axle. The 8 kip front axle was therefore placed 8.86 ft away from one end of the bridge and both of the other two axles were spaced at 14 ft from the front axle. The critical shear longitudinal location was again found by placing the rear 32 k axle directly over the supports at one end of the bridge and having the middle and front axles spaced at 14 ft from there. As determined above, the end 32 k load was distributed to the girders and placed 0.0001 in. away from the edge to accurately model the internal shear at the ends. Figure 4.17 below shows the lane 1 loading case for the Denison grillage model.

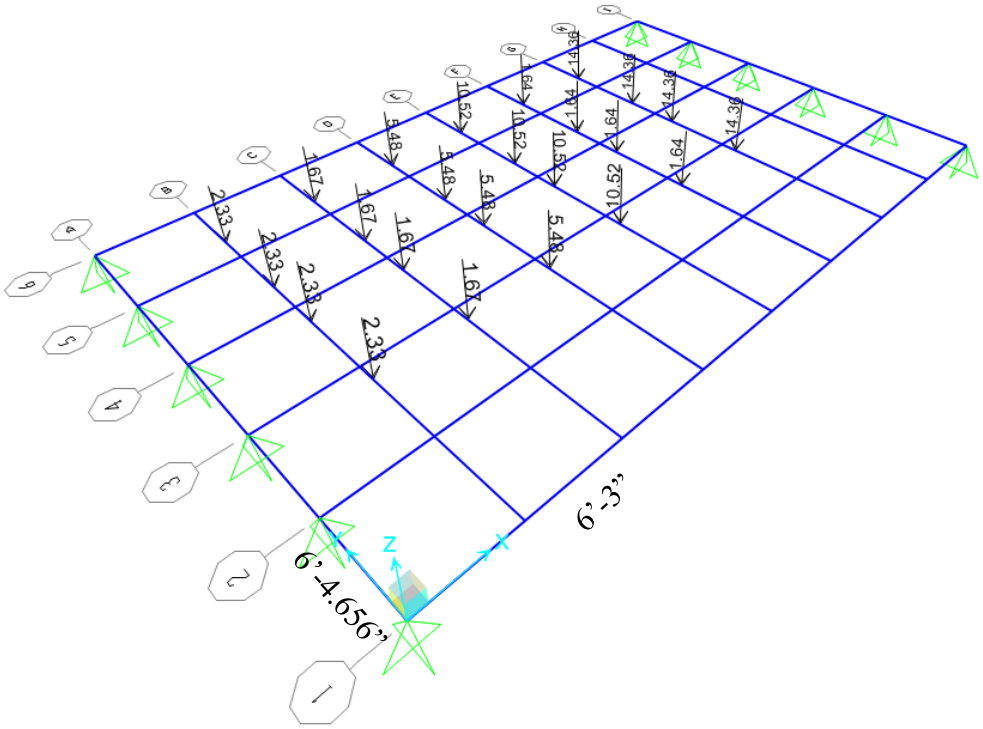

(a) Moment Load Configuration

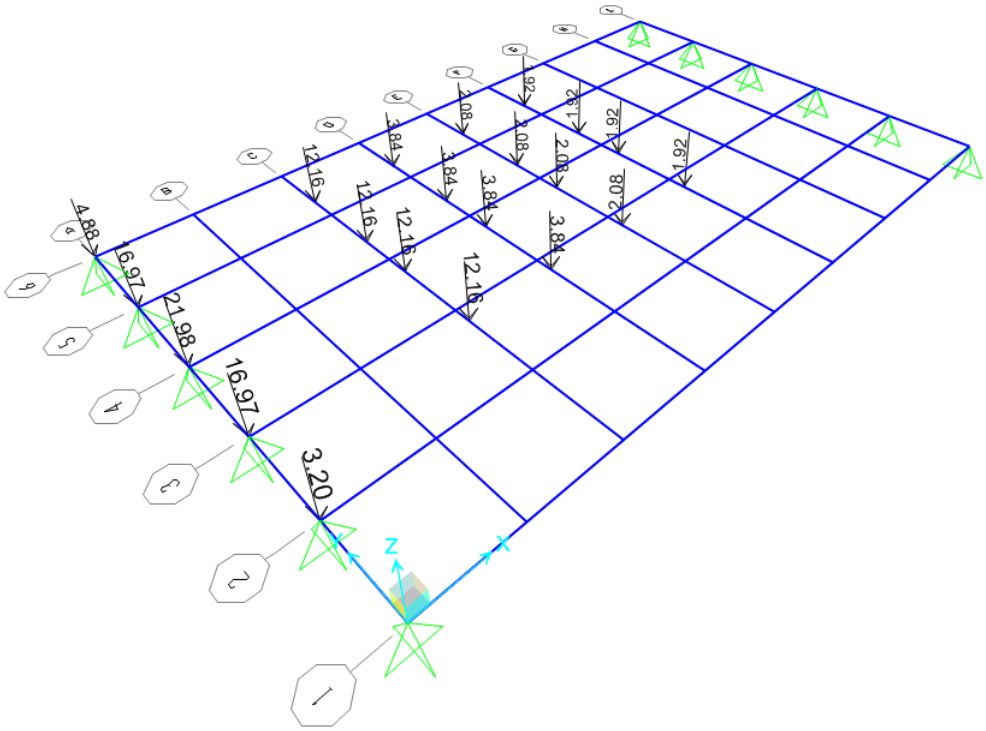

(b) Shear Load Configuration

Figure 4.17 Denison Bridge Grillage Model Lane 1 Loading

4.5.2 Results and Comparisons

The load distribution results from the grillage and FE models are presented and compared in Table 4.29 through Table 4.31 below. Since the Denison bridge has six girders, the tables include the results from the critical exterior girder, and the two interior girders closest to this critical exterior girder. The most critical of these two interior girders is the one used for interior LDF calculation but both interior girders on the loaded side are recorded for a more complete load distribution behavior comparison between the models.

Table 4.29 Exterior Girder Moment and Shear Comparisons

Loading Case	Exterior Girder - Moment			Exterior Girder - Shear		
	M_{max} [k-ft]		G/FE Ratio	V_{max} [k]		G/FE Ratio
	Grillage	FE Solid	Solid	Grillage	FE Solid	Solid
1	216.3	204.8	1.057	12.9	10.3	1.257
2	196.6	194.0	1.013	9.3	8.9	1.044
3	178.5	184.4	0.968	5.8	7.7	0.757
4	161.7	174.5	0.927	4.9	6.4	0.766

Table 4.30 Interior Girder 1 Moment and Shear Comparisons

Loading Case	Interior Girder 1 - Moment			Interior Girder 1 - Shear		
	M_{max} [k-ft]		G/FE Ratio	V_{max} [k]		G/FE Ratio
	Grillage	FE Solid	Solid	Grillage	FE Solid	Solid
1	256.4	237.2	1.081	29.3	27.0	1.084
2	244.1	228.4	1.069	28.6	25.0	1.143
3	231.5	220.2	1.051	27.6	24.0	1.152
4	218.4	211.3	1.033	23.5	22.7	1.034

Table 4.31 Interior Girder 2 Moment and Shear Comparisons

Loading Case	Interior Girder 2 - Moment			Interior Girder 2 - Shear		
	M_{max} [k-ft]		G/FE Ratio	V_{max} [k]		G/FE Ratio
	Grillage	FE Solid	Solid	Grillage	FE Solid	Solid
1	260.4	243.2	1.071	34.9	39.6	0.882
2	258.5	242.1	1.068	34.9	37.8	0.921
3	255.2	237.8	1.073	34.9	29.8	1.172
4	250.6	232.6	1.077	33.9	26.7	1.270

These tables show that the grillage analysis method for the Denison bridge as described above gives reasonably accurate and conservative results for the moment modeling. The moment values returned by the solid finite element model are assumed to be very precise. The fact that the grillage results are returning values within 10% of the solid element model is a strong indicator that the grillage model is working well for moment LDF calculation.

The shear results vary more than the moment results. The grillage model is giving conservative and reasonably accurate results for the first interior girder in all cases. However, the critical exterior girder is modeled conservatively for the first two load cases, and unconservatively for the second two load cases by the grillage model. The critical interior girder has the inverse relationship between grillage and solid element models. Since the critical load case is again the first case, closest to the edge, this results in the grillage model being conservative for the critical load cases for the exterior and first interior girders, but unconservative for the critical load case for the second interior girder. Because of the shear difference shown above, the results from all six girders were explored further in both models.

From the lever rule load distribution method, in a single beam, 81.33% of the shear force from the shear loading configuration should be transferred to the end nearest the loading and 18.67% to the far end. This calculation for the shear loading

configuration is shown in Equations 4.1 and 4.2 below, where the far end of the bridge is the one farthest away from the truck loading.

Lever rule percent of truck load distributed to the far end of the Denison bridge:

$$\frac{32\text{k}\left(\frac{0\text{ ft}}{50\text{ ft}}\right)+32\text{k}\left(\frac{14\text{ ft}}{50\text{ ft}}\right)+8\text{k}\left(\frac{28\text{ ft}}{50\text{ ft}}\right)}{72\text{k}}\times 100\% = 18.67\% \tag{4.1}$$

Lever rule percent of truck load distributed to the near end of the Denison bridge:

$$100\% - 18.67\% = 81.33\% \tag{4.2}$$

The grillage model distributed 81% of the shear to the near end and 19% to the far end, while the near end in the solid element model only carried 78% of the total shear, leaving 22% for the far end. From this comparison it would appear that both models are working very similarly in the longitudinal direction to the overall bridge superstructure lever rule simplification, they are just distributing the shear loads at the ends amongst the girders slightly differently. After this full girder investigation both models are shown to be giving reasonable and very similar results. The moment and shear trends for all girders under the critical loading case can be easily seen by examining Figure 4.18.

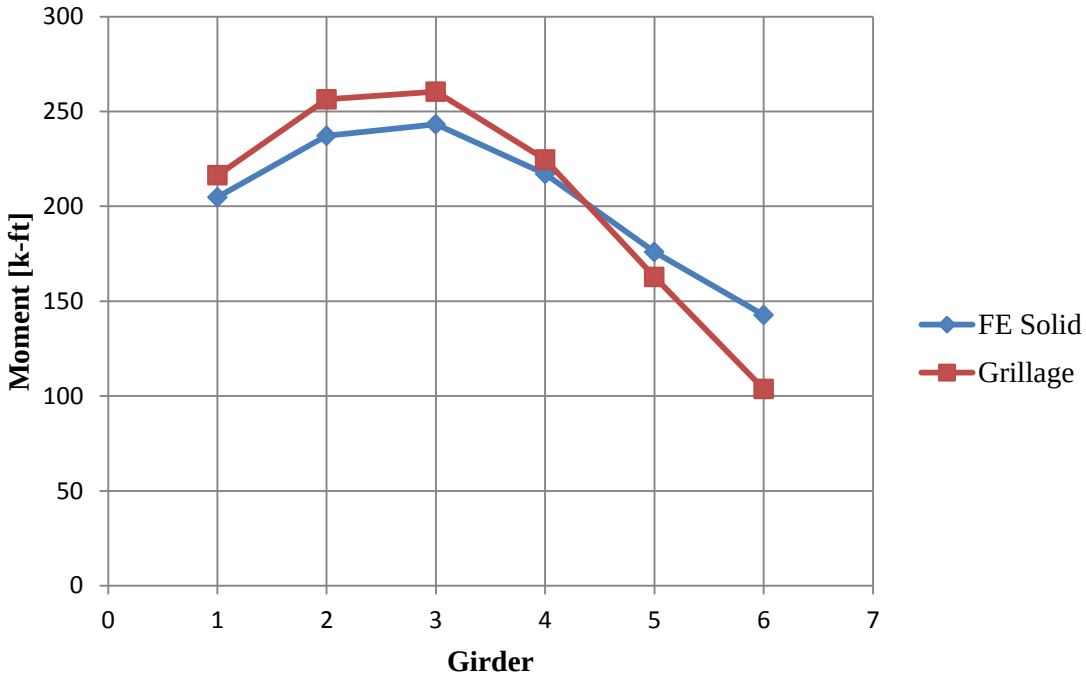

(a) Moment Loading

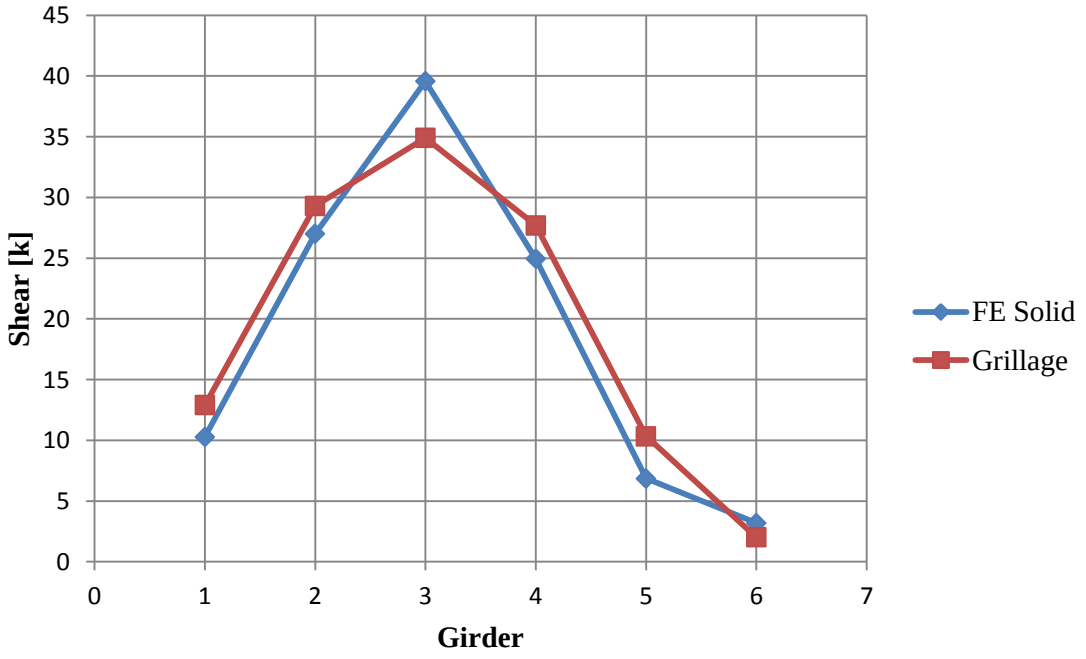

(b) Shear Loading

Figure 4.18 Maximum Response from All Denison Bridge Girders - Load Case 1

5. LOAD DISTRIBUTION RELATIONSHIPS

5.1 GENERAL

The AASHTO LRFD Bridge Design Specifications (AASHTO 2012) currently include load distribution factors for several types of bridges. The bridge types determined to be the most similar to spread prestressed slab beam bridges and the LDF equations that correspond to these bridge types are shown in Tables 2.2 through 2.5. By using these formulae to predict the load distributions in the Riverside experimental bridge and the Denison field bridge it may be possible to see which equations are closest to the correct distributions as determined by the grillage and FE modeling. This load distribution factor equation may then be altered based on parameter knowledge and differences between that bridge type and spread slab beam bridges so that the new equation will closely match the modeling results.

The LDF formulae for spread prestressed concrete box beams were assumed to be the closest mathematical model to the spread slab beam behavior and were used in the design of the Riverside experimental bridge. LDF equations for closed steel box beams, and precast concrete T-beams and I-beams will also be tested on the two slab beam bridges in this thesis for comparisons with calibrated models and the spread box beam formulae.

5.2 PREVIOUS LDF FORMULAE DEVELOPMENT

Zokaie (2000) made several assumptions during his development of the simplified mathematical models for bridge LDFs. It was assumed that the effect of each parameter on load distribution could be modeled by a power function of the form ax^b, where x is the value of the given bridge parameter under consideration, and a and b are constants that need to be determined based on the variation of the distribution factor with x. The effect of each parameter was also considered to be independent of all other parameters. The final distribution factors presented by Zokaie (2000) were modeled by a power formula of the form;

$$g = a\left(S^{b_1}\right)\left(L^{b_2}\right)\left(t^{b_3}\right)(\ldots) \tag{5.1}$$

where g is the wheel load distribution factor, a is the scale factor, and b_1, b_2 and b_3 are exponents of the corresponding parameters.

The b exponents may be calculated by changing their respective parameters and the associated distribution factor one at a time. For example the S parameter is changed in the equations below to illustrate how b_1 might be calculated.

$$g_1 = a\left(S_1^{b_1}\right)\left(L^{b_2}\right)\left(t^{b_3}\right)(\ldots) \tag{5.2}$$

$$g_2 = a\left(S_2^{b_1}\right)\left(L^{b_2}\right)\left(t^{b_3}\right)(\ldots) \tag{5.3}$$

and therefore;

$$\frac{g_1}{g_2} = \left(\frac{S_1}{S_2}\right)^{b_1} \tag{5.4}$$

or:

$$b_1 = \frac{\ln\left(\frac{g_1}{g_2}\right)}{\ln\left(\frac{S_1}{S_2}\right)} \tag{5.5}$$

If n different values of S are examined and successive pairs are used to determine the value of b_1, then (n-1) different values of b_1 can be obtained. If these b_1 values are similar, a power curve can be used to accurately model the variation of the distribution factor with S. In a similar manner the other exponents were also determined. Once all the exponents were determined the value of the constant a can be calculated as;

$$a = \frac{g_0}{\left(S_0\right)^{b_1}\left(L_0\right)^{b_2}\left(t_0\right)^{b_3}(\ldots)} \tag{5.6}$$

This procedure was applied for all other bridge types. In certain cases where a power function was not suitable to model the effect of a parameter, a slight variation from this procedure is used. However, this process worked quite well in most cases and the formulae developed by this method showed high accuracy when "g-ratios" were created and compared, as shown in Figure 2.2.

5.3 CURRENT AASHTO LRFD LDF COMPARISONS

5.3.1 Riverside Experimental Bridge

Load distribution factors for the Riverside experimental bridge were calculated using current AASHTO (2012) equations for closed steel box beams, spread prestressed concrete box beams, and prestressed concrete T-beams, and I-beams. The calculations of the spread prestressed concrete box beam interior and exterior girder load distribution factors are shown below. These were the load distribution factors used for the design of the Riverside experimental bridge.

Moment distribution factor for interior girder, one design lane loaded:

$$DFM_{in1} = \left(\frac{S}{3.0}\right)^{0.35}\left(\frac{Sd}{12.0L^2}\right)^{0.25} \tag{5.7}$$

$$= \left(\frac{9.67}{3}\right)^{0.35}\left(\frac{9.67(15)}{12\times 50^2}\right)^{0.25} = 0.397 \text{ lanes/girder}$$

where:

S = Girder spacing, ft

d = Depth of the girder, in.

L = Girder span, ft

Moment distribution factor for interior girder, two or more design lanes loaded:

$$DFM_{in2} = \left(\frac{S}{6.3}\right)^{0.6}\left(\frac{Sd}{12.0L^2}\right)^{0.125} \tag{5.8}$$

$$= \left(\frac{9.67}{6.3}\right)^{0.6}\left(\frac{9.67(15)}{12\times 50^2}\right)^{0.125} = 0.664 \text{ lanes/girder}$$

Moment distribution factor for exterior girder:

$$DFM_{ex} = DFM_{in} \times e \tag{5.9}$$

$$e = 0.97 + \frac{d_e}{28.5} \tag{5.10}$$

$$e = 0.97 + \frac{1.5}{28.5} = 1.023$$

$$DFM_{ex} = 0.664 \times 1.022 = 0.679 \text{ lanes/girder}$$

where:

e = Exterior to interior girder factor

d_e = Horizontal distance from centerline of the exterior web of exterior beam at deck level to the interior edge of curb or traffic barrier, ft

Shear distribution factor for interior girder, one design lane loaded:

$$DFV_{in1} = \left(\frac{S}{10}\right)^{0.6}\left(\frac{d}{12.0L}\right)^{0.1} \tag{5.11}$$

$$= \left(\frac{9.67}{10}\right)^{0.6}\left(\frac{15}{12 \times 50}\right)^{0.1} = 0.678 \text{ lanes/girder}$$

Shear distribution factor for interior girder, two or more design lanes loaded:

$$DFV_{in2} = \left(\frac{S}{7.4}\right)^{0.8}\left(\frac{d}{12.0L}\right)^{0.1} \tag{5.12}$$

$$= \left(\frac{9.67}{7.4}\right)^{0.8}\left(\frac{15}{12 \times 50}\right)^{0.1} = 0.856 \text{ lanes/girder}$$

Shear distribution factor for exterior girder:

$$DFV_{ex} = DFV_{in} \times e \tag{5.13}$$

$$e = 0.8 + \frac{d_e}{10} \tag{5.14}$$

$$e = 0.8 + \frac{1.5}{10} = 0.95$$

$$DFV_{ex} = 0.856 \times 0.95 = 0.813 \text{ lanes/girder}$$

The final design interior girder live load distribution factors are taken as the maximum LDF from the one and two design lanes loaded cases. In the example

calculations above, the final interior girder moment distribution factor (DFM) is 0.664 lanes/girder and the final interior girder shear distribution factor (DFV) is 0.856 lanes/girder. The case with two lanes loaded is critical for all bridges in this study.

To calculate load distribution factors from grillage and FE modeling, the maximum moment and shear results from loading a simple single beam structure with one truck's axle loads were calculated. This was done by hand using standard static analysis and equilibrium, and also by SAP2000 for confirmation. The moment and shear loadings were configured as shown in Figure 3.3 to give maximum values. Figure 5.1 shows the SAP2000 single beam models for the Riverside experimental bridge. The calculated maximum shear or moment values found from all seven of the two truck loading cases described in Section 3.4 were then divided by these single beam maximum moments and shears to give the modeling LDFs, as shown in the equations below. These maximum grillage and FE model values are shown above in Tables 5.1 and 5.3.

$$LDF_M = \frac{M_{\text{Model}}}{M_{\text{SingleBeam}}} \tag{5.15}$$

$$LDF_V = \frac{V_{\text{Model}}}{V_{\text{SingleBeam}}} \tag{5.16}$$

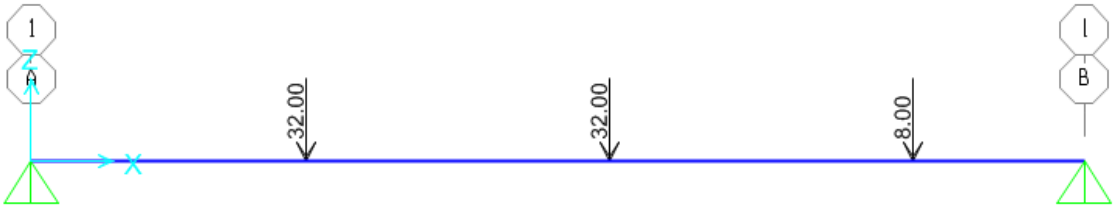

(a) Single Beam LDF Maximum Moment Reference

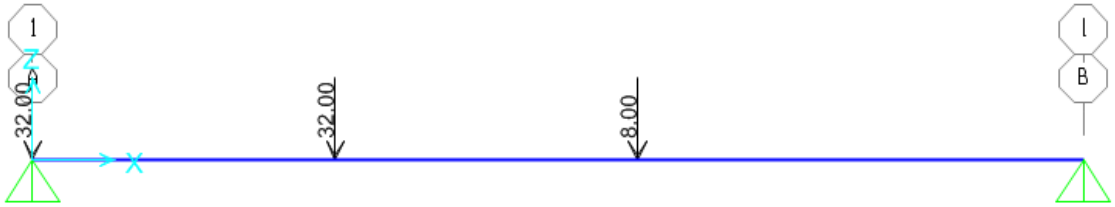

(b) Single Beam LDF Maximum Shear Reference

Figure 5.1 Riverside Experimental Bridge Single Beam LDF Reference Loading

The maximum modeling moments and shears found from all seven load cases are shown in Tables 5.1 and 5.3. These are the final values that were used to calculate the modeling LDFs for the Riverside bridge. The final modeling ratios of these critical moments and shear are also given to show the comparison between models for these critical LDF cases. The results from these modeling LDFs and from the AASHTO (2012) LDF equations for several bridge types are listed in Tables 5.2 and 5.4. A lever rule approximation of the load distribution factors is also provided for comparison.

Table 5.1 Maximum Modeling Moments and Ratios

Girder Position	Moment [k-ft]				G/FE Ratios	
	Single Beam	Grillage	FE Frame	FE Shell	Frame	Shell
Exterior	602.2	397.2	372.4	397.2	1.067	1.000
Interior		431.4	401.6	429.7	1.074	1.004

Table 5.2 Moment Load Distribution Factor Comparison

Girder Position	DFM [lanes/girder]						
	Grillage	FE Frame	FE Shell	AASHTO			Lever Rule
				Concrete Spread Box	Steel Spread Box	Concrete T- or I-Beam	
Exterior	0.66	0.62	0.66	0.68	0.69	1.35	0.63
Interior	0.72	0.67	0.71	0.66	0.69	1.27	0.97

Table 5.3 Maximum Modeling Shears and Ratios

Girder Position	Shear [k]				G/FE Ratios	
	Single Beam	Grillage	FE Frame	FE Shell	Frame	Shell
Exterior	58.7	37.8	36.2	35.8	1.044	1.056
Interior		51.7	47.9	49.4	1.079	1.047

Table 5.4 Shear Load Distribution Factor Comparison

Girder Position	DFV [lanes/girder]						
	Grillage	FE Frame	FE Shell	AASHTO			Lever Rule
				Concrete Spread Box	Steel Spread Box	Concrete T- or I-Beam	
Exterior	0.64	0.62	0.61	0.81	0.69	0.7	0.63
Interior	0.88	0.82	0.84	0.86	0.69	0.93	0.97

As can be seen in Tables 5.2 and 5.4, all models are providing similar load distributions, with the grillage model returning slightly conservative values for both moment and shear. This is ideal because it is best for the grillage model to be accurate and yet conservative for design. As expected, the AASHTO (2012) LRFD LDF equations for prestressed concrete box beams return the most similar results for DFM and DFV relative to those found from modeling the spread slab beam Riverside bridge. The lack of a typical sidewalk and curb on this bridge caused the d_e parameter to increase and reversed the typical trend of the interior girder being critical for the AASHTO moment LDF equations. These AASHTO LDFs are therefore not highly accurate and conservative for both shear and moment at all locations.

The AASHTO moment LDF for interior girders is close but unconservative for the spread concrete box beam equations, while the interior shear LDF is slightly conservative. The exterior LDF is slightly conservative for moment but overly conservative for shear. Overall the spread prestressed concrete box beam LDF equations given in the AASHTO LRFD Bridge Design Specifications (AASHTO 2012) are a reasonable approximation of the LDFs found from modeling but should still be adjusted to better capture the spread slab beam behavior.

5.3.2 Drehersville Bridge

The AASHTO (2012) LRFD LDF equations for spread box beams were also used to predict these factors for the Drehersville bridge in Pennsylvania. The calculation of these

LDFs for interior girder and exterior girders are shown below. Only the most eccentric two truck loading case (lanes 1 and 4 loaded) was explored for LDF purposes. This was because the highest moments for exterior and interior girders were both found from this loading in the modeling results and from the experimental results presented by Douglas and Vanhorn (1966). Also, the Riverside and Denison models all showed that the critical interior and exterior moments both came from the most eccentric two truck loading case possible, which for the Dreherseville bridge is the lanes 1 and 4 loading case. The exterior and interior moment LDF calculation according to the AASHTO (2012) LRFD Specification spread box beam equations is shown below.

Moment distribution factor for interior girder, one design lane loaded:

$$DFM_{in1} = \left(\frac{S}{3.0}\right)^{0.35}\left(\frac{Sd}{12.0L^2}\right)^{0.25} \tag{5.17}$$

$$= \left(\frac{7.167}{3}\right)^{0.35}\left(\frac{7.167(33)}{12\times 62.25^2}\right)^{0.25} = 0.362 \text{ lanes/girder}$$

Moment distribution factor for interior girder, two or more design lanes loaded:

$$DFM_{in2} = \left(\frac{S}{6.3}\right)^{0.6}\left(\frac{Sd}{12.0L^2}\right)^{0.125} \tag{5.18}$$

$$= \left(\frac{7.167}{6.3}\right)^{0.6}\left(\frac{7.167(33)}{12\times 62.25^2}\right)^{0.125} = 0.558 \text{ lanes/girder}$$

Moment distribution factor for exterior girder, two or more design lanes loaded:

$$DFM_{ex} = DFM_{in} \times e \tag{5.19}$$

$$e = 0.97 + \frac{d_e}{28.5} \tag{5.20}$$

$$e = 0.97 + \frac{-1.125}{28.5} = 0.931 \tag{5.21}$$

$$DFM_{ex} = 0.558 \times 0.931 = 0.519 \text{ lanes/girder}$$

The Drehersville bridge moment LDF comparisons for the interior and exterior girders are presented in Tables 5.5 through 5.7. The grillage model being used for this

comparison is the refined model with the cracked midspan diaphragm and the edge stiffening elements. All values are taken at section M for an accurate comparison and evaluation. A lever rule approximation of LDFs is also given.

Table 5.5 Drehersville Maximum Experimental and Modeling Moments

Girder Position	Moment [k-ft]					
	Single Beam	Experiment	Grillage	FE Frame	FE Shell	FE Solid
Exterior	755.9	477.1	495.4	381.3	364.8	358.4
Interior		373.0	360.6	350.7	342.1	343.1

Table 5.6 Drehersville Bridge Maximum Moment Ratio Comparisons

Girder Position	Model/Exp Ratios			
	Grillage	FE Frame	FE Shell	FE Solid
Exterior	1.038	0.799	0.765	0.751
Interior	0.967	0.940	0.917	0.920

Table 5.7 Drehersville Bridge Girder Moment Load Distribution Factors

Girder Position	DFM [lanes/girder]						
	Experiment	Grillage	FE Frame	FE Shell	FE Solid	AASHTO	Lever Rule
Exterior	0.63	0.66	0.50	0.48	0.47	0.52	0.45
Interior	0.49	0.48	0.46	0.45	0.45	0.56	0.74

As shown by Table 5.7, the grillage model of the Drehersville bridge provides the most accurate moment LDFs as compared to the experiment, although the interior girder LDF is slightly unconservative. The exterior girder LDF from the grillage model is conservative compared to the experimental results and the AASHTO equation for spread prestressed concrete box beams. The AASHTO spread box beam LDF equations

are moderately accurate and conservative for the interior girder, but unconservative for the exterior beam, when compared to the experimental results. The AASHTO equations predict that the interior beam is the critical girder, as is the case for most bridges, but for some reason, the Drehersville bridge shows a higher moment in the exterior girder. This difference is the cause of the formulae error. The original grillage model without a cracked diaphragm or edge stiffening elements gives moments less than two percent below the experimental values for the exterior girder, and six percent higher, and therefore conservative, for the interior girder.

The grillage models are the only models that give conservative moment LDFs while still providing an accurate model of the load distribution behavior of the bridge. Overall the other FE models also produce reasonable results, and could be further calibrated to the experimental results, but the grillage analysis results most closely matched the actual load sharing in the Drehersville bridge.

5.3.3 Denison Field Bridge

Live load distribution factor equations for spread prestressed concrete box beam bridges from AASHTO (2012) were used again for comparison to the LDFs found from the modeling described in section 4.5. The equations used and the calculation of these AASHTO (2012) moment and shear LDFs are shown below. The results found from these and the external girder LDF equations are listed in Table 5.8 and Table 5.9.

Moment distribution factor for interior girder, one design lane loaded:

$$DFM_{in1} = \left(\frac{S}{3.0}\right)^{0.35}\left(\frac{Sd}{12.0L^2}\right)^{0.25} \tag{5.22}$$

$$= \left(\frac{6.388}{3}\right)^{0.35}\left(\frac{6.388(15)}{12\times 50^2}\right)^{0.25} = 0.310 \text{ lanes/girder}$$

Moment distribution factor for interior girder, two or more design lanes loaded:

$$DFM_{in2} = \left(\frac{S}{6.3}\right)^{0.6}\left(\frac{Sd}{12.0L^2}\right)^{0.125} \tag{5.23}$$

$$= \left(\frac{6.388}{6.3} \right)^{0.6} \left(\frac{6.388(15)}{12 \times 50^2} \right)^{0.125} = 0.492 \text{ lanes/girder}$$

Moment distribution factor for exterior girder:

$$DFM_{ex} = DFM_{in} \times e \tag{5.24}$$

$$e = 0.97 + \frac{d_e}{28.5} \tag{5.25}$$

$$e = 0.97 + \frac{-3.5}{28.5} = 0.847$$

$$DFM_{ex} = 0.492 \times 0.847 = 0.417 \text{ lanes/girder}$$

Shear distribution factor for interior girder, one design lane loaded:

$$DFV_{in1} = \left(\frac{S}{10} \right)^{0.6} \left(\frac{d}{12.0L} \right)^{0.1} \tag{5.26}$$

$$= \left(\frac{6.388}{10} \right)^{0.6} \left(\frac{15}{12 \times 50} \right)^{0.1} = 0.528 \text{ lanes/girder}$$

Shear distribution factor for interior girder, two or more design lanes loaded:

$$DFV_{in2} = \left(\frac{S}{7.4} \right)^{0.8} \left(\frac{d}{12.0L} \right)^{0.1} \tag{5.27}$$

$$= \left(\frac{6.388}{7.4} \right)^{0.8} \left(\frac{15}{12 \times 50} \right)^{0.1} = 0.615 \text{ lanes/girder}$$

Shear distribution factor for exterior girder:

$$DFV_{ex} = DFV_{in} \times e \tag{5.28}$$

$$e = 0.8 + \frac{d_e}{10} \tag{5.29}$$

$$e = 0.8 + \frac{-3.5}{10} = 0.45$$

$$DFV_{ex} = 0.615 \times 0.45 = 0.277 \text{ lanes/girder}$$

The final interior girder moment distribution factor (DFM) is 0.492 lanes/girder and the final interior girder shear distribution factor (DFV) is 0.615 lanes/girder. These are the critical LDFs for moment and shear, respectively.

Table 5.8 Denison Bridge Maximum Moment and LDF Comparison

Girder Location	Moment [k-ft]			G/Solid Ratio	DFM [lanes/girder]		
	Single Beam	FE Solid	Grillage		FE Solid	Grillage	AASHTO
Exterior	626.7	204.8	216.3	1.057	0.33	0.35	0.42
Interior		243.2	260.4	1.071	0.39	0.42	0.49

Table 5.9 Denison Bridge Maximum Shear and LDF Comparison

Girder Location	Shear [k-ft]			G/Solid Ratio	DFV [lanes/girder]		
	Single Beam	FE Solid	Grillage		FE Solid	Grillage	AASHTO
Exterior	58.56	10.3	12.9	1.257	0.18	0.22	0.28
Interior		39.6	34.9	0.882	0.68	0.60	0.62

Tables 5.8 and 5.9 show fairly good agreement between both models and the AASHTO LDF equations for interior and exterior girders with both moment and shear. In all cases except the interior girder shear the grillage model is slightly conservative when compared to the solid finite element model, and the AASHTO spread box beam LDF equations are conservative when compared to the grillage results. The interior girders are shown to take slightly more moment than the exterior girders and significantly more shear than the exterior girders.

Based on the Denison bridge, the AASHTO LDF equations for spread prestressed concrete box beam bridges may only need adjustments to the interior beam shear to be suitable for spread slab beam bridges. However, this is only one case, and as shown by the Riverside models, some modifications need to be made to these AASHTO LDF formulae so that they are appropriately conservative for design of all spread slab

beam bridges. The AASHTO LDFs also do not take into account the median and if the median were not included in the modeling, the model results would be affected. This would likely lead to higher LDFs that would make most of the results more accurate, but possibly slightly unconservative.

5.4 INELASTIC ANALYSIS AND FAILURE LDFS

5.4.1 Overview

Load distribution factors and transverse load distribution behavior in a bridge deck can change at different loads. Typically LDF calculation is done using standard AASHTO truck loads as described in Section 3.4 and by AASHTO (2012). However, these are not always the loads acting on the bridge and may not represent the load distributions at an ultimate loading case near failure. To investigate this behavior, an inelastic push down analysis was done using the evenly spaced refined Riverside experimental bridge grillage model. This was done by assigning plastic hinges to the longitudinal grillage members and uniformly increasing all axle loads in all seven moment and shear load cases described by Tables 3.6 and 3.5. The loads were increased until the hinges failed and the force-deformation relationships in the girders became nonlinear.

5.4.2 Plastic Hinge Definition

SAP2000 does not automatically model hinges at locations of local yielding in frame elements so hinges had to be assigned to the longitudinal members. Since both ends of the bridge are modeled as pinned connections and are able to rotate about the transverse direction, only one additional free rotation point, or hinge, is needed for failure. This failure hinge will form at the location of the maximum moment but will not fail immediately upon forming, only once the entire cross-section has yielded. The maximum moment is found at midspan in all girders for the moment loading cases, while it is found at 3/8 of the full length in the girders for the shear loading cases. These maximum moment, and therefore hinge, locations were determined by examining the

results of all seven two truck service loading cases for both moment and shear load distribution factor calculation.

SAP2000 only allows hinges to be assigned to certain types of frame members. The precast concrete T-beam members that had been used for the two truck service loading did not permit the use of hinges so new longitudinal beam members were implemented. The bending moment of inertia and the torsional constant for the interior and the exterior members were recorded in Table 3.3 and new rectangular reinforced concrete beam members were created. These new members were made to be the same total depth as the previous T-members, but had prorated widths that were between the flange and web widths of the T-beams. The bending moment of inertia and torsional constant of these beams were then adjusted to match those of the original T-beams using property modifiers.

These new longitudinal grillage members were tested at the service loadings of all seven transverse load cases for moment and shear modeling. The rectangular members with the adjusted stiffness properties showed identical deflections and internal moments and shears for the service loading cases listed in Table 3.6 and Table 3.5. This confirmed that the revised SAP2000 model was consistent with the original model that used T-beams.

Due to the difference in hinge location for the critical moment and shear loading cases, two different models with rectangular beams had to be developed. One model was made for the moment loading configuration and had hinges at midspan, while the other model was made for shear loading and used 3/8 of the full length as the hinge location for all girders. Although the hinges were input in these locations they were defined so that the hinge would not start forming until the flexural capacity was reached. After this first formation the plastic hinges start to show material non-linearity in the model and the bridge starts to deform plastically, but the hinge location continues to hold moment until the full cross-section yields and the plastic moment is reached. At this point the hinge will fail, causing large deflections and zero moment capacity at that location.

The default hinge properties in SAP2000, from the Federal Emergency Management Agency (FEMA) Standard 356 (FEMA 2000) were used for these models. These hinge characteristics are dependent upon the section and material properties of the longitudinal members. They are also specified for each type of failure hinge, such as torsional, moment, or interacting moment and force, as well as the type of failure with options for force controlled (brittle) and deformation controlled (ductile). For the modeling done in this project only M3, moment about axis 3, which runs transversely across the bridge section, was used for hinge failure type, and it was assumed to be deformation controlled.

The general hinge backbone shape used by FEMA 356 (FEMA 2000) and by SAP2000 is shown in Figure 5.2. Points A through E represent different stages of structural behavior, with A being at rest with no load, B representing the first yielding in the cross-section, at C the member reaches full plastic moment, and D and E represent capacity loss and failure. IO, LS, and CP stand for Immediate Occupancy, Life Safety, and Collapse Prevention, and are described further in FEMA 356 (FEMA 2000) and set as their default values in SAP2000. The shape of this force-deformation graph also follows the shape of the moment-rotation graph for hinges. Figure 5.3 shows the hinge properties used in SAP2000 as they were set up in the models.

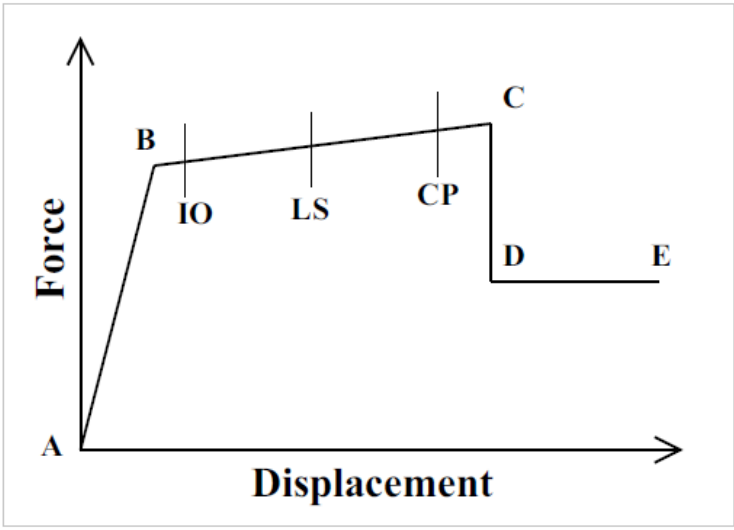

Figure 5.2 FEMA 356 Hinge Force-Deformation Relationship (Computers and Structures 2012a)

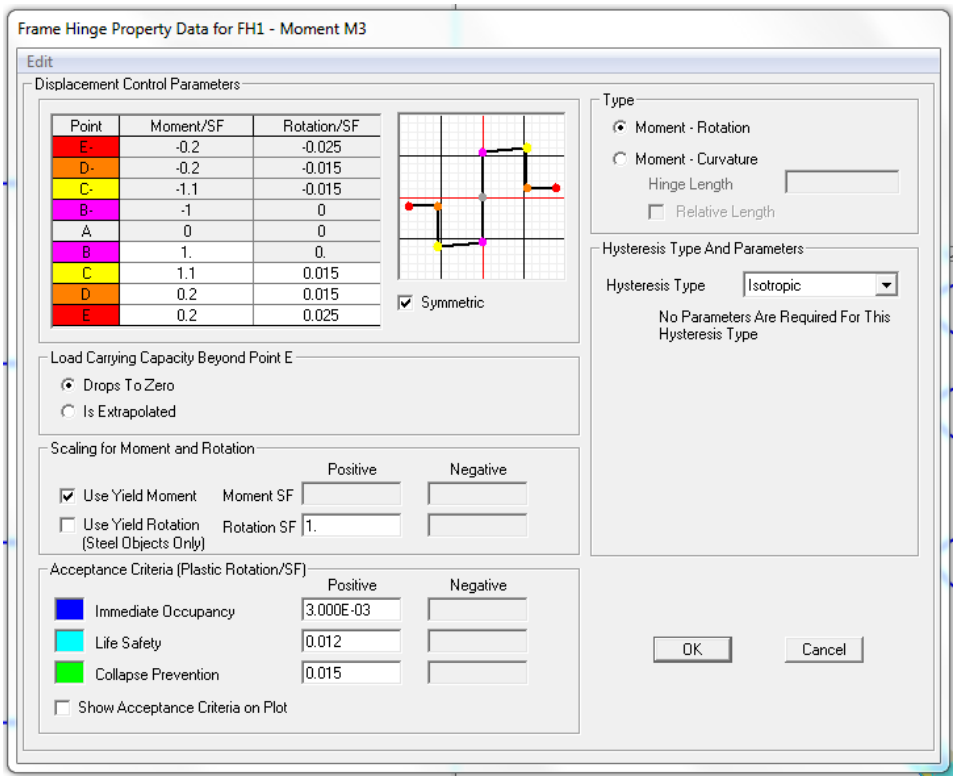

Figure 5.3 SAP2000 M3 Hinge Properties Used

5.4.3 Application of Truck Overload

The Riverside experimental bridge will only have two lanes and the critical service and design two truck loading cases described in Section 3.4 and determined from the AASHTO LRFD Bridge Design Specifications (2012) are considered to be the highest expected load the bridge will see. The two truck loading also takes up most of the driving space on the bridge as the span is relatively short and the bridge only has 32 ft of total roadway width. To test the overload capacity and to apply a reasonable ultimate load to the bridge, no additional trucks were added to the load configuration, but rather the axle loads from the two truck critical loading cases were uniformly scaled up by a certain factor. Not only were the service loading cases scaled up in SAP2000, but they were also set to take into account nonlinearities. Finally, the overload load cases were divided into twenty-five steps so that each portion of the hinge backbone shown in

Figure 5.2 would have multiple points and the hinge formation could be analyzed over several intermediate loads.

The stepped loading approach also allowed for a close determination of the failure load without having to conduct multiple trial and error loading magnitudes for every load case. The seven critical moment loading cases all required the service loading of 144 k (72 k total force for each truck) to be amplified by a factor of 2.5 to reach failure. However, due to the configuration of the critical shear loading cases which placed the trucks much closer to one end of the bridge, a factor of 4 was needed to reach failure for this configuration. Note that the model does not account for shear failures. The moment and shear results as well as the force-deformation graphs for the stepped overload cases are shown in Section 5.4.4 below and in Appendix C.

5.4.4 Inelastic Results and Comparisons

5.4.4.1 Hinge Formation

The stepped inelastic overload analysis not only gives the all the intermediate loads, moments, shears, and reactions before failure, but also shows the formation of the hinges and the level of demand for these hinges. At the step when hinges first start to form they appear as colored dots on the model which represent different regions within the hinge backbone shown in Figure 5.3. Figure 5.4 below shows several levels of hinge formation in the grillage model during the analysis of the lane 7 moment loading case (two truck centered on the bridge) until failure. The hinge colors represent different stages of the hinge backbone with the pink being IO, the dark blue representing LS, and the light blue meaning CS, as defined above. Figure 5.5 shows the hinge results as a blue dot on the hinge backbone for the final step before failure.

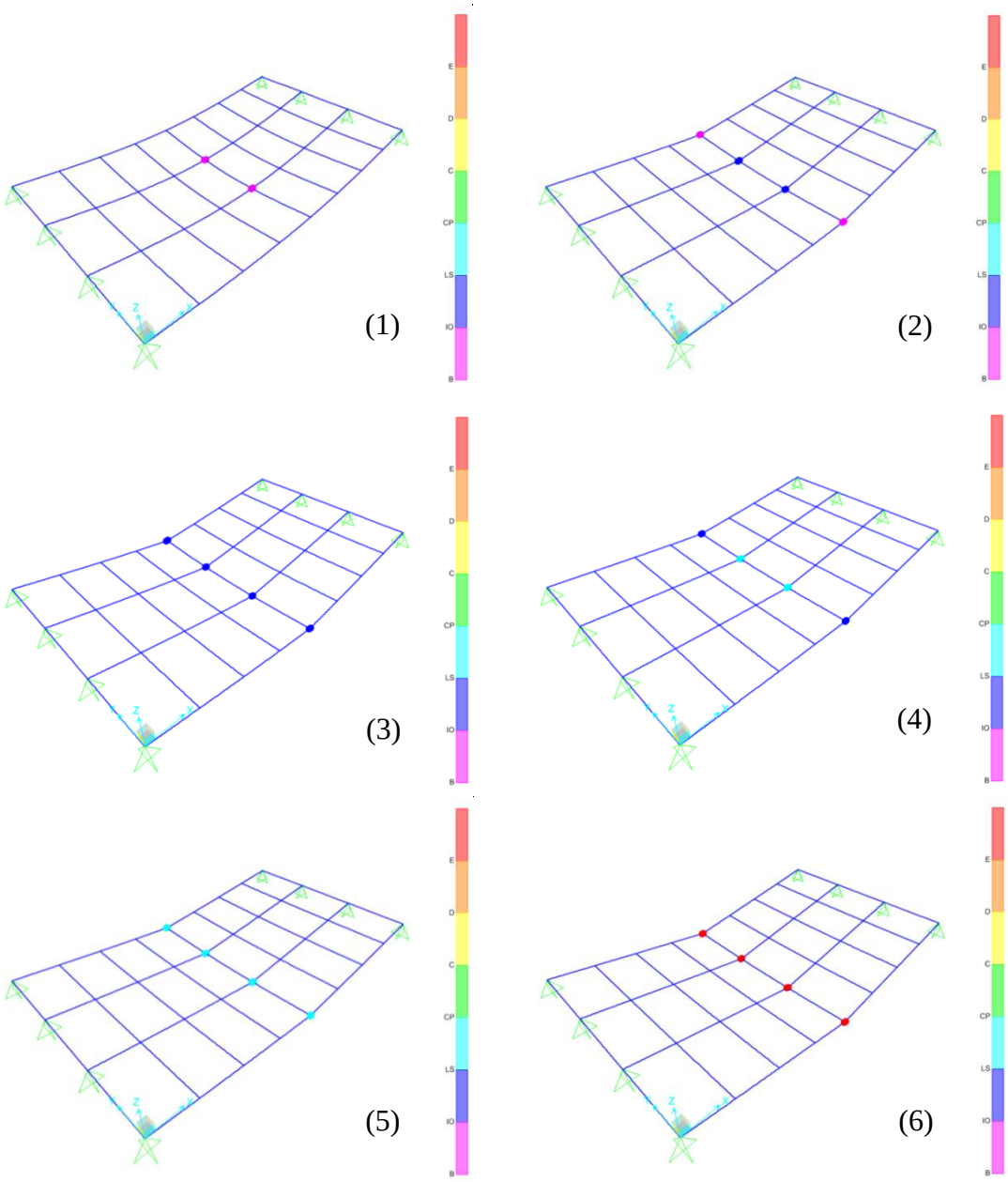

Figure 5.4 Six Steps of Hinge Formation and Failure in Grillage Moment Loading Case 7

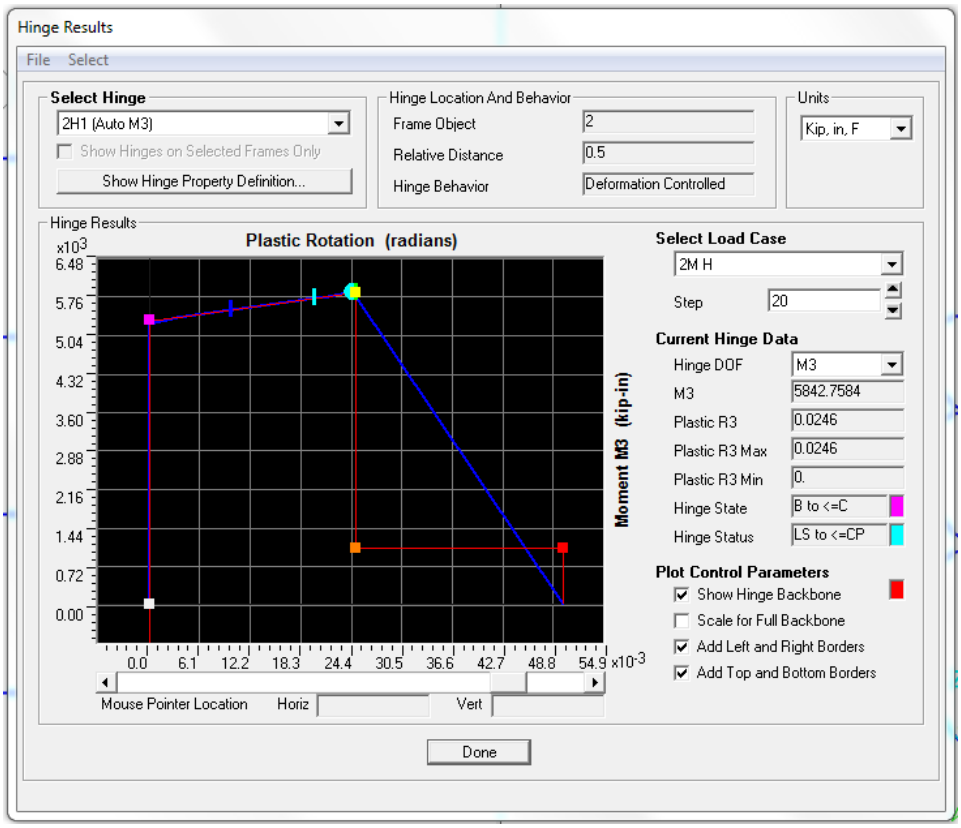

Figure 5.5 Hinge Results for Near Failure Moment Overloading Case 7

The figures above show that for the lane 7 centered loading case hinges form first in the interior girders and are followed closely by the exterior girders. It was also shown that for other loading cases that placed the loading more eccentrically on the bridge so that the exterior girder was most heavily loaded, this exterior girder formed a plastic hinge first and the far exterior girder formed a hinge last. The hinges always formed first in the longitudinal grillage member with the highest moment. This is to be expected as not all girders share the load equally and those that reach capacity first will begin to yield and cause additional loading to be placed on the adjacent girders.

5.4.4.2 Ultimate Load Distribution Factors

In order to calculate the load distribution factors from the overload case, the point loads on the single beam model had to be scaled up to be the equivalent of one overload truck load, or half of the total load on the full model just before failure. Because each load

case contained 25 steps, the load and maximum moment or shear from the step just before failure were recorded. This factor was slightly different for each loading case and had to be calculated and applied separately for all fourteen single beam load cases. The load from every step as well as the deflection of every step in every load case was also recorded to develop load deflection plots.

The ultimate load distribution factors are calculated for the step just before failure because at failure the moment capacity at the hinge drops to zero and the behavior of the bridge changes drastically. Emphasis was not placed on what happens after failure, but rather what the bridge load sharing behavior is at a near failure load. Tables 5.10 through 5.13 below show the overloading results for determination of load distribution factors. The term failure in these tables is actually used to describe the step just before failure. The service values come from the final grillage model discussed in Section 4.

Table 5.10 Overload Data from Critical Moment Loading of Grillage Model

Loading Case	Outside Wheel Location From Edge [ft]	Load Step Before Failure	Total Load At Step [k]	Load Increase Factor	Single Beam Moment [k-ft]
1	3	21	314.3	2.18	1305
2	4	20	326.4	2.27	1359
3	5	21	324.9	2.26	1353
4	6	22	330.4	2.29	1371
5	7	21	329.6	2.29	1371
6	8	23	335.6	2.33	1394.
7	9	23	341.9	2.37	1418

Table 5.11 Load Distribution Factors and Comparison for Moment Overloading

Load Case	Failure Moment [k-ft]		Interior/Exterior Ratio		DFM			
					Exterior		Interior	
	Exterior	Interior	Failure	Service	Failure	Service	Failure	Service
1	517.3	578.0	1.12	1.07	0.40	0.64	0.44	0.69
2	502.4	597.3	1.19	1.16	0.37	0.59	0.44	0.68
3	486.3	598.2	1.23	1.25	0.36	0.54	0.44	0.67
4	484.5	602.5	1.24	1.35	0.35	0.49	0.44	0.66
5	482.7	598.4	1.24	1.46	0.35	0.44	0.44	0.65
6	481.9	595.5	1.24	1.58	0.35	0.40	0.43	0.63
7	481.1	588.2	1.22	1.71	0.34	0.36	0.41	0.61

Table 5.12 Overload Data From Critical Shear Loading of Grillage Model

Loading Case	Outside Wheel Location From Edge [ft]	Load Step Before Failure	Total Load At Step [k]	Load Increase Factor	Single Beam Shear [k]
1	3	20	483.8	3.36	195.1
2	4	22	526.3	3.66	212.45
3	5	23	545.2	3.79	219.97
4	6	22	556.3	3.86	224.01
5	7	21	541.1	3.76	218.23
6	8	23	566.1	3.93	228.06
7	9	23	560.4	3.89	225.75

Table 5.13 Load Distribution Factors and Comparison for Shear Overloading

Load Case	Failure Shear [k]		Interior/Exterior Ratio		DFV			
					Exterior		Interior	
	Exterior	Interior	Failure	Service	Failure	Service	Failure	Service
1	120.4	160.7	1.34	1.37	0.62	0.65	0.82	0.89
2	107.0	167.3	1.56	1.60	0.50	0.56	0.79	0.89
3	92.6	173.3	1.87	1.91	0.42	0.47	0.79	0.89
4	76.9	177.6	2.31	2.36	0.34	0.38	0.79	0.89
5	64.4	169.1	2.63	2.73	0.30	0.32	0.77	0.87
6	56.1	168.5	3.00	3.15	0.25	0.26	0.74	0.83
7	46.0	159.6	3.47	3.75	0.20	0.21	0.71	0.79

As shown by the results above it is clear that as the load increases to an overload state the girders on the opposite side of the loading take a larger portion of the load. This is confirmed because the load distribution factors for all failure loadings are lower than those found from the service loadings. The increased load sharing amongst girders occurs when plastic hinges start forming in the critical girders, hindering their capacity as failure occurs and increasing deflections, then load is redistributed to the sections that had not initially yielded.

The interior/exterior girder moment and shear ratio comparisons between failure and service are also quite important in understanding load distribution differences between the service and overload cases. The moment ratios at failure increase slightly as the load moves towards the interior of the bridge but the interior girder never has more than 1.24 times the moment in the exterior girder. At service this difference from loading case 1 to loading case 7 is much higher, reaching 71% higher at the centered loading (load case 7). The shear interior/exterior girder ratio does not change as drastically from service loading to failure loading. The failure loading ratio is slightly less than the service ratio for all seven load cases, meaning that the exterior girder does contribute a

little more capacity at overload, but in general it shows the same distribution trends as at service for the critical load arrangement for shear.

The moment LDFs for the near failure loading were considerably less than the service LDFs for both interior and exterior girders. The final critical moment LDF for each loading case and each girder show that at service these factors are about 150% of those at failure. The failure moment LDFs are 0.40 and 0.44 lanes/girder for the exterior and interior girders respectively. The highest LDF values come from loading case 1, with axle loads nearest to the edge of the bridge. At service the moment LDFs are 0.64 and 0.69 lanes/girder for exterior and interior girders and again come from load case 1.

Shear load distribution factors showed a much higher correlation between service and failure loadings. The factors were slightly less at failure, indicating an additional contribution from the girders farthest from the loading, but overall showed that the distributions do not change very much as the load is increased for the critical shear loading arrangement. The final shear LDFs are 0.62 and 0.82 at failure and 0.65 and 0.89 at service for interior and exterior girders respectively. These maximum LDFs are once again all found from the most eccentric loading, case 1. The failure LDFs for both shear and moment did not show any closer correlation with any of the LDFs from AASHTO equations as listed in Table 5.2 and Table 5.4, and the spread box beam equations still seem the most accurate in predicting load distributions in this spread slab beam bridge.

5.4.4.3 Inelastic Force Deformation Behavior

To show the inelastic force deformation behavior of the girders, the load and maximum deformation of every step for every load case was recorded up to failure. These values were then plotted to examine how the elastic behavior changes between the shear and moment loading configuration and in each loading case. The plots for moment and shear lane loading case 1 and 7 are shown below to give the extreme loading cases. All other plots presented very similar results and are shown together in Appendix C.

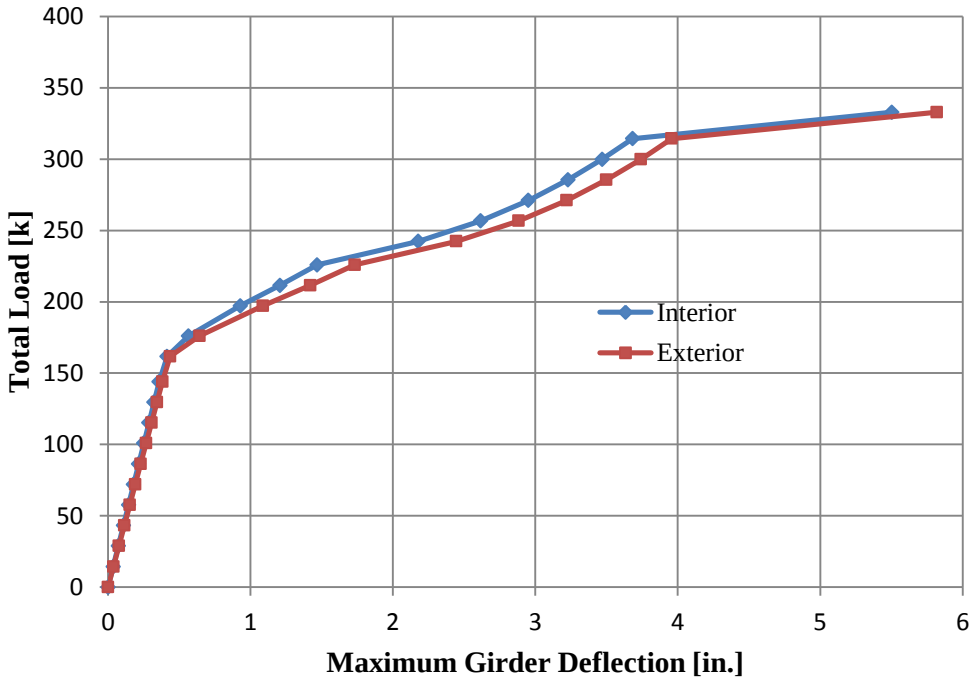

(a) Lane 1 Loading

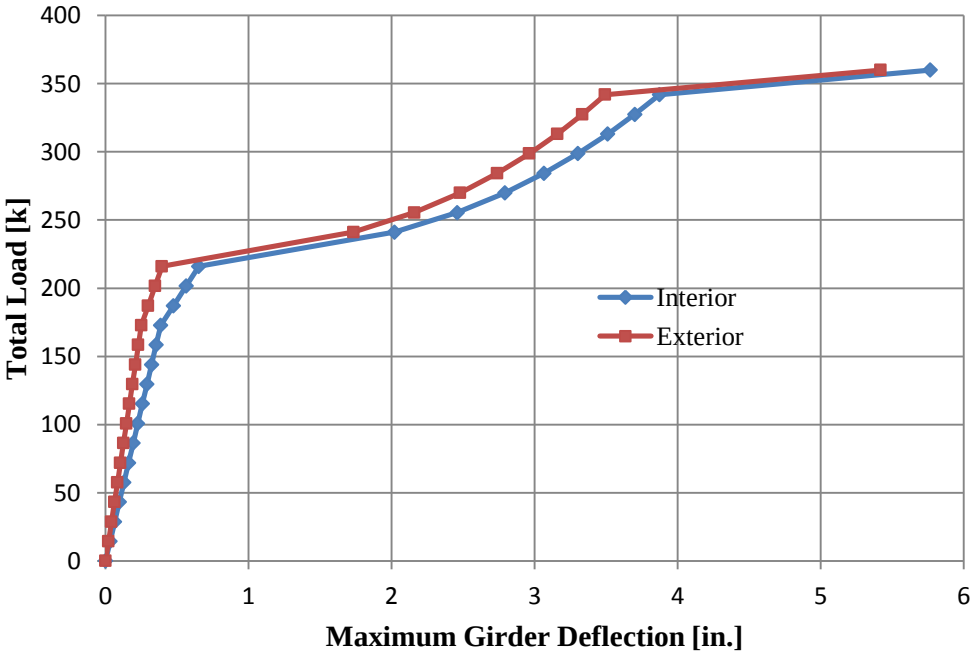

(b) Lane 7 Loading

Figure 5.6 Inelastic Force-Deformation of Extreme Moment Loading Cases

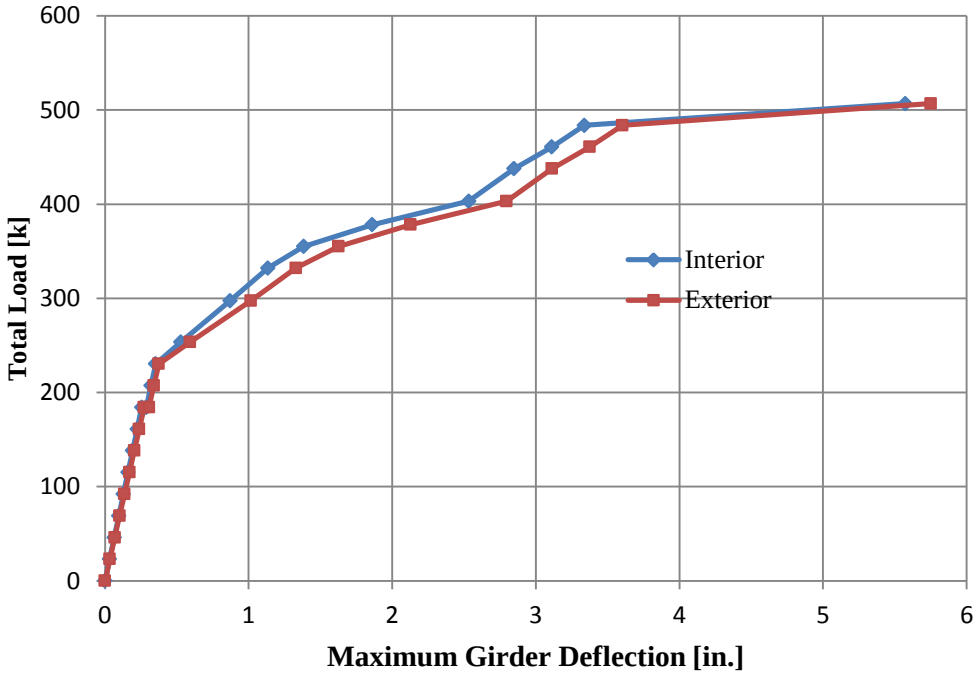

(a) Lane 1 Loading

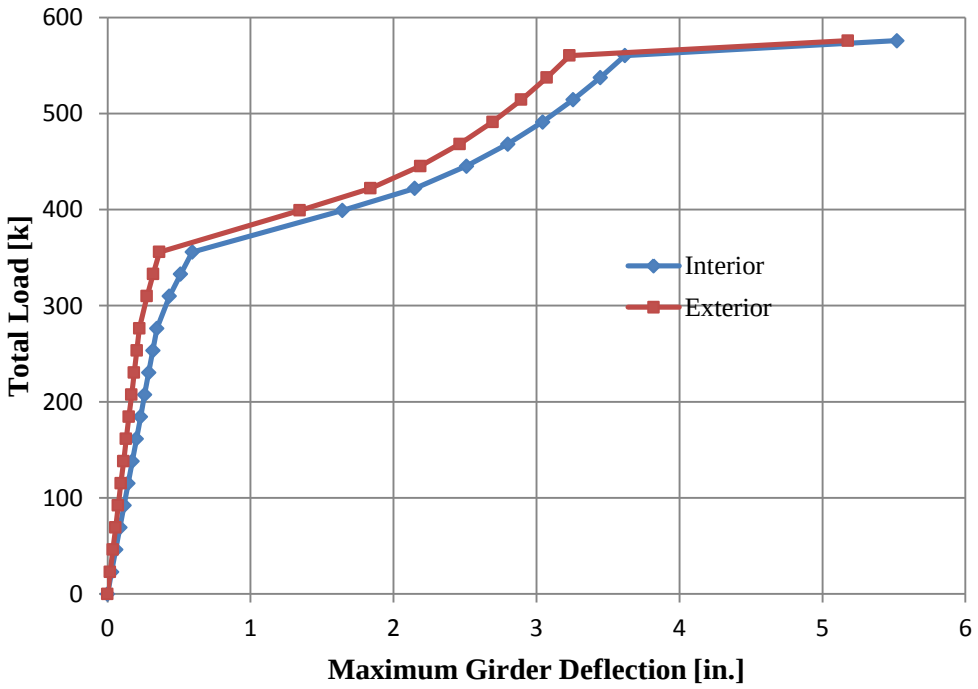

(b) Lane 7 Loading

Figure 5.7 Inelastic Force-Deformation of Extreme Shear Loading Cases

As shown by the Figures 5.6 and 5.7, as the truck loading moves in towards the center of the bridge from the outside (as the load case number increases), the exterior girder goes from a higher deformation than the interior girder to a lower deformation than the interior girder under the same load. This is intuitive and ensures that the model is correctly handling this behavior. It also shows that as the load moves closer to the center of the bridge the total load reached before failure and before the first formation of hinges and inelastic behavior increases. This may be explained as when the load is centered on the bridge all of the girders are relatively close to the centroid of the loading and the load can therefore be distributed amongst all girders more effectively.

The highest expected service loading of the bridge is two 72 k trucks for a total of 144 k. As shown by these plots, the inelastic behavior did not start until a higher load than this was reached. Even after the initial formation of hinges and inelastic behavior, the girders were able to support at least another 100 k before the hinges completely failed, which is shown by the large jump in deflection at the last point. All load cases showed that no matter what the total force was on the bridge, the inelastic hinge behavior and failure both occurred at nearly the same deflection every time.

5.4.4.4 Discussion

This overload analysis provides insight into the bridge behavior at higher loads up to failure. However, this is not considered a highly accurate overload model. The grillage model could be modified to include hinges at all intersections of longitudinal and transverse members as the load increased to consider the spreading of inelastic behavior at higher loads. Also the model has some limitations, such as lack of a shear (brittle) failure prediction model. The overload analysis results should be used as an approximation of the overload and inelastic behavior, but a more comprehensive model must be developed for accurate results.

6. SUMMARY, CONCLUSIONS, AND RECOMMENDATIONS

6.1 SUMMARY

This research was conducted as part of TxDOT project 0-6722 to examine the load distribution behavior of spread slab beam bridges, focusing on the results given by the grillage method of analysis. Three bridges were modeled in SAP2000 using the grillage method and numerous different grillage assumptions and techniques were tested. All grillage models for all three bridges were compared to more in depth finite element analysis of the same bridges and experimental data when available. The full FEA models used for calibration of the grillage analysis included frame, shell, and solid element models, with the first two being created in the program CSiBridge and the latter being developed in Abaqus. The FEA models were developed as part of the project by other researchers (Hueste et al. 2014).

The objective of this study was to determine if the simplified method of bridge superstructure analysis that is the grillage approach may be used as an expedited, conservative, and reasonably accurate method of calculating the load distribution factors for spread prestressed slab beam bridges. Bridge girder load distribution factors must be found from computer modeling or use of the lever rule in cases when no AASHTO LRFD Bridge Design Specifications (AASHTO 2012) load distribution factor formulae exist for the bridge type or bridge parameter ranges being investigated. The purpose of this study was to give recommendations for the proper use of the grillage method for load distribution factor (LDF) calculation and to investigate appropriate LDF values for spread slab beam bridges.

6.2 CONCLUSIONS

Based on the research presented in this thesis, the following major conclusions may be drawn:

1. The grillage modeling approach for bridge superstructures described in this work was effective at predicting the load distribution relationships found in existing

experimental data for a spread box beam bridge (Douglas and Vanhorn 1966) and by frame, shell, and solid element FEA of two spread slab beam bridges (Hueste et al. 2014), within a reasonable level of accuracy. This simplified method of analysis may be used to estimate load distribution factors for spread slab beam bridges and other similar bridge types that are not found in AASHTO (2012).

2. In general, the critical moment analysis conducted using the grillage models produced results that were more accurate when compared to higher levels of FE modeling and experimental data than the critical shear analysis. To improve the initial shear results, loads placed on the end transverse member had to be manually distributed to the longitudinal girders based on the lever rule and placed slightly into the member length. This technique resulted in much more realistic and agreeable internal end shear values in the longitudinal grillage members and corrected the errors caused by the end transverse member and support interaction.
3. For all bridges, the critical load cases for interior and exterior girders always placed both trucks next to one another and as far to one edge of the bridge as possible. The interior girder was shown to have higher moments and shears for both slab beam bridges, while the spread box beam bridge contradicted with the AASHTO LDF predictions and gave higher moment results in the exterior girder. Moment was distributed more evenly between girders than shear, which was mostly concentrated close to the placement of loads.
4. The AASHTO (2012) LDF equations for spread box beam bridges are the most accurate set of simplified equations for the spread slab beam bridges considered but they are not accurate and conservative for all critical cases examined. These equations may be used as a basis for developing spread slab beam bridge LDF equations once an adequate amount of slab beam bridge load distribution data has been collected and analyzed.

5. Overload LDFs from a near failure state after the formation of hinges in the girders showed that both shear and moment are distributed much more evenly amongst all girders in the bridges at ultimate when compared to service load distributions. All girders were near their full capacities at almost the same load, thereby all working together to resist the overload on the bridge, instead of having a few critical girders as in the service loading cases.

6.3 MODELING AND LDF RECOMMENDATIONS

Three different bridges were modeled as part of this research. Two of these bridges, the Riverside experimental bridge and the Denison field bridge, are spread slab beam bridges. The third bridge, the Drehersville bridge, is a spread box beam bridge. Based on the results from the full FEA computer models (Hueste et al. 2014) and from the existing experimental data on the Drehersville bridge (Douglas and Vanhorn 1966), the grillage models for these bridges were calibrated to give comparable and reasonably accurate results for all three bridges. However, due to the variation in the results between different bridges, and the relatively small number of bridges investigated as part of this thesis, the development of preliminary load distribution equations for spread slab beam bridges was shown to be impractical at this stage. At this point it is more accurate and effective to use grillage or finite element analysis to predict LDFs than to adjust a current AASHTO LDF equation for spread box beams to attempt to capture the behavior of a small number of bridge models.

The current AASHTO LDF equations for spread box beam bridges seem to give generally acceptable results for interior and exterior shear and moment cases for most loading cases in the considered bridges, but not for all cases. Overall models were consistent in the estimated bridge behavior, but none of the models matched ideally in all cases for any bridge and no model was able to completely capture the load distribution behavior shown by the Drehersville bridge experimental results. Additional experimental instrumentation data is needed from the Riverside and Denison bridges before any models may be truly calibrated and the actual bridge behavior is confirmed.

From the information available during this project, and based on the assumptions that the Drehersville bridge data, and the frame, shell, and solid element models are all reasonably accurate, recommendations for grillage modeling of LDFs are provided below.

1. Longitudinal grillage members should coincide with the centerlines of the girders and should include the transformed tributary deck section. Supports are modeled at the end of each longitudinal member and should reflect the nearest approximation of the actual support conditions. Transverse members should be modeled at a similar spacing to the longitudinal members but not over 10 ft and should only include the bridge deck. Because the bridge deck is used in both the longitudinal and transverse members, the torsional stiffness in each should be factored by half.
2. An evenly spaced grillage model will require the loads to be split to the two nearest transverse members by use of the lever rule, and will still give reasonably accurate results. A transverse grillage model spacing that is set up so that the critical axle load configuration places loads directly on certain grillage members may result in slightly more precise results. If the critical single beam shear loading configuration places an axle load directly over one of the end supports, this end axle load must be distributed away from the end transverse member in the grillage model and placed roughly 0.0001 in. into the ends of the longitudinal members. All members should be meshed so that additional nodes are created along their length, ideally at distances of 1 ft or less, and at every intersection. This will increase the resolution and give more accurate values.
3. If diaphragms exist in the bridge superstructure, model these members as part of the transverse grillages and space the grillage members accordingly. In the case that the midspan diaphragm is acting to pull the girders opposite from the load upwards, the bending and torsional stiffnesses of the diaphragm should be factored down, with a factor of 5% if it is to be modeled as fully cracked. Edge stiffening elements may be modeled by adding their torsional and bending

stiffnesses to the edge longitudinal members but they should only be included if they are considered structural elements and may be left out if the results without them are reasonable and conservative.

4. The load distribution factors are found by loading the bridge with two AASHTO design trucks or tandems placed next to each other at the critical longitudinal distance to induce the maximum girder moment or shear. The critical transverse location of the trucks or tandems can be found by testing several different transverse locations by moving the trucks over across the bridge 1 ft at a time. Consult (AASHTO 2012) Art. 3.6.1 for truck and tandem loading and spacing standards. The maximum moment or shear value found in the longitudinal members is divided by those found from a simple single beam analysis that places one truck or tandem's axle loads at the same critical longitudinal spacing. This value is then in units of design lanes per girder, which provides the load for which each girder is designed.

6.4 RECOMMENDATIONS FOR FUTURE RESEARCH

The modeling agreement between several methods in this study indicates that this work is on the right path, but before load distribution factor equations can be developed for spread slab beam bridges, much more research is required.

1. As stated above, the experimental results from the Riverside bridge and the data from the observation of the Denison bridge will greatly supplement this work and will allow for a full and accurate calibration of the models in this study if they are not already accurate.
2. If any other existing spread slab beam bridges can also be tested and modeled, either as part of TxDOT project 0-6722 or as part of another project, this will also help to confirm the modeling calibration procedures needed to precisely capture the bridges behavior of this bridge type.
3. Once the model calibration is confirmed for FE and grillage models, many more hypothetical spread slab beam bridges may be modeled by varying one parameter

at a time. With a larger database of spread slab beam bridge load distribution behavior, development of LDF expressions is possible if the results show converging trends for the effect of different bridge parameters on transverse load distributions.

REFERENCES

AASHTO (1989). *AASHTO Standard Specifications for Highway Bridges*, American Association of State Highway and Transportation Officials, Washington, DC.

AASHTO (1994a). *AASHTO Guide Specifications for Distribution of Loads for Highway Bridges*, American Association of State Highway and Transportation Officials, Washington, DC.

AASHTO (1994b). *AASHTO LRFD Bridge Design Specifications*, American Association of State Highway and Transportation Officials, Washington, DC.

AASHTO (1996). *AASHTO Standard Specifications for Highway Bridges*, American Association of State Highway and Transportation Officials, Washington, DC.

AASHTO (1998). *AASHTO LRFD Bridge Design Specifications*, American Association of State Highway and Transportation Officials, Washington, DC.

AASHTO (2002). *AASHTO Standard Specifications for Highway Bridges*, American Association of State Highway and Transportation Officials, Washington, DC.

AASHTO (2004). *AASHTO LRFD Bridge Design Specifications*, American Association of State Highway and Transportation Officials, Washington, DC.

AASHTO (2007). *AASHTO LRFD Bridge Design Specifications*, American Association of State Highway and Transportation Officials, Washington, DC.

AASHTO (2012). *AASHTO LRFD Bridge Design Specifications*, American Association of State Highway and Transportation Officials, Washington, DC.

Adnan, M. (2005). "Impact of AASHTO LRFD Specifications on the Design of Precast, Pretensioned U-Beam Bridges."MS Thesis, Texas A&M University, College Station, TX.

Barker, R. M., and Puckett, J. A. (2007). *Design of Highway Bridges: An LRFD Approach*, John Wiley & Sons, Inc., Hoboken, NJ.

Barr, P. J., Oberhard, M. O., and Stanton, J. F. (2001). "Live-Load Distribution Factors in Prestressed Concrete Girder Bridges." *ASCE Journal of Bridge Engineering*, 6(5), 298-306.

Boresi, A. P., and Schmidt, R. J. (2003). *Advanced Mechanics of Materials*, John Wiley & Sons, New York, NY.

Chen, Y., and Aswad, A. (1996). "Stretching Span Capability of Prestressed Concrete Bridges under AASHTO LRFD." *ASCE Journal of Bridge Engineering*, 1(3), 112–120.

Computers and Structures, I. (2012a). "CSI Knowledge Base." Computers and Structures, Inc., Berkeley, CA.

Computers and Structures, I. (2012b). SAP2000, version 15. Computers and Structures, Inc., Berkeley, CA.

Computers and Structures, I. (2012c). CSiBridge, version 15. Computers and Structures, Inc., Berkeley, CA.

Dassault Systemes, S. A. (2013). Abaqus, version 6. Abaqus, Inc., Velizy-Villacoublay, FR.

Douglas, W. J., and Vanhorn, D. A. (1966). "Lateral Distribution of Static Loads In A Prestressed Concrete Box-Beam Bridge. Drehersville Bridge." Lehigh University, Fritz Engineering Laboratory Report No. 350.1, Bethlehem, PA.

Eamon, C. D., and Nowak, A. S. (2002). "Effects of Edge-Stiffening Elements and Diaphragms on Bridge Resistance and Load Distribution." *ASCE Journal of Bridge Engineering*, 7(5), 258-266.

Eom, J., and Nowak, A. S. (2001). "Live Load Distribution for Steel Girder Bridges." *ASCE Journal of Bridge Engineering*, 6(6), 489-497.

FEMA (2000). "FEMA 356 Prestandard and Commentary for the Seismic Rehabilitation of Buildings." Federal Emergency Managment Agency, Washington, DC.

Goodrich, B. L., and Puckett, J. A. (2000). "Simplified Load Distribution for Vehicles with Nonstandard Axle Gauges." *Journal of the Transportation Research Board*, 1696(1), 158-170.

Hambly, E. C. (1975). "Grillage Analysis Applied to Cellular Bridge Decks." *The Structural Engineer*, 53(7), 267-276.

Hambly, E. C. (1976). *Bridge Deck Behaviour*, Halsted Press, New York, NY.

Hambly, E. C. (1991). *Bridge Deck Behaviour*, Taylor & Francis, New York, NY.

Harris, D. K. (2010). "Assessment of Flexural Lateral Load Distribution Methodologies for Stringer Bridges." *Engineering Structures*, 32(11), 3443-3451.

Harris, D. K., Cousins, T., Sotelino, E. D., and Murray, T. M. (2010). "Flexural Lateral Load Distribution Characteristics of Sandwich Plate System Bridges: Parametric Investigation." *ASCE Journal of Bridge Engineering*, 15(6), 684-694.

Hueste, M. B., Mander, J., Terzioglu, T., Petersen-Gauthier, J., and Jiang, D. (2014). "TxDOT Project 0-6722 Report: Spread Slab Beam Research." Texas Transportation Institute, College Station, TX.

Hueste, M. B. D., Adil, M. S., Adnan, M., and Keating, P. B. (2006a). "Impact of LRFD Specifications on Design of Texas Bridges Volume 1: Parametric Study." Texas Transportation Institute and Texas Department of Transportation, College Station, TX, 285-306.

Hueste, M. B. D., Adil, M. S., Adnan, M., and Keating, P. B. (2006b). "Impact of LRFD Specifications on Design of Texas Bridges Volume 2: Prestressed Concrete Bridge Girder Design Examples." Texas Transportation Institute and Texas Department of Transportation, College Station, TX, A.1-1-B.2-67.

Kaveh, A., and Talatahari, S. (2010). "Charged System Search for Optimum Grillage System Design Using the LRFD-AISC Code." *Journal of Constructional Steel Research*, 66(6), 767-771.

Kocsis, P. (2004). "Evaluation of AASHTO Live Load and Line Load Distribution Factors for I-Girder Bridge Decks." *Practice Periodical on Structural Design and Construction*, 9(4), 211-215.

Lightfoot, E., and Sawko, F. (1959). "Structural Frame Analysis by Electronic Computer: Grid Frameworks Resolved by Generalised Slope-Deflection." *Engineering*, 187, 18-20.

McKee, D. C., and Turner, H. T. (1975). "Design and Review of Precast Concrete Bridge Elements." FHWA and Luisiana Department of Highways, FHWA-LDH-LSU(75-1ST).

Newmark, N. M. (1938). *A Distribution Procedure for the Analysis of Slabs Continuous over Flexible Beams*, University of Illinois, Urbana, IL.

Nowak, A. S. (1993). "Live Load Model for Highway Bridges." *Structural Safety*, 13(1-2), 53-66.

Panak, J. J. (1982). "Economical Precast Concrete Bridges." *FHWA-TX-83-08+226-1F Final Rpt.*, FHWA and Texas Department of Highway & Public Transportation, Austin, TX.

Parke, G., and Hewson, N. (2008). *ICE Manual of Bridge Engineering*, Thomas Telford, London, UK.

Powell, G. H., and Buckle, I. (1970). *Computer Programs for Bridge Deck Analysis*, College of Engineering, Office of Research Services, University of California, Berkeley, CA.

Puckett, J. A., Mertz, D., Huo, X. S., Jablin, M. C., Peavy, M. D., and Patrick, M. D. (2005). "Simplified Live Load Distribution Factor Equations for Bridge Design." *Journal of the Transportation Research Board*, 11(S), 67-78.

Ryall, M. J., Parke, G. A. R., and Harding, J. E. (2000). *ICE Manual of Bridge Engineering*, Institution of Civil Engineers, Thomas Telford, London, UK.

Schwarz, M., and Laman, J. A. (2001). "Response of Prestressed Concrete I-Girder Bridges to Live Load." *ASCE Journal of Bridge Engineering*, 6(1), 1-8.

Sotelino, E., Liu, J., Chung, W., and Phuvoravan, K. (2004). "Simplified Load Distribution Factor for Use in LRFD Design." *Joint Transportation Research Program*, Indiana Department of Transportation and Purdue University, West Lafayette, IN, 1-148.

Srinivas, V., and Ramanjaneyulu, K. (2007). "An Integrated Approach for Optimum Design of Bridge Decks Using Genetic Algorithms and Artificial Neural Networks." *Advances in Engineering Software*, 38(7), 475-487.

Surana, C. S., and Agrawal, R. (1998). *Grillage Analogy in Bridge Deck Analysis*, Narosa Publishing House, London, UK.

Tabsh, S., and Tabatabai, M. (2001). "Live Load Distribution in Girder Bridges Subject to Oversized Trucks." *ASCE Journal of Bridge Engineering*, 6(1), 9-16.

Terzioglu, T. (2012). "Riverside Experimental Bridge Drawings." Texas Transportation Institute. Texas A&M University, College Station, TX.

Trimble, M. D., Cousins, T. E., and Seda-Sanabria, Y. (2003). "Field Study of Live Load Distribution Factors and Dynamic Load Allowance on Reinforced Concrete T-Beam Bridges." US Army Corps of Engineers, Washington, DC.

TxDOT (2010). "US 69 BNSF & Up Railroad Overpass Plans."Denison, TX.

TxDOT (2012). "Bridge Division Standards." <http://www.txdot.gov/insdtdot/orgchart/cmd/cserve/standard/bridge-e.htm>. (September 3, 2012).

Ugural, A. C., and Fenster, S. K. (2011). *Advanced Mechanics of Materials and Applied Elasticity*, Prentice Hall, Upper Saddle River, NJ.

WYDOT (1996). *Bridge Rating and Analysis of Structural Systems (Brass) User's Manual, Version 1*, Wyoming Department of Transportation, Cheyenne, WY.

Young, W. C., Budynas, R. G., and Sadegh, A. M. (2012). *Roark's Formulas for Stress and Strain*, McGraw-Hill, New York, NY.

Zokaie, T. (2000). "AASHTO-LRFD Live Load Distribution Specifications." *ASCE Journal of Bridge Engineering*, 5(2), 131-138.

Zokaie, T., Imbsen, R. A., and Osterkamp, T. A. (1991). "Distribution of Wheel Loads on Highway Bridges." *NHCRP Project Report 12-26*, Transportation Research Board, Washington, DC.

APPENDIX A

RESULTS FROM MODIFIED RIVERSIDE GRILLAGE MODELS

A.1 Riverside Grillage Model Spaced for Loading Shear Modifications

Table A.1 Bending Moment of Inertia set to 0 for Both End Transverse Members

Load Case	Outside Wheel Location From Edge [ft]	Exterior Girder - Shear							
		Grillage		FE Frame		FE Shell		G/FE Ratio	
		V_{max} [k]	LDF	V_{max} [k]	LDF	V_{max} [k]	LDF	Frame	Shell
1	3	36.9	0.634	36.2	0.622	35.8	0.615	1.019	1.030
2	4	31.1	0.534	32	0.550	31.5	0.542	0.972	0.987
3	5	25.6	0.440	27.6	0.474	27.0	0.464	0.928	0.948
4	6	20.6	0.354	23.5	0.404	22.9	0.394	0.875	0.898
5	7	16.1	0.277	19.2	0.330	18.2	0.313	0.840	0.886
6	8	12.2	0.209	15.5	0.266	14.1	0.242	0.785	0.862
7	9	8.7	0.150	11.8	0.203	10.2	0.175	0.737	0.853

Table A.2 Bending Moment of Inertia set to 0 for Both End Transverse Members

Load Case	Outside Wheel Location From Edge [ft]	Interior Girder - Shear							
		Grillage		FE Frame		FE Shell		G/FE Ratio	
		V_{max} [k]	LDF	V_{max} [k]	LDF	V_{max} [k]	LDF	Frame	Shell
1	3	54.9	0.944	47.8	0.822	49.1	0.844	1.149	1.119
2	4	55.5	0.953	47.7	0.820	49.1	0.844	1.162	1.129
3	5	55.5	0.954	47.9	0.823	49.4	0.849	1.159	1.124
4	6	55.1	0.948	47.3	0.813	48.5	0.834	1.166	1.137
5	7	54.0	0.929	46.6	0.801	48.0	0.825	1.160	1.126
6	8	52.1	0.896	45	0.774	46.6	0.801	1.158	1.118
7	9	49.5	0.850	43.3	0.744	44.9	0.772	1.142	1.102

Table A.3 Bending Moment of Inertia set to 0 for Loaded End Transverse Member

Load Case	Outside Wheel Location From Edge [ft]	Exterior Girder - Shear							
		Grillage		FE Frame		FE Shell		G/FE Ratio	
		V_{max} [k]	LDF	V_{max} [k]	LDF	V_{max} [k]	LDF	Frame	Shell
1	3	36.7	0.631	36.2	0.622	35.8	0.615	1.014	1.025
2	4	31.0	0.533	32	0.550	31.5	0.542	0.969	0.984
3	5	25.6	0.440	27.6	0.474	27.0	0.464	0.928	0.949
4	6	20.7	0.355	23.5	0.404	22.9	0.394	0.880	0.903
5	7	16.3	0.280	19.2	0.330	18.2	0.313	0.848	0.895
6	8	12.4	0.213	15.5	0.266	14.1	0.242	0.799	0.878
7	9	9.0	0.154	11.8	0.203	10.2	0.175	0.760	0.879

Table A.3 Bending Moment of Inertia set to 0 for Loaded End Transverse Member

Load Case	Outside Wheel Location From Edge [ft]	Interior Girder - Shear							
		Grillage		FE Frame		FE Shell		G/FE Ratio	
		V_{max} [k]	LDF	V_{max} [k]	LDF	V_{max} [k]	LDF	Frame	Shell
1	3	54.7	0.941	47.8	0.822	49.1	0.844	1.145	1.114
2	4	55.2	0.949	47.7	0.820	49.1	0.844	1.157	1.124
3	5	55.3	0.950	47.9	0.823	49.4	0.849	1.153	1.118
4	6	54.9	0.943	47.3	0.813	48.5	0.834	1.160	1.131
5	7	53.8	0.924	46.6	0.801	48.0	0.825	1.154	1.120
6	8	51.8	0.891	45	0.774	46.6	0.801	1.152	1.112
7	9	49.2	0.846	43.3	0.744	44.9	0.772	1.136	1.096

Table A.5 Bending and Torsional Moment of Inertia set to 0 for Loaded End Transverse Member

Load Case	Outside Wheel Location From Edge [ft]	Exterior Girder - Shear							
		Grillage		FE Frame		FE Shell		G/FE Ratio	
		V_{max} [k]	LDF	V_{max} [k]	LDF	V_{max} [k]	LDF	Frame	Shell
1	3	36.8	0.632	36.2	0.622	35.8	0.615	1.016	1.027
2	4	31.1	0.535	32	0.550	31.5	0.542	0.973	0.988
3	5	25.8	0.443	27.6	0.474	27.0	0.464	0.933	0.954
4	6	20.8	0.358	23.5	0.404	22.9	0.394	0.886	0.909
5	7	16.5	0.283	19.2	0.330	18.2	0.313	0.857	0.904
6	8	12.6	0.216	15.5	0.266	14.1	0.242	0.810	0.891
7	9	9.2	0.157	11.8	0.203	10.2	0.175	0.775	0.897

Table A.6 Bending and Torsional Moment of Inertia set to 0 for Loaded End Transverse Member

Load Case	Outside Wheel Location From Edge [ft]	Interior Girder - Shear							
		Grillage		FE Frame		FE Shell		G/FE Ratio	
		V_{max} [k]	LDF	V_{max} [k]	LDF	V_{max} [k]	LDF	Frame	Shell
1	3	54.5	0.937	47.8	0.822	49.1	0.844	1.141	1.111
2	4	55.0	0.946	47.7	0.820	49.1	0.844	1.153	1.120
3	5	55.0	0.946	47.9	0.823	49.4	0.849	1.149	1.114
4	6	54.7	0.939	47.3	0.813	48.5	0.834	1.155	1.127
5	7	53.6	0.921	46.6	0.801	48.0	0.825	1.149	1.116
6	8	51.6	0.887	45	0.774	46.6	0.801	1.147	1.108
7	9	49.0	0.843	43.3	0.744	44.9	0.772	1.132	1.092

Table A.7 End Loads Distributed from Transverse Members to Location of Girder Intersection with End Transverse Member but Still Placed on Transverse Member

Load Case	Outside Wheel Location From Edge [ft]	Exterior Girder - Shear							
		Grillage		FE Frame		FE Shell		G/FE Ratio	
		V_{max} [k]	LDF	V_{max} [k]	LDF	V_{max} [k]	LDF	Frame	Shell
1	3	38.0	0.653	36.2	0.622	35.8	0.615	1.050	1.061
2	4	32.0	0.550	32	0.550	31.5	0.542	1.001	1.017
3	5	26.3	0.451	27.6	0.474	27.0	0.464	0.951	0.973
4	6	20.7	0.356	23.5	0.404	22.9	0.394	0.882	0.905
5	7	16.8	0.289	19.2	0.330	18.2	0.313	0.875	0.923
6	8	13.4	0.229	15.5	0.266	14.1	0.242	0.861	0.947
7	9	10.1	0.173	11.8	0.203	10.2	0.175	0.855	0.989

Table A.8 End Loads Distributed from Transverse Members to Location of Girder Intersection with End Transverse Member but Still Placed on Transverse Member

Load Case	Outside Wheel Location From Edge [ft]	Interior Girder - Shear							
		Grillage		FE Frame		FE Shell		G/FE Ratio	
		V_{max} [k]	LDF	V_{max} [k]	LDF	V_{max} [k]	LDF	Frame	Shell
1	3	53.3	0.917	47.8	0.822	49.1	0.844	1.116	1.086
2	4	53.9	0.926	47.7	0.820	49.1	0.844	1.130	1.098
3	5	54.1	0.930	47.9	0.823	49.4	0.849	1.130	1.095
4	6	54.3	0.933	47.3	0.813	48.5	0.834	1.148	1.119
5	7	52.8	0.908	46.6	0.801	48.0	0.825	1.133	1.100
6	8	50.6	0.869	45	0.774	46.6	0.801	1.123	1.085
7	9	48.1	0.827	43.3	0.744	44.9	0.772	1.110	1.071

Table A.9 End Loads Distributed from Transverse Members to Girders

Load Case	Outside Wheel Location From Edge [ft]	Exterior Girder - Shear							
		Grillage		FE Frame		FE Shell		G/FE Ratio	
		V_{max} [k]	LDF	V_{max} [k]	LDF	V_{max} [k]	LDF	Frame	Shell
1	3	38.0	0.653	36.2	0.622	35.8	0.615	1.050	1.061
2	4	32.0	0.550	32	0.550	31.5	0.542	1.001	1.017
3	5	26.3	0.451	27.6	0.474	27.0	0.464	0.951	0.973
4	6	20.7	0.356	23.5	0.404	22.9	0.394	0.882	0.905
5	7	16.8	0.289	19.2	0.330	18.2	0.313	0.875	0.923
6	8	13.4	0.229	15.5	0.266	14.1	0.242	0.861	0.947
7	9	10.1	0.173	11.8	0.203	10.2	0.175	0.855	0.989

Table A.10 End Loads Distributed from Transverse Members to Girders

Load Case	Outside Wheel Location From Edge [ft]	Interior Girder - Shear							
		Grillage		FE Frame		FE Shell		G/FE Ratio	
		V_{max} [k]	LDF	V_{max} [k]	LDF	V_{max} [k]	LDF	Frame	Shell
1	3	53.3	0.917	47.8	0.822	49.1	0.844	1.116	1.086
2	4	53.9	0.926	47.7	0.820	49.1	0.844	1.130	1.098
3	5	54.1	0.930	47.9	0.823	49.4	0.849	1.130	1.095
4	6	54.3	0.933	47.3	0.813	48.5	0.834	1.148	1.119
5	7	52.8	0.908	46.6	0.801	48.0	0.825	1.133	1.100
6	8	50.6	0.869	45	0.774	46.6	0.801	1.123	1.085
7	9	48.1	0.827	43.3	0.744	44.9	0.772	1.110	1.071

Table A.11 End Loads Distributed from Transverse Members to Girders, Bending and Torsional Moment of Inertias set to 0 for Loaded End Transverse Member

Load Case	Outside Wheel Location From Edge [ft]	Exterior Girder - Shear							
		Grillage		FE Frame		FE Shell		G/FE Ratio	
		V_{max} [k]	LDF	V_{max} [k]	LDF	V_{max} [k]	LDF	Frame	Shell
1	3	38.3	0.658	36.2	0.622	35.8	0.615	1.057	1.069
2	4	32.6	0.560	32	0.550	31.5	0.542	1.019	1.035
3	5	27.1	0.465	27.6	0.474	27.0	0.464	0.981	1.003
4	6	21.7	0.373	23.5	0.404	22.9	0.394	0.923	0.948
5	7	17.9	0.308	19.2	0.330	18.2	0.313	0.934	0.986
6	8	14.6	0.251	15.5	0.266	14.1	0.242	0.941	1.035
7	9	11.4	0.196	11.8	0.203	10.2	0.175	0.965	1.117

Table A.12 End Loads Distributed from Transverse Members to Girders, Bending and Torsional Moment of Inertias set to 0 for Loaded End Transverse Member

Load Case	Outside Wheel Location From Edge [ft]	Interior Girder - Shear							
		Grillage		FE Frame		FE Shell		G/FE Ratio	
		V_{max} [k]	LDF	V_{max} [k]	LDF	V_{max} [k]	LDF	Frame	Shell
1	3	52.5	0.902	47.8	0.822	49.1	0.844	1.097	1.068
2	4	52.8	0.907	47.7	0.820	49.1	0.844	1.106	1.075
3	5	52.8	0.908	47.9	0.823	49.4	0.849	1.103	1.069
4	6	52.9	0.910	47.3	0.813	48.5	0.834	1.119	1.091
5	7	51.4	0.884	46.6	0.801	48.0	0.825	1.104	1.072
6	8	49.2	0.846	45	0.774	46.6	0.801	1.093	1.056
7	9	46.8	0.804	43.3	0.744	44.9	0.772	1.080	1.042

Table A.13 End Loads Distributed from Transverse Members to Girders and Placed 0.0001" From End

Load Case	Outside Wheel Location From Edge [ft]	Exterior Girder - Shear							
		Grillage		FE Frame		FE Shell		G/FE Ratio	
		V_{max} [k]	LDF	V_{max} [k]	LDF	V_{max} [k]	LDF	Frame	Shell
1	3	37.8	0.650	36.2	0.622	35.8	0.615	1.045	1.056
2	4	32.5	0.559	32	0.550	31.5	0.542	1.016	1.032
3	5	27.3	0.469	27.6	0.474	27.0	0.464	0.989	1.011
4	6	22.2	0.382	23.5	0.404	22.9	0.394	0.946	0.971
5	7	18.7	0.322	19.2	0.330	18.2	0.313	0.974	1.028
6	8	15.6	0.267	15.5	0.266	14.1	0.242	1.004	1.104
7	9	12.5	0.216	11.8	0.203	10.2	0.175	1.063	1.229

Table A.14 End Loads Distributed from Transverse Members to Girders and Placed 0.0001" From End

Load Case	Outside Wheel Location From Edge [ft]	Interior Girder - Shear							
		Grillage		FE Frame		FE Shell		G/FE Ratio	
		V_{max} [k]	LDF	V_{max} [k]	LDF	V_{max} [k]	LDF	Frame	Shell
1	3	51.5	0.885	47.8	0.822	49.1	0.844	1.077	1.048
2	4	51.7	0.888	47.7	0.820	49.1	0.844	1.083	1.052
3	5	51.6	0.888	47.9	0.823	49.4	0.849	1.078	1.045
4	6	51.7	0.889	47.3	0.813	48.5	0.834	1.093	1.066
5	7	50.2	0.863	46.6	0.801	48.0	0.825	1.078	1.046
6	8	48.0	0.825	45	0.774	46.6	0.801	1.067	1.030
7	9	45.6	0.784	43.3	0.744	44.9	0.772	1.054	1.016

A.2 Riverside Grillage Model Evenly Spaced Shear Alterations

Table A.15 End Loads Distributed from Transverse Members to Girders, Bending and Torsional Moment of Inertias set to 0 for Loaded End Transverse Member

Load Case	Outside Wheel Location From Edge [ft]	Exterior Girder - Shear							
		Grillage		FE Frame		FE Shell		G/FE Ratio	
		V_{max} [k]	LDF	V_{max} [k]	LDF	V_{max} [k]	LDF	Frame	Shell
1	3	38.2	0.657	36.2	0.622	35.8	0.615	1.056	1.068
2	4	32.5	0.559	32	0.550	31.5	0.542	1.015	1.031
3	5	26.9	0.463	27.6	0.474	27.0	0.464	0.976	0.997
4	6	21.6	0.370	23.5	0.404	22.9	0.394	0.917	0.941
5	7	17.7	0.305	19.2	0.330	18.2	0.313	0.924	0.975
6	8	14.4	0.247	15.5	0.266	14.1	0.242	0.927	1.019
7	9	11.2	0.192	11.8	0.203	10.2	0.175	0.946	1.094

Table A.16 End Loads Distributed from Transverse Members to Girders, Bending and Torsional Moment of Inertias set to 0 for Loaded End Transverse Member

Load Case	Outside Wheel Location From Edge [ft]	Interior Girder - Shear							
		Grillage		FE Frame		FE Shell		G/FE Ratio	
		V_{max} [k]	LDF	V_{max} [k]	LDF	V_{max} [k]	LDF	Frame	Shell
1	3	52.7	0.905	47.8	0.822	49.1	0.844	1.102	1.073
2	4	53.0	0.911	47.7	0.820	49.1	0.844	1.111	1.079
3	5	53.1	0.912	47.9	0.823	49.4	0.849	1.108	1.074
4	6	53.2	0.914	47.3	0.813	48.5	0.834	1.124	1.096
5	7	51.7	0.889	46.6	0.801	48.0	0.825	1.109	1.077
6	8	49.4	0.850	45	0.774	46.6	0.801	1.099	1.061
7	9	47.0	0.808	43.3	0.744	44.9	0.772	1.086	1.047

Table A.17 End Loads Distributed from Transverse Members to Girders 0.0001" From End

Load Case	Outside Wheel Location From Edge [ft]	Exterior Girder - Shear							
		Grillage		FE Frame		FE Shell		G/FE Ratio	
		V_{max} [k]	LDF	V_{max} [k]	LDF	V_{max} [k]	LDF	Frame	Shell
1	3	37.8	0.650	36.2	0.622	35.8	0.615	1.044	1.056
2	4	32.4	0.557	32	0.550	31.5	0.542	1.013	1.029
3	5	27.2	0.467	27.6	0.474	27.0	0.464	0.984	1.006
4	6	22.1	0.379	23.5	0.404	22.9	0.394	0.939	0.963
5	7	18.5	0.318	19.2	0.330	18.2	0.313	0.963	1.015
6	8	15.3	0.263	15.5	0.266	14.1	0.242	0.988	1.086
7	9	12.3	0.211	11.8	0.203	10.2	0.175	1.038	1.201

Table A.18 End Loads Distributed from Transverse Members to Girders 0.0001" From End

Load Case	Outside Wheel Location From Edge [ft]	Interior Girder - Shear							
		Grillage		FE Frame		FE Shell		G/FE Ratio	
		V_{max} [k]	LDF	V_{max} [k]	LDF	V_{max} [k]	LDF	Frame	Shell
1	3	51.8	0.890	47.8	0.822	49.1	0.844	1.083	1.054
2	4	51.9	0.893	47.7	0.820	49.1	0.844	1.089	1.058
3	5	51.9	0.893	47.9	0.823	49.4	0.849	1.084	1.051
4	6	52.0	0.894	47.3	0.813	48.5	0.834	1.100	1.073
5	7	50.5	0.869	46.6	0.801	48.0	0.825	1.085	1.053
6	8	48.3	0.830	45	0.774	46.6	0.801	1.073	1.036
7	9	45.9	0.789	43.3	0.744	44.9	0.772	1.061	1.023

A.3 Riverside Grillage Model Mesh Sensitivity Results

Table A.19 Half Grid Evenly Spaced, Two Truck Loading Moment

Load Case	Exterior Girder - Moment							
	Grillage		FE Frame		FE Shell		G/FE Ratio	
	M_{max} [k-ft]	LDF	M_{max} [k-ft]	LDF	M_{max} [k-ft]	LDF	Frame	Shell
1	385.0	0.639	372.4	0.618	397.2	0.660	1.034	0.969
2	354.3	0.588	344.4	0.572	364.2	0.605	1.029	0.973
3	324.6	0.539	315.6	0.524	329.7	0.548	1.029	0.985
4	296.4	0.492	288.9	0.480	298.0	0.495	1.026	0.995
5	269.5	0.448	262.9	0.437	265.2	0.440	1.025	1.016
6	243.6	0.405	238.5	0.396	234.7	0.390	1.022	1.038
7	219.0	0.364	214.9	0.357	205.0	0.340	1.019	1.068

Table A.20 Half Grid Evenly Spaced, Two Truck Loading Moment

Load Case	Interior Girder - Moment							
	Grillage		FE Frame		FE Shell		G/FE Ratio	
	M_{max} [k-ft]	LDF	M_{max} [k-ft]	LDF	M_{max} [k-ft]	LDF	Frame	Shell
1	410.2	0.681	401.6	0.667	429.7	0.714	1.021	0.955
2	407.5	0.677	396.8	0.659	426.2	0.708	1.027	0.956
3	403.2	0.670	392.4	0.652	423.5	0.703	1.027	0.952
4	397.2	0.660	385.3	0.640	416.0	0.691	1.031	0.955
5	389.3	0.646	377.1	0.626	408.8	0.679	1.032	0.952
6	379.3	0.630	365.9	0.608	397.0	0.659	1.037	0.955
7	367.6	0.610	353.8	0.588	383.7	0.637	1.039	0.958

Table A.21 Half Grid Evenly Spaced, Two Truck Loading Shear

Load Case	Exterior Girder - Shear							
	Grillage		FE Frame		FE Shell		G/FE Ratio	
	V_{max} [k]	LDF	V_{max} [k]	LDF	V_{max} [k]	LDF	Frame	Shell
1	37.6	0.646	36.2	0.622	35.8	0.615	1.038	1.049
2	32.4	0.557	32	0.550	31.5	0.542	1.012	1.028
3	27.3	0.469	27.6	0.474	27.0	0.464	0.988	1.010
4	22.3	0.384	23.5	0.404	22.9	0.394	0.949	0.974
5	18.9	0.324	19.2	0.330	18.2	0.313	0.982	1.036
6	15.8	0.271	15.5	0.266	14.1	0.242	1.017	1.118
7	12.8	0.220	11.8	0.203	10.2	0.175	1.083	1.253

Table A.22 Half Grid Evenly Spaced, Two Truck Loading Shear

Load Case	Interior Girder - Shear							
	Grillage		FE Frame		FE Shell		G/FE Ratio	
	V_{max} [k]	LDF	V_{max} [k]	LDF	V_{max} [k]	LDF	Frame	Shell
1	51.5	0.886	47.8	0.822	49.1	0.844	1.078	1.050
2	51.6	0.887	47.7	0.820	49.1	0.844	1.082	1.051
3	51.5	0.885	47.9	0.823	49.4	0.849	1.075	1.043
4	51.6	0.886	47.3	0.813	48.5	0.834	1.090	1.063
5	50.1	0.861	46.6	0.801	48.0	0.825	1.074	1.043
6	47.8	0.822	45	0.774	46.6	0.801	1.062	1.026
7	45.4	0.780	43.3	0.744	44.9	0.772	1.048	1.011

Table A.23 Double Grid Evenly Spaced, Two Truck Loading Moment

Load Case	Exterior Girder - Moment							
	Grillage		FE Frame		FE Shell		G/FE Ratio	
	M_{max} [k-ft]	LDF	M_{max} [k-ft]	LDF	M_{max} [k-ft]	LDF	Frame	Shell
1	389.1	0.646	372.4	0.618	397.2	0.660	1.045	0.980
2	356.9	0.593	344.4	0.572	364.2	0.605	1.036	0.980
3	325.8	0.541	315.6	0.524	329.7	0.548	1.032	0.988
4	296.2	0.492	288.9	0.480	298.0	0.495	1.025	0.994
5	268.1	0.445	262.9	0.437	265.2	0.440	1.020	1.011
6	241.0	0.400	238.5	0.396	234.7	0.390	1.010	1.027
7	215.2	0.357	214.9	0.357	205.0	0.340	1.001	1.050

Table A.24 Double Grid Evenly Spaced, Two Truck Loading Moment

Load Case	Interior Girder - Moment							
	Grillage		FE Frame		FE Shell		G/FE Ratio	
	M_{max} [k-ft]	LDF	M_{max} [k-ft]	LDF	M_{max} [k-ft]	LDF	Frame	Shell
1	420.9	0.699	401.6	0.667	429.7	0.714	1.048	0.979
2	418.1	0.694	396.8	0.659	426.2	0.708	1.054	0.981
3	413.7	0.687	392.4	0.652	423.5	0.703	1.054	0.977
4	408.0	0.678	385.3	0.640	416.0	0.691	1.059	0.981
5	399.9	0.664	377.1	0.626	408.8	0.679	1.060	0.978
6	389.2	0.646	365.9	0.608	397.0	0.659	1.064	0.980
7	376.2	0.625	353.8	0.588	383.7	0.637	1.063	0.981

Table A.25 Double Grid Evenly Spaced, Two Truck Loading Shear

Load Case	Exterior Girder - Shear							
	Grillage		FE Frame		FE Shell		G/FE Ratio	
	V_{max} [k]	LDF	V_{max} [k]	LDF	V_{max} [k]	LDF	Frame	Shell
1	38.0	0.653	36.2	0.622	35.8	0.615	1.050	1.061
2	32.4	0.557	32	0.550	31.5	0.542	1.012	1.028
3	26.9	0.463	27.6	0.474	27.0	0.464	0.976	0.997
4	21.7	0.372	23.5	0.404	22.9	0.394	0.921	0.945
5	17.9	0.308	19.2	0.330	18.2	0.313	0.934	0.985
6	14.6	0.252	15.5	0.266	14.1	0.242	0.945	1.038
7	11.5	0.198	11.8	0.203	10.2	0.175	0.975	1.127

Table A.26 Double Grid Evenly Spaced, Two Truck Loading Shear

Load Case	Interior Girder - Shear							
	Grillage		FE Frame		FE Shell		G/FE Ratio	
	V_{max} [k]	LDF	V_{max} [k]	LDF	V_{max} [k]	LDF	Frame	Shell
1	52.2	0.898	47.8	0.822	49.1	0.844	1.093	1.064
2	52.6	0.904	47.7	0.820	49.1	0.844	1.102	1.071
3	52.7	0.905	47.9	0.823	49.4	0.849	1.099	1.066
4	52.8	0.907	47.3	0.813	48.5	0.834	1.116	1.088
5	51.3	0.882	46.6	0.801	48.0	0.825	1.101	1.069
6	49.1	0.844	45	0.774	46.6	0.801	1.090	1.053
7	46.7	0.802	43.3	0.744	44.9	0.772	1.078	1.039

APPENDIX B

MODIFIED DREHERSVILLE GRILLAGE MODELING RESULTS

B.1 Drehersville Grillage Model Maximum Moment Results

Table B.1 Lane 4 Grillage Maximum Moment Comparisons

Lanes Loaded	Girder Location	Moment [k-ft]					
		Experiment	2005 FEA	FE Frame	FE Shell	FE Solid	Grillage
4	A	144.0	108.5	136.5	137.6	139.6	138.8
	B	158.5	162.7	152.4	151.5	150.8	160.6
	C	178.3	210.9	161.3	160.8	172.8	185.1
	D	135.5	162.7	152.4	151.5	150.8	160.6
	E	132.0	108.5	136.5	137.6	139.5	138.8

Table B.2 Lanes 1 and 4 Grillage Maximum Moment Comparisons

Lanes Loaded	Girder Location	Moment [k-ft]					
		Experiment	2005 FEA	FE Frame	FE Shell	FE Solid	Grillage
1 & 4	A	477.1	280.0	381.3	364.8	358.4	495.6
	B	373.0	339.6	350.7	342.1	343.1	393.2
	C	273.8	295.6	304.5	303.3	314.6	306.8
	D	203.2	-	248.9	256.7	261.0	209.7
	E	190.9	-	192.5	211	234.0	81.4

Table B.3 Lane 4 Grillage Maximum Moment Ratios

Lanes Loaded	Girder Location	Moment Ratio to Experimental				
		FEA/Exp	Frame/Exp	Shell/Exp	Solid/Exp	G/Exp
4	A	0.753	0.948	0.955	0.969	0.964
	B	1.027	0.962	0.956	0.951	1.014
	C	1.183	0.904	0.902	0.969	1.038
	D	1.201	1.125	1.118	1.113	1.186
	E	0.822	1.034	1.043	1.057	1.052

Table B.4 Lanes 1 and 4 Grillage Maximum Moment Ratios

Lanes Loaded	Girder Location	Moment Ratio to Experimental				
		FEA/Exp	Frame/Exp	Shell/Exp	Solid/Exp	G/Exp
1 & 4	A	0.587	0.799	0.765	0.751	1.039
	B	0.910	0.940	0.917	0.920	1.054
	C	1.080	1.112	1.108	1.149	1.121
	D	-	1.225	1.263	1.285	1.032
	E	-	1.008	1.105	1.226	0.427

B.2 Drehersville Grillage Model Cracked Diaphragm Results

Table B.5 Cracked Diaphragm in Grillage Model, Lane 4 Moment Comparisons

Lanes Loaded	Girder Location	Moment [k-ft]					
		Experiment	2005 FEA	FE Frame	FE Shell	FE Solid	Grillage
4	A	144.0	108.5	136.5	137.6	139.6	116.3
	B	158.5	162.7	152.4	151.5	150.8	159.2
	C	178.3	210.9	161.3	160.8	172.8	167.1
	D	135.5	162.7	152.4	151.5	150.8	159.2
	E	132.0	108.5	136.5	137.6	139.5	116.3

Table B.6 Cracked Diaphragm in Grillage Model, Lanes 1 and 4 Moment Comparisons

Lanes Loaded	Girder Location	Moment [k-ft]					
		Experiment	2005 FEA	FE Frame	FE Shell	FE Solid	Grillage
1 & 4	A	477.1	280.0	381.3	364.8	358.4	465.1
	B	373.0	339.6	350.7	342.1	343.1	394.1
	C	273.8	295.6	304.5	303.3	314.6	307.0
	D	203.2	-	248.9	256.7	261.0	201.0
	E	190.9	-	192.5	211	234.0	69.0

Table B.7 Cracked Diaphragm in Grillage Model, Lane 4 Moment Ratios

Lanes Loaded	Girder Location	Moment Ratio to Experimental				
		FEA/Exp	Frame/Exp	Shell/Exp	Solid/Exp	G/Exp
4	A	0.753	0.948	0.955	0.969	0.808
	B	1.027	0.962	0.956	0.951	1.004
	C	1.183	0.904	0.902	0.969	0.937
	D	1.201	1.125	1.118	1.113	1.175
	E	0.822	1.034	1.043	1.057	0.881

Table B.8 Cracked Diaphragm in Grillage Model, Lanes 1 and 4 Moment Ratios

Lanes Loaded	Girder Location	Moment Ratio to Experimental				
		FEA/Exp	Frame/Exp	Shell/Exp	Solid/Exp	G/Exp
1 & 4	A	0.587	0.799	0.765	0.751	0.975
	B	0.910	0.940	0.917	0.920	1.056
	C	1.080	1.112	1.108	1.149	1.121
	D	-	1.225	1.263	1.285	0.989
	E	-	1.008	1.105	1.226	0.361

B.3 Drehersville Grillage Model Edge Stiffening Results

Table B.9 Edge Stiffening Elements in Grillage Model, Lane 4 Moment Comparisons

Lanes Loaded	Girder Location	Moment [k-ft]					
		Experiment	2005 FEA	FE Frame	FE Shell	FE Solid	Grillage
4	A	144.0	108.5	136.5	137.6	139.6	136.0
	B	158.5	162.7	152.4	151.5	150.8	147.7
	C	178.3	210.9	161.3	160.8	172.8	150.7
	D	135.5	162.7	152.4	151.5	150.8	147.7
	E	132.0	108.5	136.5	137.6	139.5	136.0

Table B.10 Edge Stiffening Elements in Grillage Model, Lanes 1 and 4 Moment Comparisons

Lanes Loaded	Girder Location	Moment [k-ft]					
		Experiment	2005 FEA	FE Frame	FE Shell	FE Solid	Grillage
1 & 4	A	477.1	280.0	381.3	364.8	358.4	529.4
	B	373.0	339.6	350.7	342.1	343.1	361.1
	C	273.8	295.6	304.5	303.3	314.6	283.4
	D	203.2	-	248.9	256.7	261.0	196.1
	E	190.9	-	192.5	211	234.0	98.5

Table B.11 Edge Stiffening Elements in Grillage Model, Lane 4 Moment Ratios

Lanes Loaded	Girder Location	Moment Ratio to Experimental				
		FEA/Exp	Frame/Exp	Shell/Exp	Solid/Exp	G/Exp
4	A	0.753	0.948	0.955	0.969	0.944
	B	1.027	0.962	0.956	0.951	0.932
	C	1.183	0.904	0.902	0.969	0.845
	D	1.201	1.125	1.118	1.113	1.090
	E	0.822	1.034	1.043	1.057	1.031

Table B.12 Edge Stiffening Elements in Grillage Model, Lanes 1 and 4 Moment Ratios

Lanes Loaded	Girder Location	Moment Ratio to Experimental				
		FEA/Exp	Frame/Exp	Shell/Exp	Solid/Exp	G/Exp
1 & 4	A	0.587	0.799	0.765	0.751	1.110
	B	0.910	0.940	0.917	0.920	0.968
	C	1.080	1.112	1.108	1.149	1.035
	D	-	1.225	1.263	1.285	0.965
	E	-	1.008	1.105	1.226	0.516

B.4 Drehersville Grillage Model with Edge Stiffening Elements and Cracked Midspan Diaphragm Deflection Results

Table B.13 Lane 4 Altered Grillage Deflection Comparisons

Lanes Loaded	Girder Location	Deflection [in.]				
		Experiment	FE Frame	FE Shell	FE Solid	Grillage
4	A	0.0398	0.060	0.06	0.060	0.136
	B	0.0574	0.068	0.065	0.066	0.098
	C	0.0700	0.074	0.069	0.070	0.055
	D	0.0552	0.068	0.065	0.066	0.098
	E	0.0404	0.060	0.058	0.060	0.136

Table B.14 Lanes 1 and 4 Altered Grillage Deflection Comparisons

Lanes Loaded	Girder Location	Deflection [in.]				
		Experiment	FE Frame	FE Shell	FE Solid	Grillage
1 & 4	A	0.115	0.170	0.156	0.154	0.180
	B	0.127	0.157	0.146	0.146	0.165
	C	0.120	0.137	0.13	0.133	0.134
	D	0.086	0.110	0.11	0.115	0.086
	E	0.061	0.085	0.09	0.099	0.033

Table B.15 Lane 4 Altered Grillage Deflection Ratios

Lanes Loaded	Girder Location	Deflection Ratio to Experimental			
		Frame/Exp	Shell/Exp	Solid/Exp	G/Exp
4	A	1.509	1.509	1.509	3.419
	B	1.185	1.133	1.151	1.705
	C	1.057	0.985	1.000	0.790
	D	1.233	1.178	1.196	1.773
	E	1.484	1.434	1.484	3.362

Table B.16 Lanes 1 and 4 Altered Grillage Deflection Ratios

Lanes Loaded	Girder Location	Deflection Ratio to Experimental			
		Frame/Exp	Shell/Exp	Solid/Exp	G/Exp
1 & 4	A	1.477	1.355	1.338	1.568
	B	1.234	1.147	1.147	1.299
	C	1.141	1.083	1.108	1.120
	D	1.283	1.283	1.341	1.007
	E	1.398	1.481	1.629	0.551

APPENDIX C

RIVERSIDE INELASTIC OVERLOAD ANALYSIS RESULTS

C.1 Riverside Moment Overload Analysis Force-Deformation Results

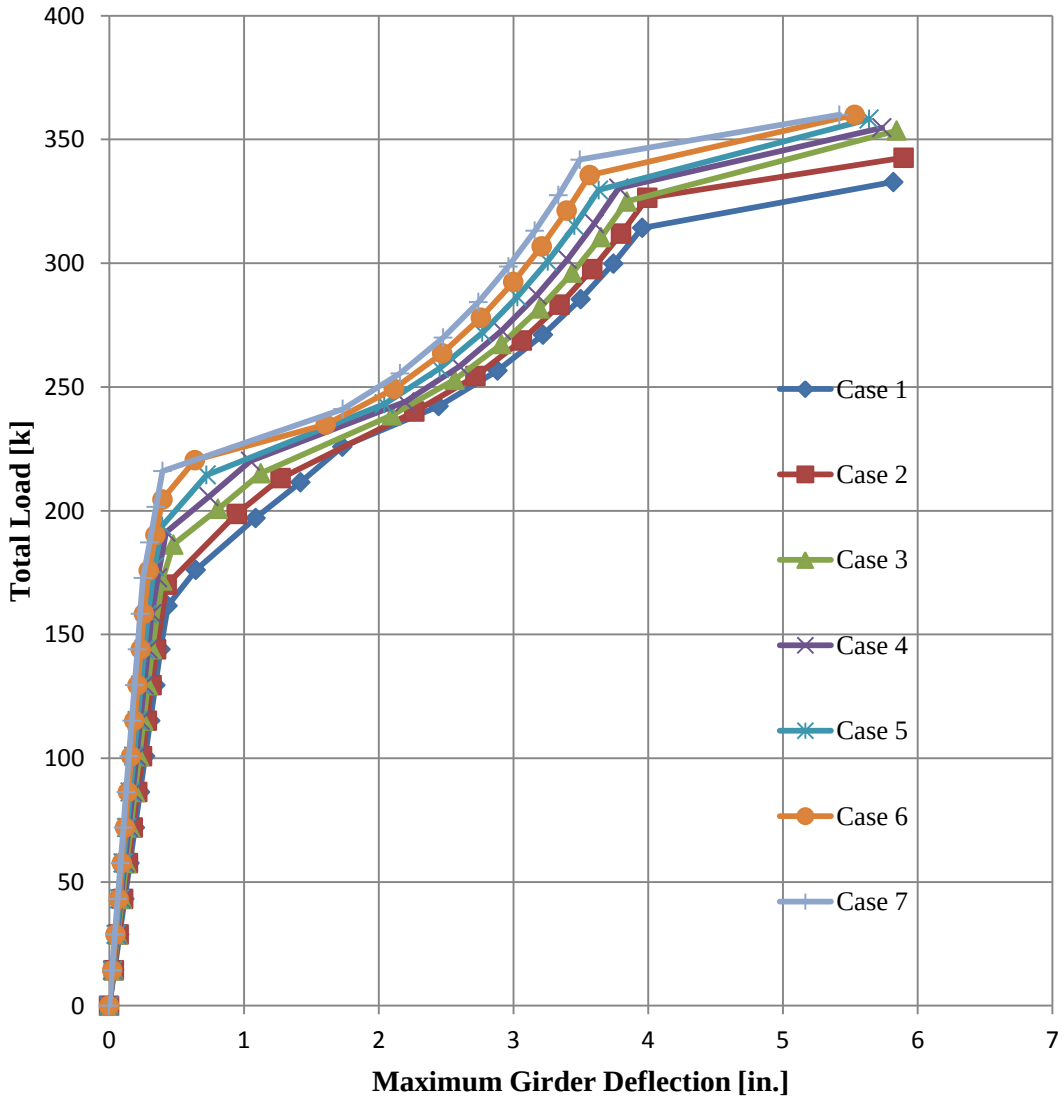

Figure C.1 Inelastic Force-Deformation Response for Exterior Girder – All Seven Loading Cases (Critical Moment Load Configuration)

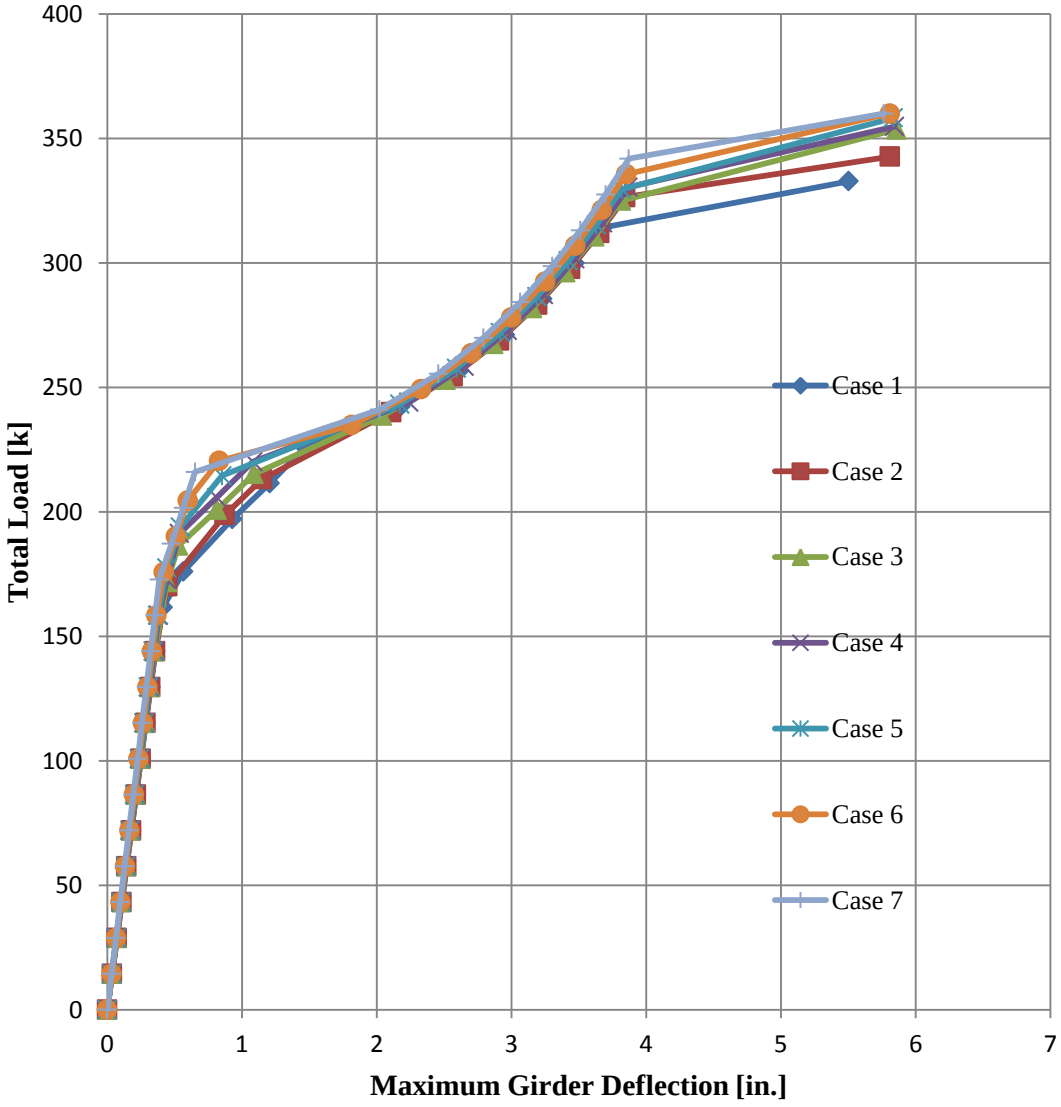

Figure C.2 Inelastic Force-Deformation Response for Interior Girder – All Seven Loading Cases (Critical Moment Load Configuration)

C.2 Riverside Shear Overload Analysis Force-Deformation Results

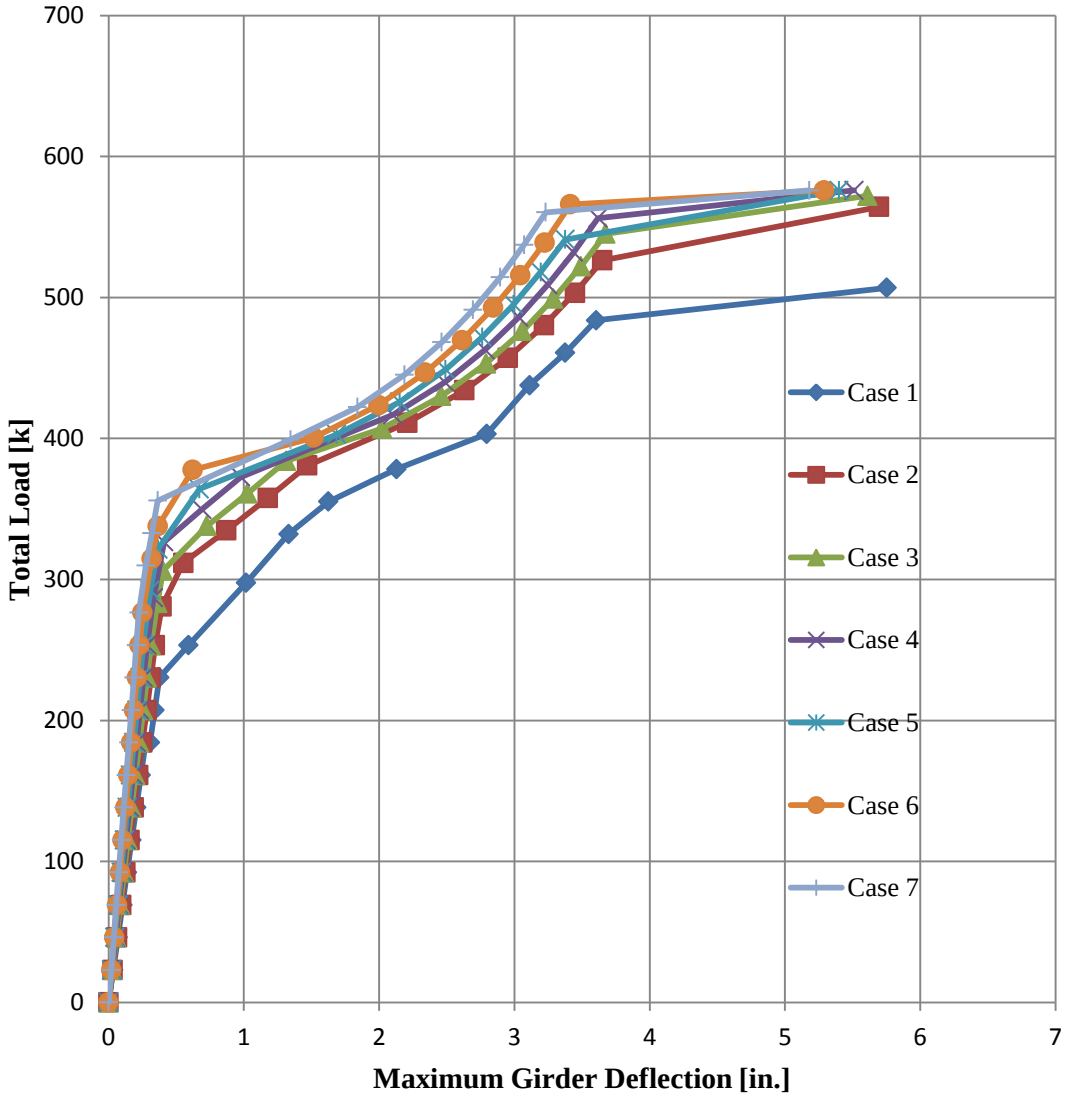

Figure C.3 Inelastic Force-Deformation Response for Exterior Girder – All Seven Loading Cases (Critical Shear Load Configuration)

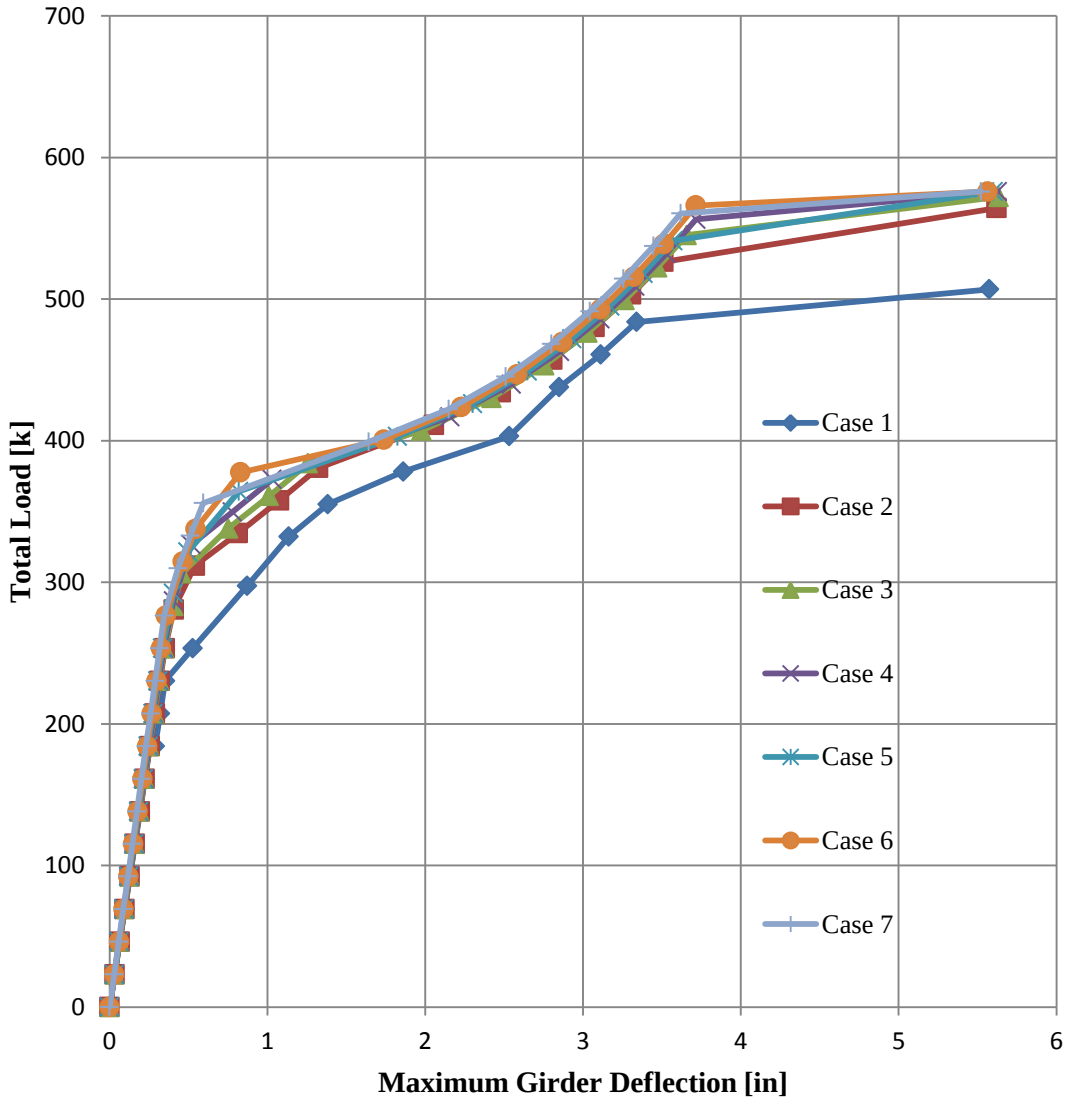

Figure C.4 Inelastic Force-Deformation Response for Interior Girder – All Seven Loading Cases (Critical Shear Load Configuration)